

ENERGY AND EXERGY ANALYSES OF ACTIVE SOLAR STILLS USING WATER LOADED NANOFLUID

by

DHARAMVEER

(Roll No-2K16/PHD/ME/53)

Mechanical Engineering

Submitted

in the fulfillment of the requirements of the degree of

Doctor of Philosophy

Under the supervision of

Prof. Samsher
(Professor)
Deptt. of Mechanical Engg.

Dr. Anil Kumar
(Associate Professor)
Deptt. of Mechanical Engg.



Department of Mechanical Engineering

Delhi Technological University

Shahbad, Daulatpur, Bawana Road, Delhi-110042, India

February 2022

DECLARATION

I hereby declare that the thesis titled “**Energy and Exergy Analyses of Active Solar Stills Using Water loaded Nanofluid**” is an original work carried out by me under the supervision of Dr. Samsheer, Professor, and Dr. Anil Kumar, Associate Professor, Department of Mechanical Engineering, Delhi Technological University, Delhi. This thesis has been prepared in conformity with the rules and regulations of Delhi Technological University, Delhi. The research work reported and the results presented in this have not been submitted either in part or full to any other University or institute for the award of diploma or degree.

DHARAMVEER

(2K16/PHD/ME/53)

Department of Mechanical Engineering

Delhi Technological University,

Delhi-110042, India

Date: February 23, 2022

Place: Delhi, India

CERTIFICATE

This is to certify that the work embodied in the thesis entitled “**Energy and Exergy Analyses of Active Solar Stills Using Water loaded Nanofluid**” by **Dharamveer** (Roll No. **2K16/PHD/ME/53**) student to the **Delhi Technological University, Delhi**, in partial fulfillment of requirements for the award of Degree of **Doctor of Philosophy in Mechanical Engineering** specialization in **Thermal Engineering**, is a record of bonafide research work carried out by him. He has worked under our guidance and supervision and has fulfilled the requirement, which to my knowledge, have reached the requisite standard for the submission of this thesis.

The results contained in this thesis have not been submitted in part or full any other University or Institute for the award of any degree or diploma.

(Prof. Samsheer)
Professor
Mechanical Engineering Department
Delhi Technological University
Delhi- 110042
India

(Dr. Anil Kumar)
Associate Professor
Mechanical Engineering Department
Delhi Technological University
Delhi- 110042
India

**Dedicated to my loving parents and family, whose constant support
strengthened me in completing this research**

ACKNOWLEDGEMENT

In the beginning, I would like to express deep and heartily gratitude to my research supervisor Prof. Samsher for his supervision, valuable advice and regular direction to carry out this research work. He provided me continuous encouragement and support in different ways, which motivated me to carry out the research work.

I am highly obliged and thankful to my research Jt-supervisor Dr. Anil Kumar, for his real scientist intuition idea and enthusiasm in science, inspired and enriched my growth as a researcher and a scientist. He provided me continuous support and motivation to carry out this research work.

I am also thankful to Prof. P. V. Ramkumar as my teacher in my college time. I could never have embarked and started all of this without his prior teachings, and I would forever be thankful to him for his leadership and blessings. I am highly grateful to DRC chairman Prof. S. K. Garg, Expert from department within DTU Prof. Raj Kumar Singh, Department of Mechanical Engineering and outside the Department Prof. Rakesh Kumar of Department of Civil Engineering, Delhi Technological University, Delhi, for their kind, moral support and advice time to time.

I am highly obliged and grateful to Prof. Prabal Talukdar and Prof. Sangeeta Kohli, Department of Mechanical Engineering, Indian Institute of Technology Delhi, for their valuable guidance and suggestions to carry out my research.

My words fail to express my appreciation to my respected parents Shri Mashi Charan and Late Smt. Rama Devi whose blessings have helped me to achieve my goal. My wife Ms. Lata Singh and younger son Gatik deserve thanks for their inseparable support and patience. My elder son Aakersh deserves special thanks for their valuable suggestions and help in carrying out this work. At last, I would like to thank everyone who helped for the successful realization of this thesis and express my regret that I could not mention it personally one by one.

DHARAMVEER
(2K16/PHD/ME/53)
Department of Mechanical Engineering
Delhi Technological University,
Delhi-110042
India

ABSTRACT

The basin type active solar still with CuO nanoparticles has been investigated in the current study and energy, exergy analysis, energy matrices, exergoeconomic parameter, environoeconomic parameter, and productivity has been presented. The prime objective of this design is to develop an energy efficient solar distillation system and produce potable water at a reasonable price. The single and double slope solar distillation systems N-PVT-CPC-HE with water loaded CuO nanoparticles have been studied in detail.

A mathematical model developed for the proposed systems and life cycle cost analysis for single and double solar distiller units with N-PVT-CPC using a helically coiled heat exchanger with water loaded CuO nanoparticles has emanated out. The analysis of four different weather conditions viz type a, b, c and d days for each month of year has been done. Detailed computation of energy, exergy, and yield optimized at $N=4$ number of collectors and various parameters like cost of distillate, CO₂ mitigation, carbon credit earned, environoeconomic, productivity and exergoeconomic also have been computed. Generally, exergoeconomic parameters are computed by lost exergy per unit cost for the systems like mechanical, thermal, etc. as many researchers reported, while in proposed study to compute the exergy gain per unit cost because solar energy is free of cost available. Solar distillation is carried out at 0.14 m depth of water, N-PVT-Compound parabolic concentrator collectors and optimum flow rate for the composite climate condition of New Delhi, India. Water production cost in ₹/kg and \$/kg has also been calculated. Solar distiller performance in terms of hourly productivity of distiller unit has for optimum number of collectors ($N = 4$), flow rate, and relative water depth have been determined.

It has been concluded that double slope N-PVT-CPC active solar distiller unit with heat exchanger using CuO nanoparticles gives the best performance based on average energy, exergy,

yield, cost of distillate, CO₂ mitigation, carbon credit earned, environoeconomic, productivity and exergoeconomic etc.

Following contributions are made by annual analysis of the proposed systems with CuO nanoparticles.

1. Distillate cost is less for system-B than system-A. Annual distillate costs for 30 yrs at rate of interest 10% are 0.30₹/kg for system-B, 0.344₹/kg for system-A, and 0.338₹/kg for system-C.
2. System-A gives a higher value of carbon dioxide mitigation and carbon credit earned based on thermal energy and exergy. Mitigation per ton based on energy and exergy for system-A is 15.76% and 53.5% higher than system-B and system- C, respectively.
3. Annual productivity of system-B for 15, 20, 30, 50 years are 209.44%, 230.63%, 251.28%, and 262.04% respectively.
4. Exergoeconomic analysis based on exergoeconomic parameter (Rex) of the system-B for 15, 20, 30, 50 years are 0.0312, 0.0344, 0.03746, and 0.03906 kWh/₹, respectively.

LIST OF CONTENTS

	Page No.
Declaration	ii
Certificate	iii
Dedication	iv
Acknowledgements	v
Abstract	vi
List of Contents	viii
List of Figures	xii
List of Tables	xiv
Nomenclature	xviii
CHAPTER 1 GENERAL INTRODUCTION	1-11
1.1 Introduction	1
1.2 What is distillation	5
1.2.1 Solar distillation	5
1.3 Material used in construction of solar still	7
1.4 Modes of heat transfer	7
1.4.1 Internal heat transfer	7
1.4.2 External heat transfer	7
1.5 Basic concept of solar distillation	8
1.6 Solar distiller quality of water	9
1.7 The parameters for solar distillation performance	9
1.8 Applications of distillate	10
CHAPTER 2 LITERATURE REVIEW	12-21
2.1 Historical background	12
2.2 Research gaps	18
2.3 Research objectives	18
2.4 Methodology to be adopted	19
2.5 The thesis plan	20
CHAPTER 3 METHODOLOGY	22-76
3.1 Energy and exergy analysis of active solar distiller unit (single and double slope)	22-46

3.1a	Energy and exergy analysis of 25% partially covered active solar distiller (single slope)	22-32
3.1a.1	System description	22
3.1a.2	Thermal modeling	28
3.1a.2.1	Governing equations of energy for various part of the distiller unit of active single slope (System-A)	28
3.1a.2.2	Procedure to be adopted	31
3.1b	Energy and exergy analysis of 25% incorporating PVT-CPC active solar distiller unit (double slope)	33-46
3.1b.1	System description	33
3.1b.2	Thermal modeling	38
3.1b.2.1	Governing equations of energy for various part of the distiller unit of active single slope (System-B)	39
3.1b.2.2	Procedure to be adopted	45
3.2	Energy matrices and life cycle cost analysis of 25% PVT incorporating N- CPC-HE active solar distiller unit (single and double	47-65
3.2a	Energy matrices and life cycle cost analysis of single slope solar distiller	47-55
3.2a.1	Analysis	47
3.2a.1.1	Energy analysis	47
3.2a.1.2	Exergy analysis	49
3.2a.2	Matrices analysis	51
3.2a.2.1	Payback time of energy (EPT)	51
3.2a.2.2	Payback factor of energy (EPF)	52
3.2.a.2. 3	Life cycle cost efficiency (LCCE)	52
3.2b	Energy matrices and life cycle cost analysis of active solar distiller	56-65
3.2b.1	Analysis	56
3.2b.1.1	Energy analysis	56
3.2b.1.2	Exergy analysis	59
3.2b.2	Energy matrices	61
3.2b.2.1	Payback time of energy (EPT)	61
3.2b.2.2	Production factor of energy (EPF)	61
3.2b.2.3	Life cycle cost efficiency (LCCE)	61

3.3	Enviroeconomic and exergoeconomic analysis of 25% partially covered (N-PVT-CPC-HE) active solar distillers (single and double slope)	65-76
3.3a	Economic analysis of 25% partially covered active solar distiller (single and double slope)	66-72
3.3a.1	Capital cost	66
3.3a.2	Lifetime of the system	66
3.3a.3	Salvage value	66
3.3a.4	Maintenance cost annually (AMC)	66
3.3a.5	Capital recovery factor (CRF)	67
3.3a.6	Shrinking fund factor (SFF)	67
3.3a.7	First annually cost obtained	67
3.3a.8	The total annual cost obtained	67
3.3a.9	Cost of distillate per kg obtained	67
3.3b	Environ-economic analysis 25% partially covered (N-PVT-CPC-HE) active solar distiller (single and double slope)	73-73
3.3b.1	CO ₂ Emission	73
3.3b.2	CO ₂ Mitigation	73
3.3b.3	Carbon credit earned	73
3.3c	Exergoeconomic analyses of 25% partly covered (N-PVT-CPC-HE) active solar distiller (single and double slope)	74-76
3.3c.1	Parameter (R_{ex}) is used to expressed the exergoeconomic	74
CHAPTER 4	RESULT AND DISCUSSION	77-111
4.1	Discussion on results	77
4.1a	Energy and exergy analyses of 25% incorporating PVT-CPC active solar distiller unit (single slope)	77-86
4.1b	Energy and exergy analysis of 25% partially covered N-PVT-CPC-DS-HE solar distiller unit (double slope)	86-97
4.2a	Energy matrices and life cycle cost analysis of active solar distiller (single slope)	97-101
4.2b	Energy matrices and life cycle cot analysis of active solar distiller (double slope)	101-105
4.3a	Economic analysis of 25% partly incorporating (N-PVT-CPC-HE) active solar distiller (single and double slope)	105-105

4.3b	Environ-economic analysis 25% partly incorporating (N-PVT-CPC-HE) active solar distiller (single and double slope)	105-108
4.3c	Exergo-economic analysis of 25% partly incorporating (N-PVT-CPC-HE) active solar distiller (single and double slope)	108-111
CHAPTER 5	CONCLUSIONS AND FUTURE SCOPE	112-114
5.1	Conclusion	112
5.2	Future scope	113
REFERENCES		115-125
APPENDIX		126-128
PUBLICATIONS		129
Bio – Data		130

LIST OF FIGURES

S. No.	Title	Page No.
Fig. 1.1	Water availability on earth's surface in percentage	2
Fig. 1.2	Need of fresh water in low income countries	3
Fig. 1.3	Need of fresh water in high income countries	4
Fig. 1.4	Overall need of fresh water in world	4
Fig. 1.5	Opened cycle distillation process	5
Fig. 1.6	Classification of solar distillation system	6
Fig. 3.1	Active single slope solar distiller incorporating 25% PVT with compound parabolic concentrator (N-PVT-CPC-SS-HE) system-A	23
Fig. 3.1a	View of helically coiled heat exchanger	24
Fig.3.1b	Sectioned view of 25% enclosed N-PVT-CPC	24
Fig. 3.1c	Cut section YY elevation of 25% covered N-PVT-CPC	25
Fig. 3.2	Active double slope solar distiller incorporating 25% PVT with flat plate collector (N-PVT-FPC-DS-HE)	31
Fig. 3.3	Flow chart to show the procedure adopted	32
Fig. 3.4	Active double slope solar distiller incorporating 25% PVT with compound parabolic concentrator (N-PVT-CPC-DS-HE) system-B.	35
Fig. 3.4a	View of helically coiled heat exchanger	35
Fig. 3.4b	Sectioned view of 25% enclosed N-PVT-CPC	36
Fig. 3.4c	Cut section YY elevation of 25% covered N-PVT-CPC	36
Fig. 3.5	Flow chart shows the methodology used	46
Fig. 4.1	Ambient temperature and solar radiation of typical day in May	77
Fig. 4.2	Per hour variation in temperature of basin water in °C for a-Type days	78
Fig. 4.3	Monthly variation in mean basin water temperature vs yield	79
Fig. 4.4	Hourly variation in collector outlet water temperature in °C month-wise in a-Type days	80
Fig. 4.5	Monthly variation in mean collector outlet water temperature vs yield	80
Fig. 4.6	Per hour variation of inside glass temperature month-wise in a -Type days	81
Fig. 4.7	per hour variation of temperatures (T_w , T_{gi} , T_{woN} , T_{cN} and T_a) in May for a-Type days	82
Fig. 4.8	Average thermal exergy vs T_w month wise	83
Fig. 4.9	Mean electrical exergy in kWh month-wise	84

Fig. 4.10	Monthly variation in average yield	85
Fig. 4.11	Comparative analysis of proposed and previous system [38]	86
Fig. 4.12	Per hour variation of solar radiation for New Delhi climatic conditions	88
Fig. 4.13	Per hour variation of ambient temperature in May for a-Type days	89
Fig. 4.14	Monthly variation in temperature of basin water	90
Fig. 4.15	Per month inside glass temperature variation in Eastside	91
Fig. 4.16	Per month inside glass temperature variation in Westside	91
Fig. 4.17	Monthly variation of heat energy (East side)	92
Fig. 4.18	Monthly variation of heat energy (West side)	93
Fig. 4.19	Monthly variation in heat transfer coefficient (east side)	94
Fig. 4.20	Monthly variation in heat transfer coefficient (west side)	94
Fig. 4.21	Mean electrical exergy	95
Fig. 4.22	Monthly average variation in thermal exergy	96
Fig. 4.23	Daily yield in kg of the proposed system	97
Fig. 4.24	Energy matrices observations for the proposed systems based on energy	99
Fig. 4.25	Energy matrices observations for the proposed systems based on exergy	100
Fig. 4.26	Economic observations for proposed system (system-A)	101
Fig. 4.27	Energy matrices observations for the proposed systems based on energy	103
Fig. 4.28	Energy matrices observations for the proposed systems based on exergy	103
Fig. 4.29	Economic observations for proposed system (system-A)	104
Fig. 4.30	Environ-economic analysis for 15 years	106
Fig. 4.31	Environ-economic analysis for 20 years	106
Fig. 4.32	Environ-economic analysis for 30 years	107
Fig. 4.33	Environ-economic analysis for 50 years	107
Fig. 4.34	Exergoeconomic analyses for 15 years	109
Fig. 4.35	Exergoeconomic analyses for 20 years	109
Fig. 4.36	Exergoeconomic analyses for 30 years	110
Fig. 4.37	Exergoeconomic analyses for 50 years	110

LIST OF TABLES

S. No.	Title	Page No.
Table 3.1	Parameters and specifications used in active solar distiller (single slope) N-PVT-CPC-SS-HE	25
Table 3.2	Thermophysical properties of CuO nanoparticles	27
Table 3.3	Average air velocity	27
Table 3.4	Different parameters used in calculations [22 and 41]	37
Table 3.5	Annual energy system-A (N-PVT-CPC-SS-HE)	47
Table 3.6a	Annual energy system-B (N-PVT-FPC-DS-HE) East side	48
Table 3.6b	Annual energy system-B (N-PVT-FPC-DS-HE) West side	48
Table 3.7	Daily, monthly and annually yield system-A (N-PVT-CPC-SS-HE)	49
Table 3.8	Daily, monthly and annually yield system-B (N-PVT-FPC-DS-HE)	49
Table 3.9	Per day, monthly and annum thermal exergy system-A (N-PVT-CPC-SS-HE)	50
Table 3.10	Per day, per month and per annum thermal exergy system-B (N-PVT-FPC-DS-HE)	50
Table 3.11	Annual thermal energy, annual thermal exergy and annual yield obtained from system-A (N-PVT-CPC-DS-HE) and system-B (N-PVT-FPC-DS-HE)	51
Table 3.12	Embodied energy of various components of system-A (N-PVT-CPC-SS-HE) and system-B (N-PVT-FPC-DS-HE)	52
Table 3.13	Embodied energy of various components of system-A (N-PVT-CPC-SS-HE) and system-B (N-PVT-CPC-DS-HE)	53
Table 3.14	Capital investment and cost of different components of system-A (N-PVT-CPC-SS-HE) and system-B (N-PVT-FPC-DS-HE)	53
Table 3.15	Capital investment and cost of different components of system-A (N-PVT-CPC-SS-HE) and system-B (N-PVT-CPC-DS-HE)	54
Table 3.16	Embodied energy (E_{in}), the conversion efficiency of the life cycle (LCCE), energy payback factor (EPF), and energy payback time for (N-PVT-FPC-DS-HE) and (N-PVT-CPC-SS-HE) for 30 years	54
Table 3.17	Embodied energy (E_{in}), the conversion efficiency of the life cycle (LCCE), energy payback factor (EPF), and energy payback time for (N-PVT-FPC-DS-HE) and (N-PVT-CPC-SS-HE) for 50 years	55

Table 3.18a	Annual energy system-A (N-PVT-CPC-DS-HE), Eastside	56
Table 3.18b	Annual energy system-A (N-PVT-CPC-DS-HE) west side	57
Table 3.19a	Annual energy system-B (N-PVT-FPC-DS-HE) East side	57
Table 3.19b	Annual energy system-B (N-PVT-FPC-DS-HE) West side	57
Table 3.20	Daily, monthly and annually yield system-A (N-PVT-CPC-DS-HE)	58
Table 3.21	Daily, monthly and annually yield system-B (N-PVT-FPC-DS-HE)	58
Table 3.22	Per day, monthly and annually thermal exergy of system-A (N-PVT-CPC-DS-HE)	59
Table 3.23	Per day, monthly and annually thermal exergy of system-B (N-PVT-FPC-DS-HE)	60
Table 3.24	Annual thermal energy, annual thermal exergy and annual yield obtained from system-A (N-PVT-CPC-DS-HE) and system-B (N-PVT-FPC-DS-HE)	60
Table 3.25	Embodied energy of different components of system (N-PVT-FPC-DS-HE) and system (N-PVT-CPC-DS-HE)	62
Table 3.26	Capital investment and cost of different components of flat plat double slope (N-PVT-FPC-DS-HE) and CPC double slope (N-PVT-CPC-DS-HE)	62
Table 3.27	Embodied energy (E_{in}), the conversion efficiency of the life cycle (LCCE), energy payback factor (EPF), and energy payback time for (N-PVT-FPC-DS-HE) and (N-PVT-CPC-DS-HE) for 30 years	63
Table 3.28	Embodied energy (E_{in}), the conversion efficiency of the life cycle (LCCE), energy payback factor (EPF), and energy payback time for (N-PVT-FPC-DS-HE) and (N-PVT-CPC-DS-HE) for 50 years	64
Table 3.29	Embodied energy (E_{in}), the conversion efficiency of the life cycle (LCCE), energy payback factor (EPF), and energy payback time for single slope (N-PVT-CPC-SS-HE) and double slope (N-PVT-CPC-DS-HE) for 30 years	64
Table 3.30	Embodied energy (E_{in}), the conversion efficiency of the life cycle (LCCE), energy payback factor (EPF), and energy payback time for single slope (N-PVT-CPC-SS-HE) and double slope (N-PVT-CPC-DS-HE) for 50 years	65
Table 3.31	Economic analysis of N-incorporating PVT-CPC active single slope	67

	solar distiller with helically coiled heat exchanger using CuO nanoparticles for 30 years	
Table 3.32	Economic analysis of N-incorporating PVT-CPC active single slope solar distiller with helically coiled heat exchanger using CuO nanoparticles for 50 years	68
Table 3.33	Economic analysis N-PVT-FPC collector active solar distiller (double slope) with helically coiled heat exchanger using CuO nanoparticles for 30 years	69
Table 3.34	Economic analysis N-PVT-FPC collector active solar distiller (double slope) with helically coiled heat exchanger using CuO nanoparticles for 50 years	69
Table 3.35	Economic analysis N-PVT-CPC collector active solar distiller (single slope) with helically coiled heat exchanger using CuO nanoparticles for 30 years	70
Table 3.36	Economic analysis N-PVT-CPC collector active solar distiller (double slope) with helically coiled heat exchanger using CuO nanoparticles for 50 years	71
Table 3.37	The total annual cost, factor of shrinking fund, and factor of capital recovery, and distillate cost\$/kg and ₹/kg for system-A (N-PVT-CPC-SS-HE), system-B (N-PVT-CPC-DS-HE), and system-C (N-PVT-CPC-DS-HE) for 30, 50 years	71
Table 3.38	The total annual cost, factor of shrinking fund, and factor of capital recovery, and distillate cost \$/kg and ₹/kg for system-A (N-PVT-CPC-SS-HE), system-B (N-PVT-CPC-DS-HE), and system-C (N-PVT-CPC-DS-HE) for 15, 20 years	72
Table 3.39	Exergoeconomic analyses of N-PVT-CPC collector active solar distiller (single slope) with a helically coiled heat exchanger using CuO nanoparticles for 30 years	74
Table 3.40	Exergoeconomic analyses of N-PVT-CPC collector active solar distiller (double slope) with a helically coiled heat exchanger using CuO nanoparticles for 30 years	74
Table 3.41	Exergoeconomic analyses of N-PVT-FPC collector active solar distiller (double slope) with a helically coiled heat exchanger using	75

	CuO nanoparticles for 30 years	
Table 3.42	Exergoeconomic analyses of N-PVT-CPC collector active solar distiller (single slope) with a helically coiled heat exchanger using CuO nanoparticles for 50 years	75
Table 3.43	Exergo-economic analyses of N-PVT-CPC collector active solar distiller (double slope) with a helically coiled heat exchanger using CuO nanoparticales for 50 years	75
Table 3.44	Exergo-economic analyses of N-PVT-FPC collector active solar distiller (double slope) with a helically coiled heat exchanger using CuO nanoparticales for 50 years	76
Table 4.1	Enhancement in the daily thermal energy and thermal exergy of proposed and previous systems using CuO nanaoparticles	86
Table 4.2	Enhancement in annual yield, obtained by proposed system and previous systems using CuO nanoparticles [ref.38]	87
Table 4.3	Enhancement in average daily yield, average thermal energy and average thermal exergy of proposed system over the previous research	97

NOMENCLATURE

A_b	Basin region in (m^2)
A_c	Under glazing region of collector in m^2
A_{gE}	East side glass cover area in m^2
A_{gW}	West side glass cover area in m^2
A_m	PVT area in m^2
a	Blue sky (clear days)
b	Hazy days
C_p	Heat nanoparticle (specific in J/kgK)
C_{bf}	Basefluid heat (specific in J/kgK)
C_{nf}	Heat nanofluid (specific in J/kgK)
D_i	Collector tube dia in m
d_p	Nanoparticle dia in nm
CPC	Compound parabolic concentrator
c	Partially foggy and unclear days
d	Fully unclear days
DS	Distiller unit with double slope
F'	Collector efficiency factor
h_i	Coefficient of heat transfer glazing and absorbing plate in $W/m^2 K$
h_o	Coefficient of heat transfer PVT to ambient in $W/m^2 K$
h_{pw}	Coefficient of heat transfer blackened plate to fluid in $W/m^2 K$
h_{bw}	Coefficient of heat transfer basin liner to water in $W/m^2 K$
h_{ba}	Coefficient of heat transfer basin liner to ambient in $W/m^2 K$
h_{CPC}	Coefficient of convective heat transfer, at CPC in $W/m^2 K$
h_{HE}	Coefficient of convective heat transfer, in heat exchanger in $W/m^2 K$
h_{rwgE}	Coefficient of radiant heat transfer water surface to inside of glass cover in east, $W/m^2 K$
h_{rwgW}	Coefficient of radiant heat transfer water surface to inside of glass cover in west, $W/m^2 K$
h_{cwgE}	Coefficient of convective heat transfer, surface water to inside glass cover in east, $W/m^2 K$
h_{cwgW}	Coefficient of heat transfer convective, water surface to inside of glass cover in west, $W/m^2 K$

h_{ewgE}	Coefficient of heat transfer evaporative, water surface to inside of glass cover in east $W/m^2 K$
h_{ewgW}	Coefficient of heat transfer evaporative, water surface to inside of glass cover in west $W/m^2 K$
h_{1gE}	Coefficient of total heat transfer in east $W/m^2 K$
h_{1gW}	Coefficient of total heat transfer in west $W/m^2 K$
h_{1wE}	Coefficient of total heat transfer amid fluid area and glass cover in east $W/m^2 K$
h_{1wW}	Coefficient of total heat transfer amid fluid area and glass cover in west $W/m^2 K$
I_b	Radiant energy falls on collector, W/m^2
I_{sE}	Radiant energy falls on glass cover in east, W/m^2
I_{sW}	Radiant energy falls on glass cover in west, W/m^2
K_g	Glass thermal conductivity, $W/m K$
K_i	Insulation thermal conductivity, $W/m K$
K_p	Absorption plate thermal conductivity, $W/m K$
k_p	Nanoparticle thermal conductivity, $W/m K$
K_{nf}	Nanoparticle thermal conductivity, $W/m K$
K_{bf}	Basefluid thermal conductivity, $W/m K$
L	Helical coiled heat exchanger length in (m)
L_c	Under glazing collector length in (m)
L_i	Insulation thickness in (m)
L_g	Glass cover thickness in (m)
L_m	PV module length in (m)
L_p	Absorption plate thickness in (m)
M_w	Mass of basin water in (k_g)
M_{ew}	Per annum water generation in (k_g)
m_f	Flow rate of water, (K_g/s)
PVT	Photovoltaic thermal
PF ₁	Penalty factor by glass cover module
PF ₂	Penalty element with a suction plate under the module
PF ₃	Penalty element with a suction plate on the polished assignment
PF _c	Penalty factor by glass covers to glazed portion
P_{gi}	Partially pressure of saturated vapor of glass cover in N/m^2

r_{11}	Outside dia of helical coiled heat exchanger in (m)
r_{22}	Inside dia of the helical coiled heat exchanger in (m)
T_{giE}	Temperature inside glass cover of solar distiller in east ($^{\circ}C$)
T_{giW}	Temperature of inner glass cover of solar distiller in west ($^{\circ}C$)
T_{goE}	Temperature outside glass cover of solar distiller in east ($^{\circ}C$)
T_{goW}	Temperature of outside glass cover of solar distiller in west ($^{\circ}C$)
N-PVT-CPC-DS N^{th} serially connected PVT-CPC double slope solar distiller unit	
Q_{uN}	Usable heat to N alike partly covered PVT-CPC in (kWh)
R	Reflectivity
r	Fraction of per day diffused to per day total radiation
T_a	Ambient temperature in ($^{\circ}C$)
T_c	Solar cell temperature in ($^{\circ}C$)
T_{cN}	Average solar cell temperature in ($^{\circ}C$)
T_{wi}	Input water temperature of collector in ($^{\circ}C$)
T_{bf}	Temperature of basefluid in collector in ($^{\circ}C$)
T_{woN}	Output water temperature of collector in ($^{\circ}C$)
T_{nf}	Nanoparticle temperature in ($^{\circ}C$)
T_p	Temperature of absorption plate in ($^{\circ}C$)
T_s	Temperature of sun in ($^{\circ}C$)
T_v	Vapor temperature in ($^{\circ}C$)
T_w	Temperature in basin water in ($^{\circ}C$)
T_{wo}	Temperature of water in $^{\circ}C$ at $t = 0$
ΔT_{DSSS}	Temperature difference amid nanoparticle to basefluid in distiller unit, ($^{\circ}C$)
ΔT_{CPC}	Temperature difference amid nanoparticle to base fluid at the output of PVT collector, in ($^{\circ}C$)
ΔT_{HE}	Temperature difference amid nanoparticle to base fluid in heat exchanger, in ($^{\circ}C$)
ΔT	Temperature difference amid T_w , in $^{\circ}C$ and $\frac{T_{giE}}{T_{giW}}$, in h
U_{tca}	Total heat transfer coefficient, cell to ambient in ($W/m^2 K$)
U_{tpa}	Total heat transfer coefficient, suction plate to ambient in ($W/m^2 K$)
U_{lm}	Total heat transfer coefficient, PV module to ambient in ($W/m^2 K$)
U_{lc}	Total heat transfer coefficient, glazing to ambient in ($W/m^2 K$)
U_{ga}	Coefficient of total heat transfer, condensing cover to ambient in ($W/m^2 K$)

U_{ba}	Total heat transfer coefficient, base liner to ambient in ($W/m^2 K$)
U_{gaE}	Total heat transfer coefficient, condensing cover of east side to ambient in ($W/m^2 K$)
U_{gaW}	Total heat transfer coefficient, condensing cover of west side to ambient in ($W/m^2 K$)
$U_{tc,p}$	Total heat transfer coefficient, cell to absorption plate in ($W/m^2 K$)
X	Characteristic length of solar distiller unit, in (m)

Greek Letter's

α_g	Condensing cover absorbed solar radiation
α_b	Basin surface absorbed solar radiation
α_f	Water absorbed solar radiation
α_c	Solar cell absorbed solar radiation
τ_g	Top glass cover transmitted solar radiation
\emptyset_g	Volume fraction of NPs in (%)
η_g	Collector efficiency in (%)
β	Packing factor
β_p	Coefficient of thermal expansion of nanoparticle, in (K^{-1})
β_{nf}	Coefficient of thermal expansion of nanofluid, in (K^{-1})
β_{bf}	Coefficient of thermal expansion of basefluid, in (K^{-1})
μ_{bf}	Basefluid dynamic viscosity, in (Ns/m^2)
μ_{nf}	Nanofluid dynamic viscosity, in (Ns/m^2)
ρ_p	Nanoparticle density, in (Kg/m^3)
ρ_{nf}	Nanofluid density, in (Kg/m^3)
ρ_{bf}	Basefluid density, in (Kg/m^3)
β	Packing factor
τ_g	Solar energy fraction transmitted from top glass cover of PVT-CPC collector

Subscripts

a	Ambient air
b	Basin area
v	Vapour
g_i	Inside condensing cover
g_o	Outside condensing cover
w	Water (fluid)

p	Particles
th	Thermal
sol	Solar
W	Western side
ann	Per annum
ex	Exergy
en	Energy
a_n	Annual
E	East side
E_{in}	Input embodied energy
E_{out}	Output embodied energy
E_{sol}	Annual solar energy
f	Fluid
i	Rate of interest
n	Life time period

Abbreviation

AMC	Maintenance cost annually
ASC	Salvage cost annually
BF	Basefluid
CRF	Capital recovery factor
C	Per liter yield price
CM	Carbon dioxide mitigation
CPC	Compound parabolic concentrator
DS	Double slope solar distiller unit
DSSS	Solar distiller unit of double slope
EPT	Payback time of energy
EPF	Payback factor of energy
FAC	Fixed annual cost
FPC	Collector, flat plate
HE	Heat exchanger
HTC	Factor of heat transfer coefficient
LCCE	Efficiency of life cycle conversion

NPs	Nanoparticles
NF	Mixture of nanoparticle and glycol
N-PVT-CPC-DS-HE	N^{th} identical photovoltaic thermal compound parabolic concentrator collector double slope with helical coiled heat exchanger
PCC	Primary capital cost
PVT	Photovoltaic thermal
R	Reflectors
SFF	Shrinking fund factor
S	Value of future salvage
TAC	Total annual cost

GENERAL INTRODUCTION

1.1 Introduction

Solar distillation by using solar still to get potable water through the closed natural hydrological cycle is a process that uses solar energy. Hence, government needs to pay more attention to it. The use of solar energy rises day by day for desalination purposes. This could be the best substitute to overcome the scarcity of water up to a great extent. Any living thing on earth is possible due to water, whether plants, animals, and human beings. Potable water is in dire need by human for the functioning of body cells. Shortage of water in human body may cause dehydration. Availability of water on earth is huge, but it is very less as far as potable water is concerned. Earth surface is covered with water about 67%. Out of total water availability, 97% is in sea, and lakes that are not pure water have 35000 to 45000 ppm and have lots of impurities. According to World Health Organization (WHO) only 1000 ppm of salinity water can be consumed by human body. The rest is more than 2% of pure water in glaciers, and 0.97% is potable. Fig.1 represents the existence of water locations on earth's surface. As per United Nations (UN), more than two billion face problems accessing drinking water [1].

Scarcity of potable water will be faced by 67% of the world's population by 2025. Later it was concluded that the available water quality is poor and will not be potable. There are many methods available to purify the water, but solar distillation is eco-friendly, low cost, renewable and easy in operation technology to purify the water.

First, the world population is being multiplied rapidly; therefore, water resources have to be grown accordingly. Second, the rise in population with factors like urbanization and

industrialization will increase demand for potable water. If demand for potable water is not fulfilled, it will negatively impact human health and the environment.

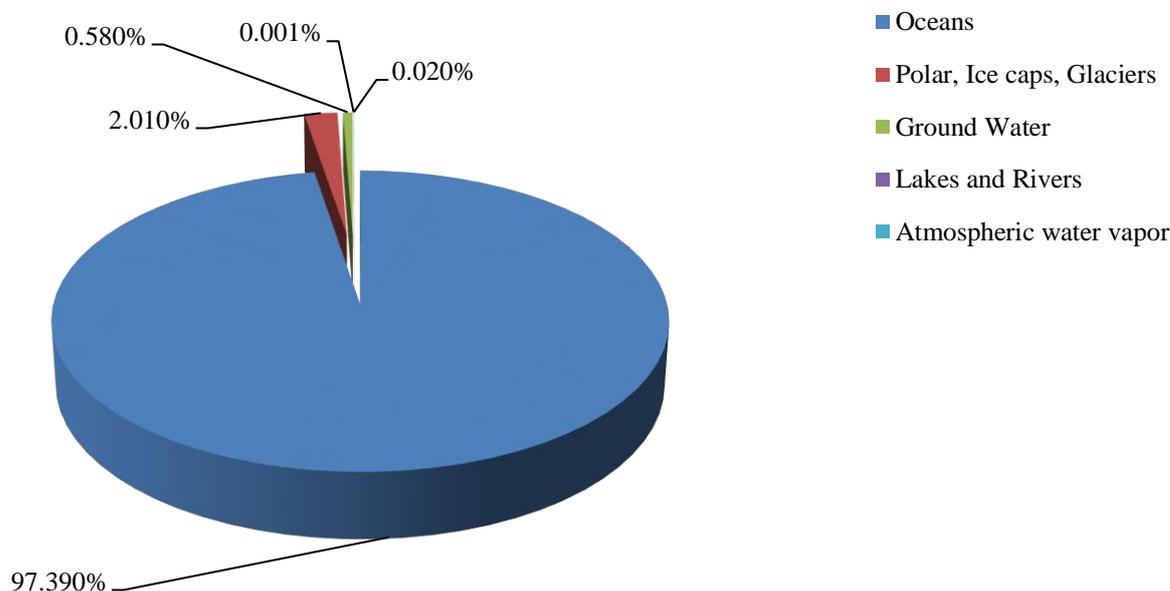


Fig. 1.1 Water availability on earth's surface [1]

As per UNICEF [1] report, every sixth person will be unable to access potable water and face lack of water for sanitation. In [2] WHO reported 443 school days missed annually [UNDP (2006)] due to water enduring diseases in this world. Scarcity of potable water is being faced in several places of India, most of the rural and costal zones. Approx. 60 to 70% of rural areas residents of developing countries face problems with potable water. Due to the use of contaminated water, there is a risk of related diseases.

Water crisis has been found by the World Water Vision Report [3]. The main cause of water shortage is not less water but poor water management. As a result, people and the environment have to bear it. Before the worst situation, there is need to take corrective measures. There is a need to make people aware of the limitation of fresh water sources and realize its need to be protected in terms of quality and quantity. Second World Water Forum's

key message is that “water is everyone’s business”. Water agenda must be in on high priority in decision maker’s list. Human rights permit everybody to take adequate water for domestic and potable use. Adequate amount of water is required to prevent dehydration and other water risk diseases. Moreover, the water sources are gradually reducing due to industrial waste contamination. It is the policy maker’s responsibility to make a policy to overcome the problem of water.

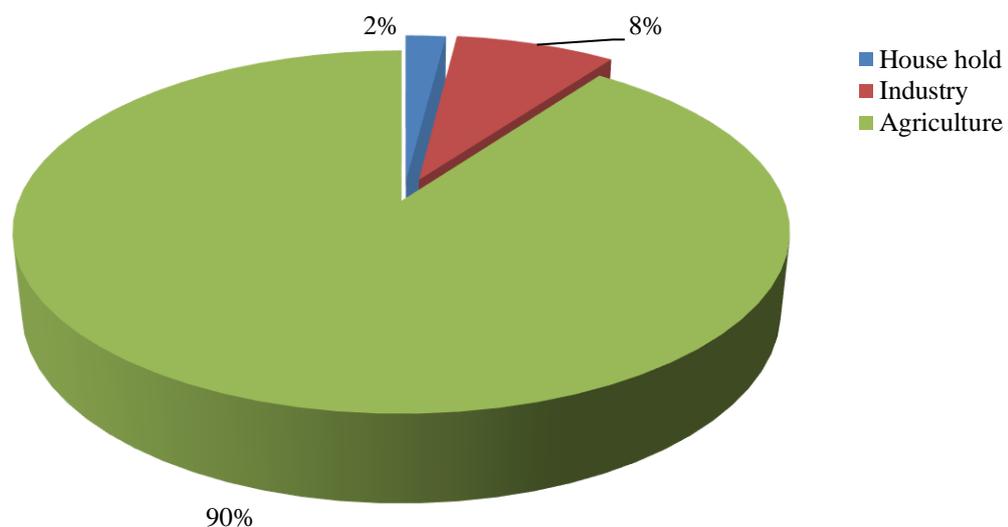


Fig. 1.2 Need for fresh water in low income countries [3]

Countries have varying levels of fresh water resources and the prime areas of fresh water requirement are domestic, industrial and agriculture. Fig. 1.2 and Fig. 1.3 show the water requirement according to countries' incomes.

The distilled water filters micro-nutrients and essential minerals from water necessary to the human body, but purity favors the human body. It is needed to eliminate harmful minerals and deduces toxicity in waste water, but limitation of distillation methods is chlorine and fluorine are also evaporated when steam produces. Solar distillation is used prevailing because of low temperature evaporation to overcome this problem. At places where brackish

water is present, the water demand is low. In a place where hot climatic conditions are present throughout the years, the rainfall is less than 50 cm in a year, transportation cost is high, and purification through solar distillation is useful in producing potable water in such places.

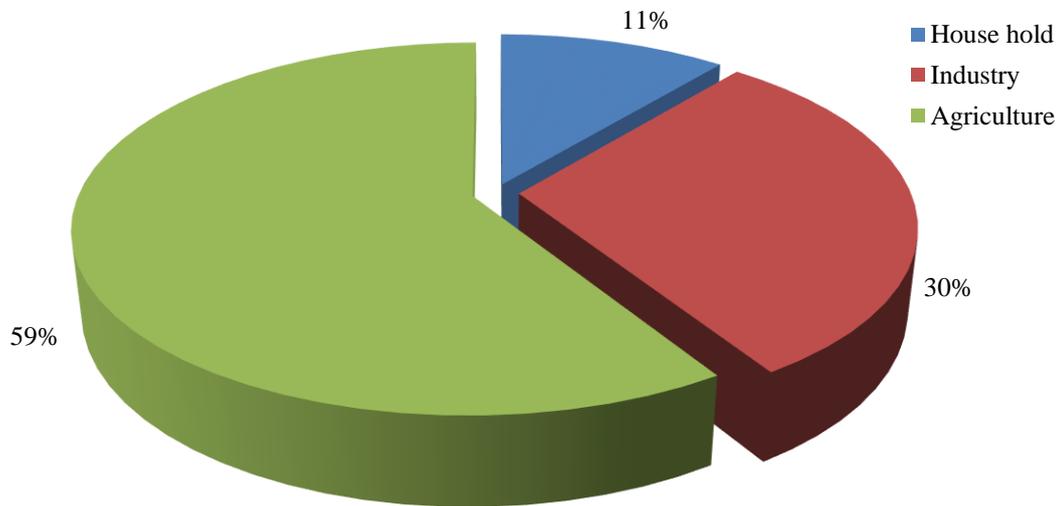


Fig. 1.3 Need for fresh water in high income countries [3]

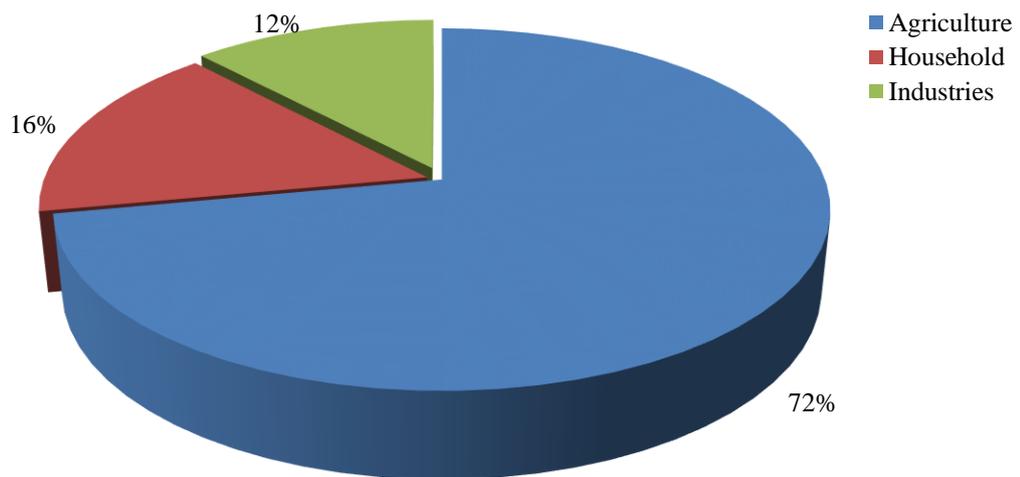


Fig. 1.4 Overall need for fresh water in world [3]

1.2 What is distillation?

Distillation is the process of purifying the liquid to separate the substances by condensation and boiling. When the heat energy is fed to liquids/ water, it gets vaporized. Later the vapor is condensed and forms distillate Fig. 1.5 shows an open cycle.

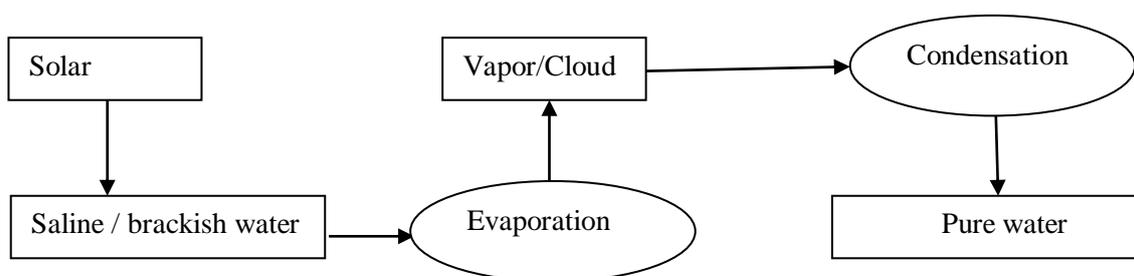


Fig. 1.5 Opened cycle distillation process

1.2.1 Solar distillation

Distillation process is due to solar radiation is called solar distillation. It is a natural process with the help of solar energy in closed cycle. Further, solar distillation can be classified as;

- (i) Passive solar distillation process
- (ii) Active solar distillation process

In passive solar distillation process, the brackish water is directly fed to basin without the help of external sources, while in active solar distillation process secondary source is provided to feed the water. This additional heat energy increases evaporation rates. Secondary sources of heat addition include the collector, concentrators, etc., further classified as single and double slope solar distiller units based on structure and positioning. To get maximum amount of solar energy, the orientation of single slope is southern facing and double slope is east-west facing. Fig. 1.6 represents complete classifications. Further passive solar distiller can be divided into symmetrical and unsymmetrical types. Glass cover inclination matters in the symmetric or unsymmetric distiller unit. Active solar distiller unit can further be divided into two types high

temperature and nocturnal and high temperature can further be divided into two parts auxiliary and heating by collectors. Heating by collectors is again divided into three parts that are flat plate collector (FPC), compound parabolic concentrator (CPC), and evacuated tube collector (ETC).

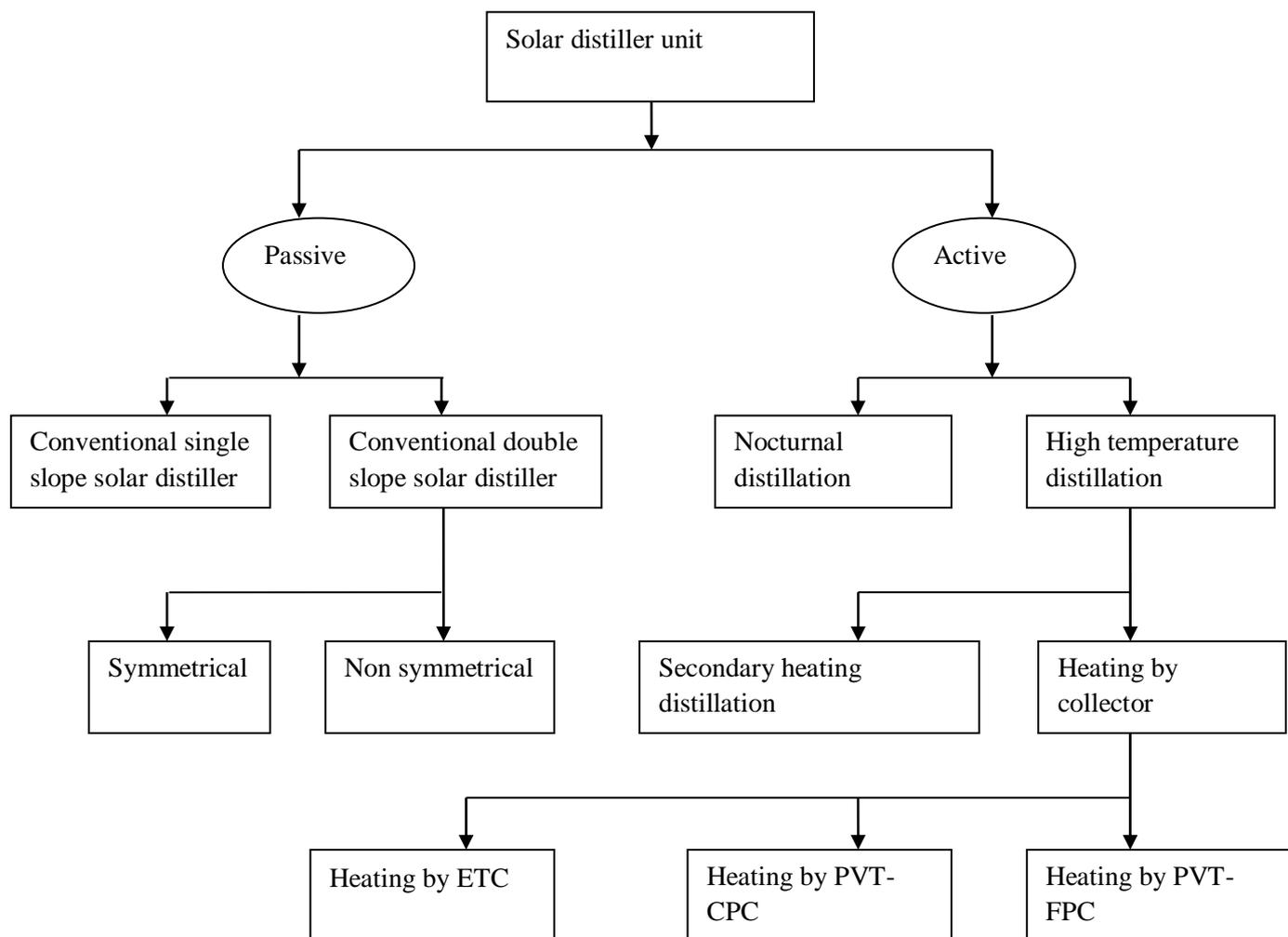


Fig. 1.6 Classification of solar distillation system

To develop self sustainable system flat plate collector (FPC) is used with fully or partly covered surface. Later on, flat plate collector can be attached compound parabolic concentrator while flat plate of PVT is alone used for electricity generation by converting thermal into electrical energy. This electrical energy is mainly used to run the pump and remaining for other

work. Recent research focuses on active solar distiller single and double slope with a helically coiled heat exchanger attached with N-incorporating photovoltaic compound parabolic concentrator collectors (N-PVT-CPC).

1.3 Construction material of solar still

Fabrication of solar distiller is very simple even local material can be used to construct. However, the good quality material will raise the cost of distiller. The material used must be strong against wind and minor earthquakes. It should not be toxic, encourage different tastes at temperature rise and vapor released. It should be compact to easily be carried by local transport and should have corrosive resistance to saline water.

Condensation must be occurred film wise on the glass covers because drop-wise condensation reduces the intensity of solar radiant energy. The following materials can be used to construct a solar distiller unit: fiber reinforced plastic, G. I. sheet, concrete and top cover materials like glass and plastic.

1.4 Mode of heat transfer

Heat transfer modes in active single and double slope solar distiller incorporating photovoltaic thermal are conduction, convection, radiation, and evaporation, which further can be categorized as internal and external heat transfer.

1.4.1 Internal heat transfer mode

Inside solar distiller heat transfer from condensing cover to water surface occurs by radiation, evaporation, and convection.

1.4.2 External heat transfer mode

In solar distiller, the external heat transfer occurs by convection and radiation from top.

The heat transfer from sides, and bottom, occurs in environment by convection and conduction.

1.5 Basic concept of solar distillation

Greenhouse effect is basic principle of condensation/evaporation of water. To obtain potable water, with the help of solar distiller the source of heat energy is solar radiation. Fig. 3.1 shows the schematic diagram of conventional single slope active solar distiller. The box is constructed of fiber reinforced plastic (FRP), G. I. sheet, wood/concrete coated with insulated materials, which reduce heat from sides and bottom wall. Top of the box is closed with glass cover, which is inclined to trick down the condensed water. Due to gravitational force, the condensed water moves down to inner surface and is collected into a jar. The blackened bottom surface absorbs almost all the radiation falling on the box. This blackened bottom surface is known as basin liner.

Solar radiation fall son glass cover after transmittance, significant portion is absorbed in basin water. The small amount of radiant energy approaching the water surface gets back, and the blackened surface mostly absorbs the rest. The reduction of solar radiant energy in water depth depends on absorptivity and depth which basin liner temperature increases. Later by convection, most of it's heat transmit to water mass, and very small part is lost to environment by conduction. Therefore, temperature difference amid glass and water surfaces increases because water temperature increases. The water mass evaporates and undergoes film-wise condensation on inner surface of glass by releasing latent heat. The condensed water trickles down into jar and emanates out for further use. The distillate obtained is not fit directly for drinking, but it will be suitable for drinking and cooking after adding the minerals.

The per day production from single slope passive distiller unit varies from 0.5 kg/m² to 2.5 kg/m², single slope solar distiller thermal efficiency from 5 to 40% in a year.

The merits of solar distiller unit over other distiller technologies are as follows.

- i. There is no moving part in passive solar distiller.
- ii. It is cheap and easy technology for providing potable water.
- iii. It is renewable and non-polluted for its operation.
- iv. Unskilled or semi-skilled labor can operate it.
- v. Can repair and manufacture locally.
- vi. This system is very useful areas where brackish/saline water is available.
- vii. Self-sustainability emphasizes more and photovoltaic thermal module can generate excess electricity to requirement.
- viii. It is easy to use and more satisfying unit as water treatment plant.

Moreover, a system has merits and demerits that make technology limited for mass production. It is included the following (a) weather dependent unit, (b) large solar collection area is needed for commercial purpose, (c) less interest of investors, (d) low performance, (e) initially higher investment (f) continuous feeding and flashing is needed and (g) robust system are needed for open system.

1.6 Solar distiller quality of water

The water quality, i.e., taste, depends on the pH value. In solar distillation processes, the pH value of water does not change. Therefore, water taste is very good as water does not get boiled. Solar distilled water is purest form and does not contain biological elements and salt. Harmful bacteria and arsenic are also removed during solar distillation. EI Paso Energy Association (EPSEA) works on distillate water and found it beneficial for health. It means water created by solar distillation is more pure and free from impurities.

1.7 Parameters for solar distillation performance

The performance parameters for solar distiller are; water temperature, condensing cover temperature, heat transfer coefficient; radiation receives by glazing, yield etc. Moreover, the

flow of condensate does not affect the trickled water. However, need to clean the glass cover regularly. Hence, the film-wise condensation will occur automatically. The glass cover slope slightly matters because of the following reasons.

- i. More material is needed to cover if slope angle increases for give basin area.
- ii. The volume and mass of solar still will increase due to increase in slope.
- iii. A high amount of air will enter and reduce system performance in volume.

The lower condensing covers temperature and higher water temperature result in higher yield. For higher yield, the vapor leakage should be lower and heat transfer from side and bottom should also be low, resulting in increased yield. Large solar radiation absorbed means higher water temperature. For good radiation absorbing basin, liner is needed for lower absorption glazing. Low water depth is also one option to increase water temperature.

1.8 Applications of distillate

Solar energy is freely available and no need to pay a single penny. However, investment in fabrication of distiller unit makes the cost of distilled water and requirement of large area. That is why large-scale production is not economical, such as domestic supply, industrial use, agriculture purposes, etc. Therefore it is used only to purify water for domestic use and for some laboratory and greenhouse applications.

The solar distilled water can be utilized for drinking, bathing, washing, cooking purposes, laboratory for analytical purposes, and in hospitals for sterilization uses. It can also be used for maintenance of telephone exchange in battery. It can also be used in agriculture, industry for different purposes.

It is not an attractive economy but can be used for salt recovery. From sewage, recovery of potable water may be possible, but some odorous gases may evaporate, condensed, and mixed with distillate. The production of alcohol can also be played a role in solar distillation.

LITERATURE REVIEW

2.1 Historical background

Solar distillation is the process that uses solar energy and a device known as solar still to get the fresh water that can be used for drinking after mixing some minerals. The potable water obtained from solar still can be directly used for other purposes like agriculture, industry etc. Mouchot [4] was the first solar distiller unit documented in the 16th century by Arab alchemist. Della porta [5] invented earthen pots, this pot was used to heat the water to get evaporation and finally, condensation took place and water was collected into containers. Colebrook [6] studied a particular transition area amid smooth and rough surfaces for turbulent flow. Soliman [7] recommended the concept of feeding external heat energy input from solar collector into the basin. Rai and Tiwari [8] analyzed the flow rate effects with a sole basin solar distiller unit attached to flat plate collector and observed a yield increase 24%. Zaki et al. [9] observed that an active solar distiller produces 33% higher yield than conventional unit. Lawrence and Tiwari [10] calculated active solar distiller in natural type with heat exchanging to extend empirical formulas. Collector addition increases the water temperature, which improves the system's efficiency. Overall, increasing water depth decreases efficiency. Popiel and Wojtkowiak [11] developed the formulas for the thermophysical properties of water at 0 to 150°C like specific heat, latent heat, saturated vapor etc., and calculated heat transfer to heat exchanger. Pak and Cho [12] studied hydrodynamic heat transfer of dispersed fluid using oxides. Kumar and Tiwari [13] have optimized the active double slope solar distiller unit and got the highest water generation at a 1.8 m/s flow rate using theoretical model. The effects of water depth, basin area, and collector area are considered. Tiwari. [14] used solar energy fundamentals to design, model, and applications with economic aspects for solar desalination and presented numerous applications, such as water distillation, water heating, and biogas

digestion. Delyannis et al. [15] studied the historical developments of solar desalination while taking care of energy and the environment. Tiwari et al. [16] reviewed the gradual development of solar distillation systems, such as the availability of potable water, purification methods, and water demand. Boukar and Harmim [17] explained the one-sided vertical solar distiller for the climatic conditions of Algeria and found the yield 0.275 to 1.31 kg/m², overall efficiency 7.85 to 21.19% and energy varies 8.42 to 14.71 MJ. Tiwari and Tiwari [18] discussed water scarcity and possible solar distiller solutions. Fundamentals of thermal modeling, design effects, passive and active solar distillers are covered. Barden [19] experimentally studied the single slope for different parameters and found productivity 51% greater during day and 16% greater at night also concluded that reducing water depth will increase yield. Hwang et al. [20] studied experimentally and showed that water-based nanofluid in a rectangular cavity is more stable than water. Ho et al. [21] analyzed thermal conductivity and viscosity uncertainties in a square enclosure of natural convection. Dubey and Tiwari [22] analyzed the thermal exergy, energy, and weather conditions for different cities like Jodhpur, New Delhi, Mumbai etc. Research evaluated carbon credit earned for hybrid solar distiller systems. Dev and Tiwari [23] linear and nonlinear characteristic equations were developed for different inclined angle and depth of water. It was concluded that the lower depth gives better efficiency for passive still. Otanicar and Golden [24] analyzed the enviroeconomic aspect of solar collectors using nanofluid and found it neutralizes 74 kg for 15 years. Singh et al. [25] investigated entropy generation of Al₂O₃-water nanofluids theoretically and developed equations to predict micro channel and conventional channel. Dev and Tiwari [26] analyzed linear and nonlinear curves for active solar still and observed that the performance of nonlinear equations is better than linear equations. Gaur and Tiwari [27] analyzed the maximum yield for four (N=4) collectors and 50 kg mass of fluid in solar distiller unit. Patel et al. [28] investigated enhancement experimentally in thermal conductivity with

metallic and oxide nanofluids. Sharma et al. [29] developed turbulent flow and found heat transfer coefficients of water-based nanofluids to predict friction in forced convection. Dev et al. [30-32] developed characteristic equations for active and passive solar distiller units. In an active solar distiller unit, solar energy is fed to water as external thermal energy, and water is pumped mechanically in forced mode by using solar energy with the help of photovoltaic technology to improve the passive solar distiller. Khanafer and Vafai [33] studied the impacts of thermal conductivity and viscosity on yield and developed correlations. Elzen et al. [34] estimated to lead 11 to 14% reduction in baseline emissions 12 to 18% low. The global abate cost was estimated 60 to 100 billion \$. Khullar and Tyagi [35] analyzed and reported emissions of 103kg approx./household/year reduced for a solar heating device for nanofluids. Clean energy can help to reduce greenhouse effect. Balan et al. [36] review on passive solar distillation included history and modes important to heat transfer and analyzed various designs. Yiamsawasd et al. [37] studied the effects of nanofluid specific heat in desalination process. Dispersion of TiO_2 and Al_2O_3 was noticed with concentration of 0 to 8 volume % between temperatures of 15 to 65°C as specific heat lower with temperature increased. Faizel et al. [38] analyzed the flat plate collector (FPC) cost using tin oxide, copper oxide, titanium oxide, and aluminum oxide nanofluids. Performance of CuO nanofluid is better credited to its high density, low specific heat, and thermal conductivity. Liu et al. [39] have evaluated the economic analysis of the integrated solar distiller unit of the evacuated tube. Mathematical model was developed and cost analysis was done. Khairul et al. [40] theoretically investigated CuO, Al_2O_3 , ZnO water-loaded nanofluids. Application of nanofluids increases heat transfer coefficient and entropy decreases. Mahian et al. [41] examined solar collector performance based on the micro-channel using CuO, Al_2O_3 , TiO_2 , and SiO_2 nanofluids. Collector outlet temperature follows the order: $CuO > Al_2O_3 > TiO_2 > SiO_2$. Mahian et al. [42] studied water aluminum oxide nanofluids in the solar collector and various thermo-physical models to find

entropy. Kabeel et al. [43] analyzed a vacuum fan solo inclined solar distiller using water-based (Al_2O_3) nanofluids. Mahian et al. [44] analyzed pressure drop effect of heat transfer, pH via, and generation of entropy in a solar collector using SiO_2 /water nanofluids. Shyam et al. [45] developed an expression for connected N-PVT-water collectors for temperature-dependent electrical efficiency of two different configurations in series that gives almost the same outcomes. Atheaya et al. [46] developed mathematical expression for a partly roofed PVT compound parabolic concentrator (CPC). Sekhar and Sharma [47] also studied specific heat, viscosity for Al_2O_3 , ZnO nanofluids. Elango et al. [48] determined performance of single slope solar distiller based on exergy and productivity using nanofluids. Omara et al. [49] performed on corrugated wick type and simple solar distiller unit using nanofluids. Tiwari et al. [50] performed no. of experiments on active solar distiller for the exergoeconomic and enviroeconomic parameters using water-based nanofluid. Sharon and Reddy [51] analyzed the annual economics of an active solar distiller loaded with saline water. Sahota et al. [52] analyzed active double slope solar distiller unit performance using nanofluids. Aluminum oxide-based nanofluid gives better performance than others. Singh et al. [53] analyzed energy matrices and life cycle cost analysis of single and double conventional distiller units and found 0.144 and 0.137 per unit cost, respectively. Sahota and Tiwari [54] analyzed performance of double slope passive solar distiller using nanofluids. Energy and exergy efficiency is better with Al_2O_3 than CuO and TiO_2 ; however, productivity was greater with CuO . Singh and Tiwari [55] analyzed the energy matrices, life cycle cost conversion efficiency of an active partly PVT-CPC solar distiller. Annual yield 5%, EPF 12.73%, and LCCE 22.22% were higher than the prior 0.019m. Shyam et al. [56] evaluated N-photovoltaic thermal (PVT) water collectors partially covered by a photovoltaic module connected in series. Mwesigye et al. [57] used Monte-Carlo ray tracing method to analyze effect of CuO nanofluid. It gives greater yield for passive double slope solar distiller units. Tripathi and Tiwari [58] studied the comparison

between N-PVT-FPC and N-PVT-CPC solar distiller and found that at 25% PV, the thermal exergy, energy, 13.67kWh and 150.45 kWh. [59] MathWorks Inc., MATLAB-R2016a (9.0.0.341360). Menbari et al. [60] analyzed heat transfer on direct absorption concentrating collector using CuO-water nanofluid. Tiwari and Sahota [61] reviewed the energy efficiency and economics of different (passive and active) solar distiller units. Sahota and Tiwari [62] found maximum evaporative heat transfer coefficient (HTCs), which gives high rate of yield compared to the other distiller units and developed characteristic curve for nanofluid based distillation system (N-PVT-FPC-DS-HE). Sahota et al. [63] analyzed environoeconomic and exergoeconomic for passive double slope solar distiller using water-loaded nanofluid (CuO, Al₂O₃, TiO₂) and found payback time of energy is low. Sahota and Tiwari [64] analyzed exergoeconomic and environoeconomic with or without heat exchanger double slope solar distiller unit loaded using nanofluid and found CuO > Al₂O₃> TiO₂ performance in a given order. Chen et al. [65] found good stability of weak luminous with nanofluid in solar distiller unit. Mahian et al. [66] found that the heat exchanger was not noteworthy at a temperature lower than 50°C, and yield was two times greater than without a heat exchanger. Singh and Tiwari [67] noticed augmentation in energy matrices of N-PVT-FPC partly double slope solar distiller. Saleha et al. [68] analyzed the effect of solvent ZnO and found it effective in solar distiller units. Shashir et al. [69] analyzed the performance of nanoparticles like copper oxide and graphite micro-flakes on solar distiller units with different cooling of toughened glass cover. Tiwari and Sahota [70] made thermal modeling the advanced solar distiller. Joshi and Tiwari [71] analyzed a single slope N identical PVT-CPC and single slope FPC solar distiller. Daily yield with FPC was 37.9 kg and with CPC, electricity was found 13% higher. Singh et al. [72] reviewed active solar distillation systems using nanofluids. It is focused on advancement of nanofluids to solar distillation. Singh et al. [73] analyzed for single slope partly covered PVT-FPC system for various efficiencies and depth of water under optimized conditions. Singh

et al. [74] investigated single slope distiller unit of partly covered PVT flat plate collector at different water depths for efficiency and productivity. Dharamveer et al. [75] reviewed nanofluids with an active solar distiller unit. It is concluded that nanofluids reduce pump work by reducing viscosity and increasing water output. Prasad et al. [76] analyzed N-PVT-CPC system using one at a time technique (OAT). Power increases with increasing flow rate and depth of water analyzed from 0.07 to 0.14m. Ahmed et al. [77] studied for energy and exergy of a flat-plate collector (FPC) solar distiller using MWCNT/water nanofluid with thermosiphon forced-circulation mode. Singh et al. [78] estimated energy payback time for N identical compound parabolic concentrator collector of the single-slope without nanofluid. Singh et al. [79] observed that exergoeconomic parameter decrease with the mass flow rate increase. Dharamveer and Samsheer [80] evaluated energy matrices and enviroeconomics for active and passive solar distiller units. Improved distillate performance 119%, embodied energy 5602.94 kWh, and carbon reduction 102% for 30 years were noticed. Sharma et al. [81] discussed double slope evacuated tube collector with and without CPC. Instantaneous energy and exergy efficiency were 46.18, and 56.99% and 81.27 and 92.25% for respective systems. Sharma et al. [82] theoretically investigated double slope solar distiller unit with parabolic concentrator collector (CPC) and evacuated tube collector (ETC). Based on thermal exergy, the energy payback is 88.5% low and based on LCCE, 51.93% high and daily exergy 78.01% high. Dhivagar et al. [83] analyzed grate crude shrewd heat storage single slope solar still energy, exergy, and economic assessment. Gupta et al. [84] discussed the performance of fully covered N = 6 CPC collectors and developed characteristic equations. Performance of four systems was evaluated and found instantaneous efficiency higher. Zhang et al.[85] presented sustainable clean technology focused on utilizing green energy. Arora et al. [86] studied incorporating carbon nanotubes using N-PVT-CPC solar distiller double slope and found 46.4%, 46.7%, 76.7% enhancement in heat transfer coefficients and yield 65.7% and 28.1% higher

respectively for MWCNT. Bharti et al. [87] analyzed sensitivity on N alike double slope solar distiller with photovoltaic thermal (PVT) flat plate collectors (FPC). Electricity increased 29.63% yield and EPO was found 0.303 and 0.992, respectively.

2.2 Research gaps

The extant literature survey shows that many works have been done on solar distiller units (active and Passive). However, not much literature is available on analyzing an active solar distiller loaded with nanofluids based water. Only double slope solar distiller incorporating with flat plate collector (FPC) using water loaded nanofluids has been analyzed so far. Analysis of single slope solar distiller integrated with flat plate collector (FPC) having nanofluids based water loaded nanofluid has not been reported by any researchers.

Further, any researchers have not analyzed single and double slope solar distiller incorporating compound parabolic concentrator/evacuated tubular collectors loaded with nanofluid-based water. Hence, the proposed research will analyze single and double slope solar distiller unit integrated with compound parabolic concentrator collector and loaded with nanofluid based water. Solar desalination systems will be analyzed in terms of energy metrics, exergoeconomic parameter, enviroeconomic parameters, various efficiencies and productivity. The results of analysis of proposed system will also be compared with results of earlier researchers.

2.3 Research objectives

Based on the research gaps in the literature, the following objectives of the present study have been framed:

- i. Energy and exergy analysis of active solar distiller using nanofluid based water
- ii. Energy matrices of active solar stills using nanofluid
- iii. Efficiencies of active solar stills using nanofluid
- iv. Life cycle cost analysis of an active solar distiller using nanofluid

- v. Environoeconomic and exergoeconomic analysis of active solar distiller using nanofluid

2.4 Methodology to be adopted

The methodology is adopted to carry out the study of the proposed system follows the following steps:

Step-I

Firstly Lui and Jordon formulae for beam solar radiation (I_b) and global irradiation (I_s) is used to calculate proposed systems for the annual. Further calculate per day radiant energy with number of days according to clear, hazy, hazy and cloudy, and cloudy days given in a month.

Step-II

All the parameters are optimized to maximize the collector's output temperature (T_{woN}), basin water temperature computed based on hourly, monthly and annually.

Step-III

Thermal energy and thermal exergy and hourly, daily and monthly yield according to clear, hazy, hazy and cloudy and cloudy days given in month have estimated.

Step-IV

Energy matrices (EPT, EPF, and LCCE) have been computed.

Step-V

Enviroeconomic and exergoeconomic parameters have been evaluated.

Step-VI

Proposed systems are compared based on numerically computed values with previous system.

2.5 Thesis plan

The thesis entitled “**Energy and exergy analyses of active solar stills using water loaded nanofluid**” has been divided into four chapters.

Chapter 1 includes introduction, types of solar distiller, historical background and material required, working principle, mode of heat transfer, merits and demerits, and research work have been discussed. The last part of this chapter deals with water quality, performance parameters, including climatic, design parameters and application of distilled water.

Chapter 2 includes literature review exist. The passive and active solar distiller systems are discussed. The effect of parameters like basin temperature, heat transfer coefficients, thermal energy, thermal exergy, yield, effect of inclined angle of glass cover, depth of water etc has been presented in this part. In the active solar distiller units are surveyed. The various parameters are studied like effect of depth of basin water, effect of flow rate, additional heat collectors like FPC/CPC/ETC using partly or fully covered photovoltaic thermal, using pump, heat exchanger internal as well external, and with or without nanofluids.

- Historical background
- Research gap
- Research objective
- Methodology to be adopted
- Thesis plan

Chapter 3 Methodology

It is about analyzing energy and exergy of active solar distillers of N-identical photovoltaic thermal compound parabolic concentrator collectors with a helically coiled heat exchanger (N-PVT-CPC-HE) using CuO nanoparticles for single and double slope. Comparative study of active solar distillers N-PVT-CPC-HE has also been considered for yearly four climatic conditions type-a, type-b, type-c, and type-d for every month. Various

parameters, including basin water temperature, collector outlet temperature, energy, exergy, and electrical exergy have been calculated.

Talks about energy matrices, life cycle cost for active solar distillers of N-identical photovoltaic thermal compound parabolic concentrator collectors with a helically coiled heat exchanger (N-PVT-CPC-HE) using CuO nanoparticles for single and double slope. Comparative studies for these two systems have been considered using various parameters like payback time of energy, energy payback factor, and life cycle cost analysis based on energy and exergy, embodied energy, and economics.

This analysis of environmental, exergoeconomic, productivity for active solar distillers of N-identical photovoltaic thermal compound parabolic concentrator collectors with a helically coiled heat exchanger (N-PVT-CPC-HE) using CuO nanoparticles for single and double slope. These two systems have been comparatively analyzed based on various parameters like interest rate, life of span 30 and 50 years (n), productivity, total annual cost, etc.

Chapter 4 Results and discussion

Result and discussions for incorporating photovoltaic thermal compound parabolic concentrator collector with a helically coiled heat exchanger (N-PVT-CPC-HE) using CuO nanoparticles for active solar distillers (single and double slope) have been presented.

Chapter 5 Conclusions and future scope

Present the conclusions and future scopes for active solar distillers incorporating photovoltaic thermal compound parabolic concentrator collectors with a helically coiled heat exchanger (N-PVT-CPC-HE) using CuO nanoparticles (single and double slope). The recommendations have been made last to follow up on the present research.

METHODOLOGY

This chapter explains the methodology that has been adopted to find the objectives. For a detailed discussion, it has been divided into three sections. Section 3.1 explains the energy and exergy, in section 3.2 energy matrices, in section 3.3 enviroeconomic and exergoeconomic analysis of N-PVT-CPC-HE of active solar distiller using CuO nanofluid (single and double slope).

3.1 Energy and exergy analysis of active solar distiller unit (single and double slope)

3.1a Energy and exergy analysis of 25% partially covered active solar distiller (single slope) – Analytical study of N-incorporating photovoltaic thermal compound parabolic concentrator collectors active solar distiller (single slope) with helically coiled heat exchanger using CuO nanoparticles.

3.1a.1 System description

Fig. 3.1 shows N-identical 25% partly covered photovoltaic thermal compound parabolic concentrator collector with helically coiled heat exchanger active solar distiller unit (single slope) (N-PVT-CPC-SS-HE). Collectors are serially connected in series and put at an angle of 45° south-facing. Parabolic concentrator collector reflects the beam radiation which falls on receiver area radiation falls on direct collector surface gets absorbed. Radiation on the PV module is the cause of electricity generation, which operates the DC motor and runs the pump, and access can utilize for other applications. The specifications and other components of the proposed system are given in Table 3.1. The system is oriented southern face at an inclination angle of glass cover of 30° to horizontal. Maximum solar radiation falls on the glass cover absorbed by the basin liner. Through the heat exchanger, the nanoparticles exchange heat to basin fluid. It is found in the literature survey that the helically coiled heat exchanger is more effective than a simple tube heat exchanger. The CuO nanoparticles exchange more heat as

found in literature due to more heat-absorbing capacities. The nanoparticles cover more surface area in a solar distiller unit (single slope) with a heat exchanger, and volume increases basin fluid temperature. Getting thermal energy combined by single slope solar distiller unit, and externally from PVT-CPC collectors using CuO nanoparticles. Absorbing heat due to solar radiation via collectors and distiller unit, enhance the water temperature of solar distiller unit. Finally, the vapor droplets condense by realizing the latent heat, and these have been collected in basin inclined glass cover at lower ends.

The proposed hybrid system generates potable water as well as electricity. This kind of system requires low maintenance and can install easily at a small and large scale to fulfill the demand for potable water for domestic and industrial purposes.

In the present research, emphasis has been given to producing maximum potable water; therefore, CPC collectors were partly covered by PV modules..

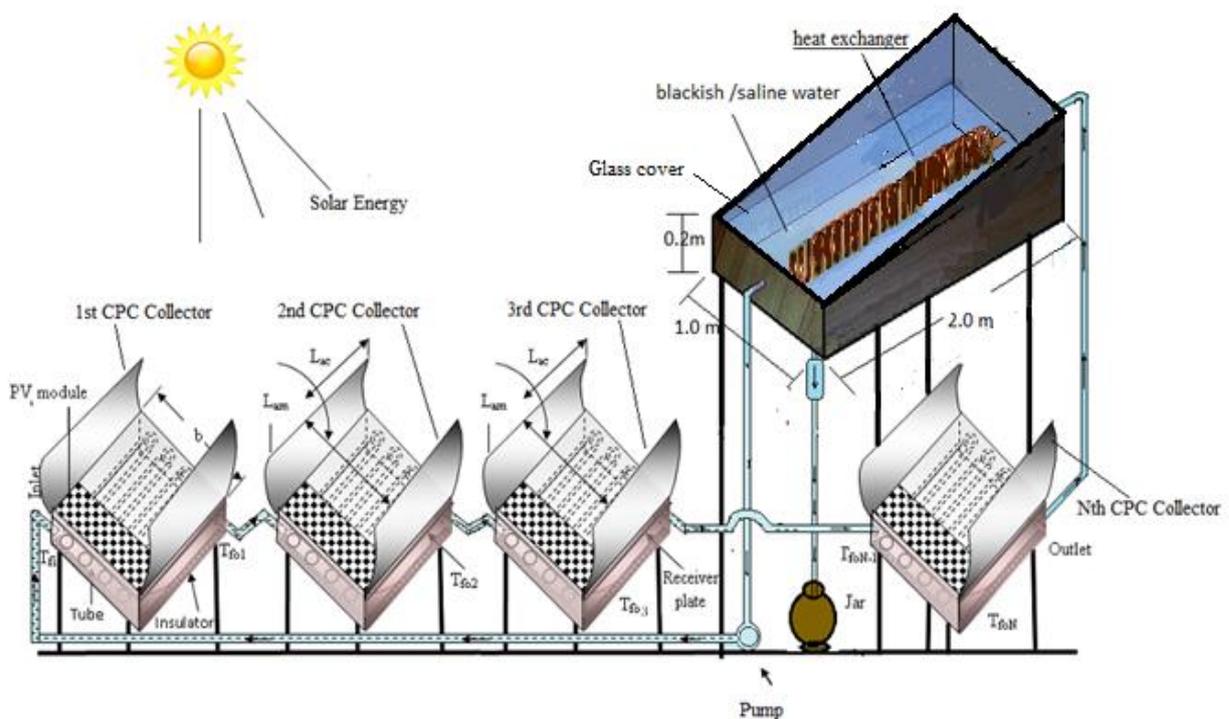


Fig. 3.1 Active single slope solar distiller incorporating 25% PVT with compound parabolic concentrator (N-PVT-CPC-SS-HE) system-A

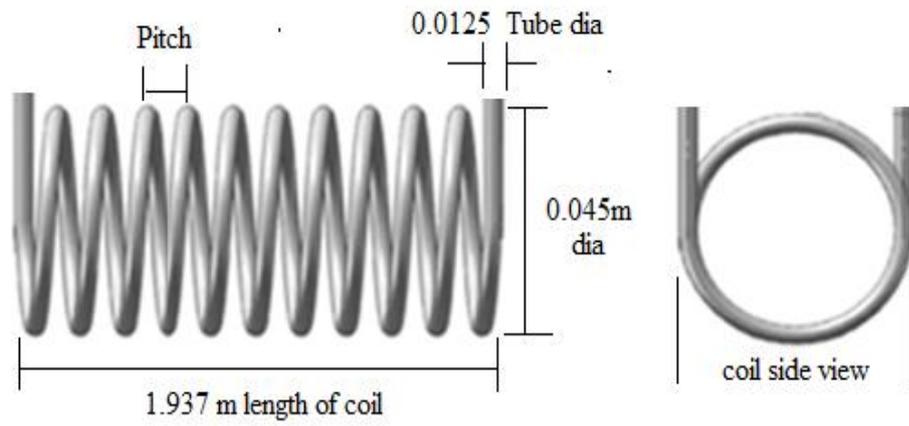


Fig.3.1a. Helically coiled heat exchanger

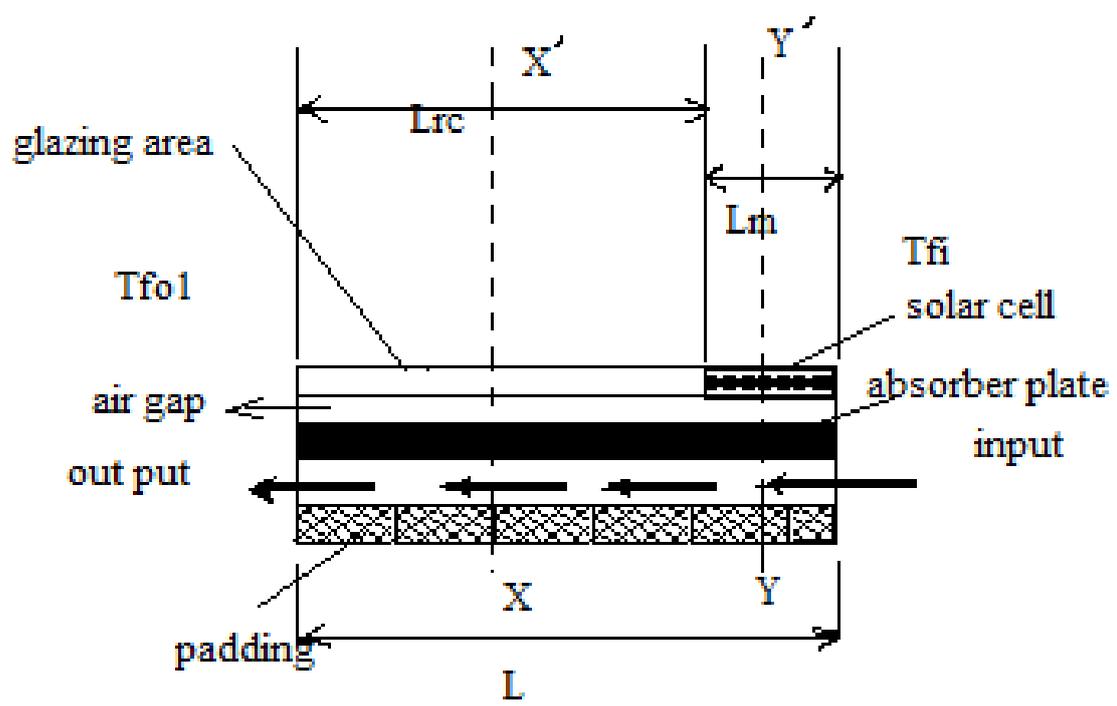
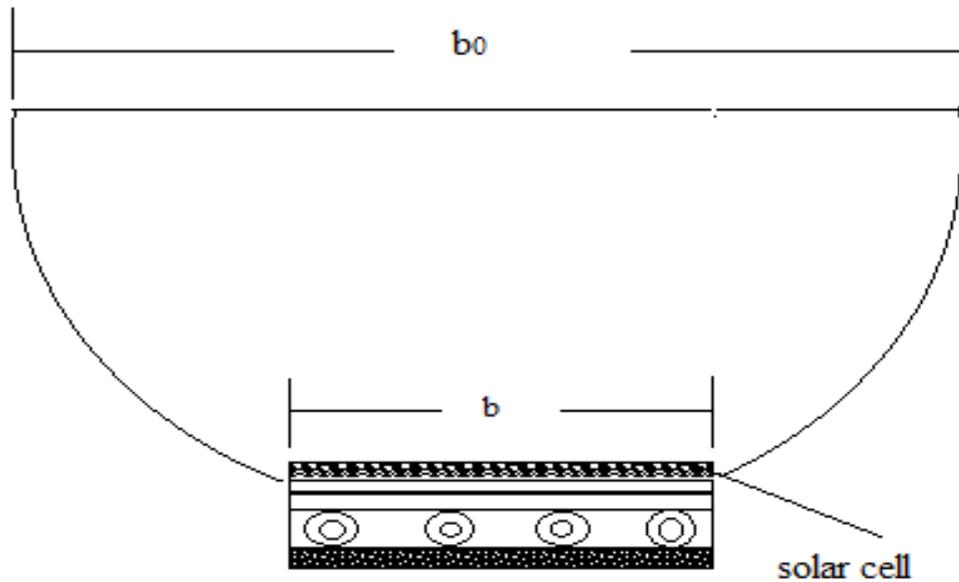


Fig.3.1b. X -X' sectioned view



(c)

Fig.3.1c. Cut section Y – Y' elevation

Although, the proposed system is compared with the previous system based on the following i.e. basin water temperature, glass cover temperature, fluid outlet temperature from N-CPC collectors, overall thermal energy, overall thermal exergy, electrical exergy, and yield. The nanoparticles' sedimentation possibility is higher in water. Therefore the critical value of the size of nanoparticles leads to change aggregation. Further, this can remove by using sophisticated and advanced types of equipment.

However, some separation methods, i.e., electrophoresis, centrifugation, filtration, and chemical methods, can be used to extract from this problem.

Table 3.1

Parameters and specifications used in active solar distiller (single) N-PVT-CPC-SS-HE

Components	Numerical Value
Specifications for single slope distiller[45]	
Length of basin	2 m
Width of basin	1 m

Glass cover inclination	15°
Body material	FRP (fiber-reinforced plastic)
Stand material	MS
Condensing cover	Glass
Orientation	South

Helically coiled heat exchanger [59]

Number of turns	12
Length of heat exchanger	1.937 m
Dia of coil tube	0.0125 m
Coil dia	0.045 m

Specifications for CPC collectors [43]

Specific heat	4200
K_g	0.78 W/mK
L_g	0.003 m
K_i	0.166 W/mK
L_i	0.1 m
$U_{tc,p}$	2.67 W/m ² K
$U_{tc,a}$	19.34 W/m ² K
PF_1	0.12
PF_2	0.58
h_{pf}	100 W/m ² K
h_i	2.8 W/m ² K
ρ	0.84
τ_g	0.95
α_p	0.6
β_c	0.8
α_c	0.7
α_p	0.6
η_0	0.15
$F/$	0.96
Length of copper tubes	1 m
Dia of tube	0.0125 m
CPC thickness	0.004 m
CPC angle to Horizontal	30°
Area of aperture	2 m ²
Module's aperture area	0.5, 2 and 0 m ²
Module's receiver area	0.25, 1 and 0 m ²
Area of receiver	1 m ²
Receiver's aperture area	1.5, 0 and 2 m ²
Receiver's collector area	0.75, 0 and 1 m ²
Type of collectors	Tube and plate type
Number of collectors	4
No of solar cells	36

Area of solar cell	0.007 m ²
D. C. motor	12 V, 24 W
<hr/>	
Nanoparticle specifications [59]	
Nanoparticles	CuO
Density	6.3*10 ³ kg/m ³
Conductivity	17.6 W/mK
Specific heat	550 J/kgK

Table 3.2

Thermophysical properties of CuO nanoparticles [59]

Density	$\rho_{nf} = \emptyset_p \rho_p + (1 - \emptyset_p) \rho_{bf}$
Thermal expansion coefficient	$\beta_{nf} = \emptyset_p \beta_p + (1 - \emptyset_p) \beta_{bf}$
	k_{nf} $= k_{bf} [0.9843$ $+ (0.398)(\emptyset_p)^{0.467} \left(\frac{\mu_{nf}}{\mu_{bf}}\right)^{0.0235} \left(\frac{1}{d_p(\text{nm})}\right)^{0.2246}$ $- (3.951) \left(\frac{\emptyset_p}{T_{nf}}\right) + (34.034) \left(\frac{\emptyset_p^2}{T_{nf}}\right) + 32.51 \left(\frac{\emptyset_p}{T_{nf}}\right)]$ $0 < \emptyset_p < 10\%; 20 < T_{nf} < 70^\circ\text{C}; 11 < d_p$ $< 150\text{nm} \text{ (CuO - water)}$
Viscosity	$\mu_{nf} = (2.41410^{-5}) 10^{\frac{247.8}{(T_{nf}-140)}}$ $0 \leq \emptyset_p \leq 10; 11 \leq d_p \leq 150\text{nm}; 20 \leq T_{nf}$ $\leq 70^\circ\text{C} \text{ (CuO - water)}$
Specific heat	$C_{nf} = 0.8429 \left(1 + \frac{T_{nf}}{50}\right)^{-0.3037} \left(1 + \frac{\emptyset_p}{100}\right)^{2.272} \left(1 + \frac{d_p}{50}\right)^{0.4167}$ $15 < d_p < 50 \text{ nm}; 0 < \emptyset_p < 4\%; 20 < T_{nf}$ $< 50^\circ\text{C} \text{ (CuO - water)}$

Table 3.3

Average air velocity

Month	Jan	Feb	Mar	Apr	May	Jun	Jul	Aug	Sep	Oct	Nov	Dec
Velocity (m/s)	2.77	3.13	3.46	3.87	4.02	4.11	3.39	2.91	2.85	2.16	1.83	2.4

3.1a.2 Thermal modeling

All modes of heat transfer to be considered for thermal modeling and different system components express them in balancing equations.

Following assumptions are considered to develop the characteristic equation for the proposed system:

- i. Level of water is constant
- ii. Ohmic losses are neglected in solar cells
- iii. Solar distiller unit is leak proof
- iv. Film condensation over the entire surface of the glass
- v. Quasi-static state for the part covered the active solar distiller unit

3.1a2.1 Governing equations of energy for various part of the distiller unit of active single slope (System-A) [48]

- a. Balancing equation for energy of semi-transparent PV module

$$\rho\alpha_c\tau_g\beta_c I_b A_{rm} = [U_{tc,a}(T_c - T_a) + U_{tc,p}(T_c - T_p)]A_{rm} + \rho\eta_m I_b A_{am} \quad (3.1)$$

- b. Energy balance for an absorber plate below the PV module

$$\rho\alpha_p\tau_g\tau_g^2(1 - \beta_c)I_b A_{am} + U_{tc,p}(T_c - T_p) = [U_{tc,a}(T_p - T_w)A_{rm} + F/h_{pf}(T_p - T_w)]A_{rm} \quad (3.2)$$

- c. Below absorber flowing fluid energy balance equation

$$m_f C_f \frac{dT_f}{dx} dx = F/[h_{pf}(T_p - T_w)]bdx \quad (3.3)$$

- d. Basin liner

$$\alpha_b I_b A_b = h_{bw}(T_b - T_w)A_b + h_{ba}(T_b - T_a)A_b \quad (3.4)$$

- e. Inside and outside glass cover

$$h_{kg}(T_{gi} - T_{go})A_g = h_1(T_{go} - T_{wi})A_g \quad (3.5)$$

$$\alpha_g I_b A_g = h_2(T_w - T_{gi})A_b + h_{kg}(T_{gi} - T_{go})A_g \quad (3.6)$$

- f. For mass of basin water

$$Q_{uN} + \alpha_w I_b A_b + h_{bw}(T_b - T_w)A_b = m_f C_f \frac{dT_f}{dx} d_x + h_2(T_w - T_{gi})A_b \quad (3.7)$$

g. Energy balance equation for immersed helically coiled heat exchanger of single slope solar distiller unit

$$m_f C_f \frac{dT_f}{dx} d_x = -2\pi r_1 U(T_{wi} - T_w) \quad (3.8)$$

Applying boundary conditions

$$T_w(x = 0) = T_{woN}, \text{ and } T_w(x = L) = T_{wi}$$

$$T_{wi} = T_{woN} \exp\left(\frac{-2\pi r_1 UL}{m_f C_f}\right) + T_w \left(1 - \exp\left(\frac{-2\pi r_1 UL}{m_f C_f}\right)\right) \quad (3.9)$$

Where

$$U = \left[\frac{1}{h_w} + \left(\frac{r_1}{k_1}\right) \log\left(\frac{r_2}{r_1}\right) + \left(\frac{r_1}{r_2}\right) \frac{1}{h_w}\right]^{-1} \quad (3.10)$$

$$T_{woN} = \left[\frac{(AF_R(\alpha\tau))_1(1-K_p^N)}{m_f C_f(1-K_p)}\right] I_b + \left[\frac{(AF_R(UL))_1(1-K_p^N)}{m_f C_f(1-K_p)}\right] T_a + T_{wi} K_m^N \quad (3.11)$$

By solving equations 5 and 7 we get

$$T_{woN} = \left[\left[\frac{(AF_R(\alpha\tau))_1(1-K_p^N)}{m_f C_f(1-K_p)}\right] \left(\frac{1}{(1-e^z K_m^N)}\right)\right] I_b + \left[\left[\frac{(AF_R(UL))_1(1-K_p^N)}{m_f C_f(1-K_p)}\right] \left(\frac{1}{(1-e^z K_m^N)}\right)\right] T_a + T_{HE} \left(\frac{(1-e^z)K_m^N}{(1-e^z K_m^N)}\right) \quad (3.12)$$

Now the heat energy gain is computed using the following relation for N-PVT-CPC-SS-HE

$$Q_{uN} = m_f C_f (T_{woN} - T_{wi}) \quad (3.13)$$

From Equations 3.11 and 3.12 the water output temperature of N-PVT-CPC collector is

$$T_{HE} > T_{wi} > T_w$$

$$Q_{uN} = \left[\left(\frac{(AF_R(\alpha\tau))_1(1-K_p^N)}{(1-K_p)}\right) \left(\frac{1}{(1-e^z K_m^N)}\right)\right] I_b + \left[\left(\frac{(AF_R(UL))_1(1-K_p^N)}{(1-K_p)}\right) \left(\frac{1}{(1-e^z K_m^N)}\right)\right] T_a + m_f C_f (T_{HE} \left(\frac{(1-e^z)K_m^N}{(1-e^z K_m^N)}\right) - T_{wi}) \quad (3.14)$$

$$Q_{uN} = [D_1 I_b + D_2 T_a + D_3]$$

Where the unknown terms $(AF_R(\alpha\tau))_1, (AF_R(UL))_1, D_1, D_2$ and D_3 are given in appendix-A

The first order equation can be used for solution

$$\frac{dT_w}{dt} + a_2 T_w = f_2(t) \quad (3.15)$$

First order differential equation can be written as

$$T_w = \frac{f(t)_1}{a_1} \left(1 - \frac{(1 - \exp(-a_1 t))}{a_1 t} \right) + T_{wi} \frac{1 - \exp(-a_1 t)}{a_1 t} \quad (3.16)$$

Solving, Equations 3.5 and 3.6 on substituting the value of T_{gi} , T_b and Q_{uN} we get we get Equations. 3.15 and

$$T_w = \frac{f(t)_2}{a_1} (1 - \exp(-a_2 \Delta t)) + T_{wo} \exp(-a_2 \Delta t) \quad (3.17)$$

0.933 is used as solar radiation exchange constant for exergy. The mentioned equation can calculate hourly water generation of the proposed system.

$$M_w = \frac{q_{ew}}{L_v} 3600 = \frac{h_{ew} A_b (T_w - T_{gi})}{L_v} 3600 \quad (3.18)$$

Where, the latent heat of vaporization is expressed as [14]:

$$L_v = 3.162510^6 + [1 - (7.61610^{-4} T_v)] \text{ For } T_v > 70 \text{ } ^\circ\text{C}$$

$$L_v = 2.493510^6 [1 - (9.477910^{-4} T_v) + (1.313210^{-7} T_v^2) - (4.797410^{-3} T_v^3)] \text{ For } T_v < 70 \text{ } ^\circ\text{C}$$

Where the unknown terms a_2 , $T_w T_{go} T_{gi} C_1$ and S are given in appendix-A

$$E_{hourlyEn} = h_{1w} (T_w - T_{gi}) A_b \quad (3.19)$$

$$E_{hourlyEx} = h_{1w} \left[(T_w - T_{go}) - (T_a + 273) \ln \left(\frac{T_w + 273}{T_{gi} + 273} \right) \right] A_b \quad (3.20)$$

Per hour variations in water temperature, thermal energy, thermal exergy, and distillate output have been obtained using equations 3.16, 3.18, 3.19 and 3.20.

Although, the proposed system is compared with the previous system based on the following parameters such as; basin water temperature, inside glass temperature, fluid outlet temperature, from N-CPC collectors, overall thermal energy, overall thermal exergy, electrical exergy, and yield. The nanoparticles' sedimentation possibility is higher in water. Therefore

the critical value of the size of nanoparticles leads to change aggregation. Further, this can remove by using sophisticated and advanced types of equipment.

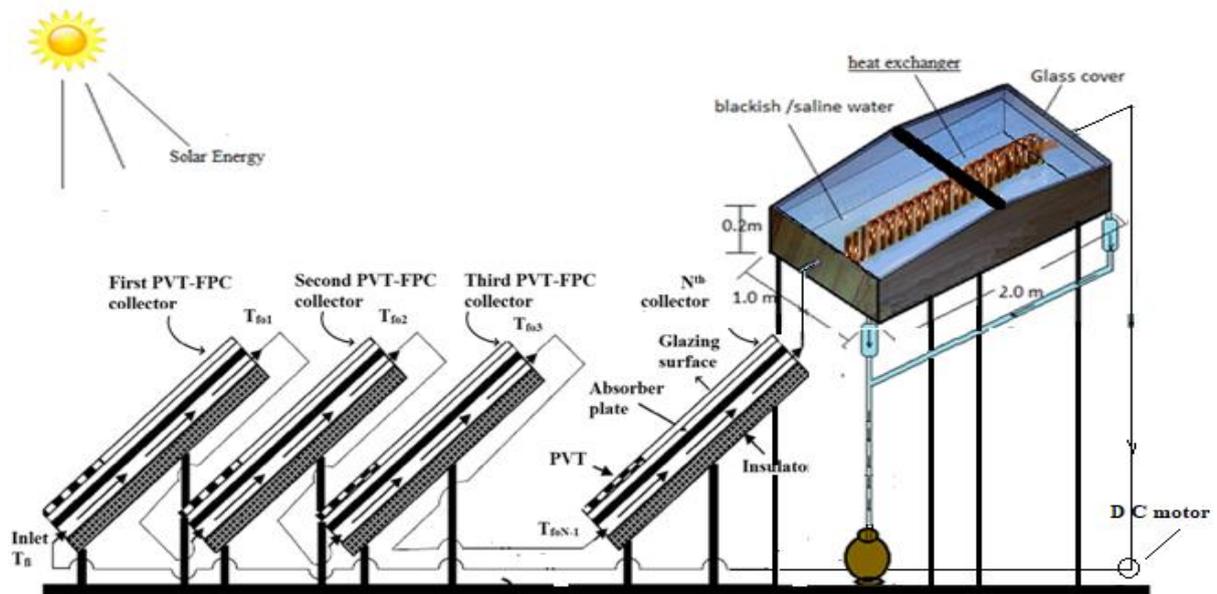


Fig. 3.2 Active double slope solar distiller incorporating 25% PVT with flat plate collector (N-PVT-FPC-DS-HE) system-C

3.1a.2.2 Procedure to be adopted

The following steps are adopted in methodology to carry out the study of the proposed system:

Step-I

Firstly Lui and Jordon formulae [11], solar radiation (I_b) and global irradiation (I_s) is used to calculate proposed system (N-PVT-CPC-SS-HE) for the annual. Further, per day solar radiant energy with number of days according to clear, hazy, hazy, and cloudy days is given in a month.

Step-II

All the parameters are optimized to maximize the collector's output temperature, basin water temperature computed based on hourly, monthly, and annually.

Step-III

Later on, thermal energy and thermal exergy and yield hourly, daily, and monthly yield

according to clear, hazy, hazy and cloudy, and cloudy days given in a month.

Step-IV

The proposed system is compared based on numerically computed values with the previous system. To easily understand the procedure, a flow chart is shown in Fig. 3.3.

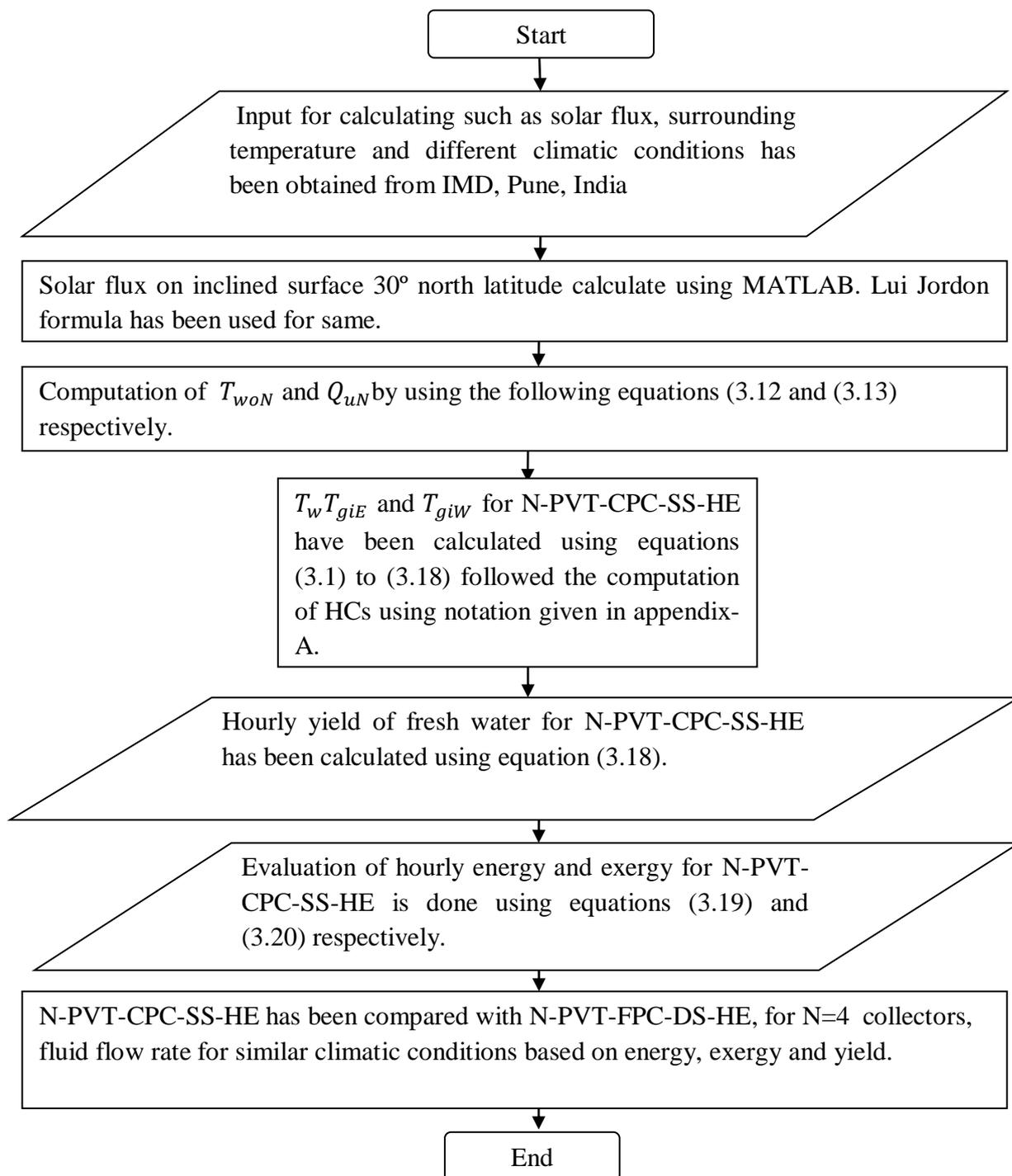


Fig.3.3Flow chart of procedure adopted

3.1b Energy and exergy analysis of 25% incorporating PVT-CPC active solar

distiller (double slope)-Analytical study of N^{th} identical photovoltaic thermal (PVT) compound parabolic concentrator (CPC) active double slope solar distiller with a helical coiled heat exchanger using CuO nanoparticles.

3.1b.1 System description

The proposed system Fig.3.15, 3.15a, 3.15b, 3.15c and the previous system in Fig.3.16 illustrate the schematic diagram. The proposed system is comprised of N^{th} identically 25% enclosed photovoltaic thermal compound parabolic concentrator collector active solar distiller (double slope) using a helically coiled heat exchanger (N-PVT-CPC-DS-HE). The heat exchanger has dipped adequately in the basin, which is oriented in east and west. The basin is made of toughened glass with an inclination of top cover being 30° , and the basin area of fiber-reinforced plastic is $2 \times 1 \text{ m}^2$. N-PVT-CPCs have a south-facing inclination of 45° . PVT generates electricity that operates on the DC motor as well as the pump. It has a fixed and accurate place for heat exchanging devices as per the basin water depth. The double slope distiller base sides are dyed mat black. The specifications of the proposed system are specified in Table 3.7. This study proposes a system with a partly covered CPC collector constructed as in Fig.1 and $A_a > A_r$, $L_{rm} = 0.25\text{m}$ and $L_{rc} = 0.75\text{m}$. A glazed partly covered flat plate collector, and remaining area is considered as receiver area (A_r). The aperture gets radiation from the beam reflected on the collector area of PVT covered, and the semi-transparent PV module is below the flat plate collector (FPC). The collector is shown in Figs. 3.15b and 3.15c. This transformation of thermal energy raises water temperature.

The intensity of solar via fluid of basin (BF/NF) directly penetrates the distiller unit's blackened surface, which is absorbed on basin liner. The irradiation gets thermally stored and raises the basin water temperature. The nanoparticles' electromagnetic wave produces intense

absorption that interacts and produces mutual oscillation as Plasmon response. In the infrared and ultraviolet region, Plasmon has high modes of NPs. The higher concentration of nanoparticles is increased to a large basin surface area and increases the temperature of the heat exchanger. Vapor gets condensed and collected into the jar when latent heat is released. Due to this, the system becomes complex but enhances production. Due to the sedimentation and dispersion of nanoparticles, the system demands more maintenance. Advanced and classy tools are needed to eliminate the problems. Various separation methods have been developed, depending on dimension, geometry, and a fraction of volume. Therefore, sets of NPs are required to reuse after rejecting brine for an extended period as per the requirement to avoid the complexity of the additional saline water. The previous system is also an active double slope solar distiller unit of photovoltaic thermalth identically 25% incorporating FPC with helically coiled heat exchanger (N-PVT-FPC-DS-HE) Fig. 3.16. Specifications of both systems are same except compound parabolic collector, which is attached to the proposed system. The basin size (2×1) and mass of water are taken into consideration 280 kg while 100 kg by previous researchers [62]. The orientation of the double slope basin is from the east-west side, and the flat plate collectors are facing south. Therefore, the distiller unit can absorb solar energy in the maximum amount. Nth compound parabolic collectors are coupled with basin in the proposed system, while in the previous system, Nth flat plate collectors are coupled with basin.

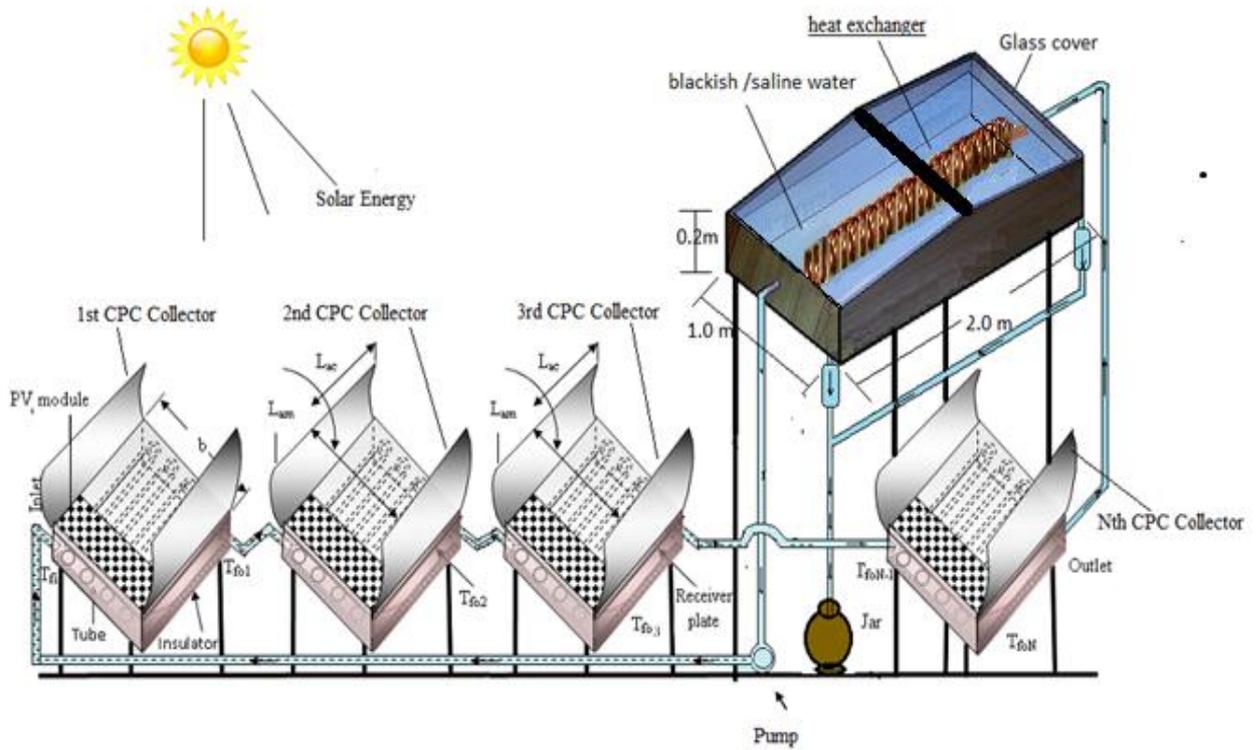


Fig. 3.4 Active double slope solar distiller incorporating 25% PVT with compound parabolic concentrator (N-PVT-CPC-DS-HE) system-B

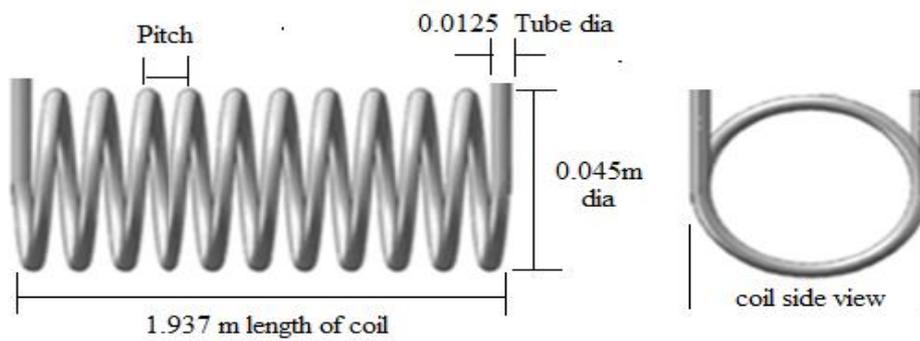


Fig. 3.4a Helically coiled heat exchanger

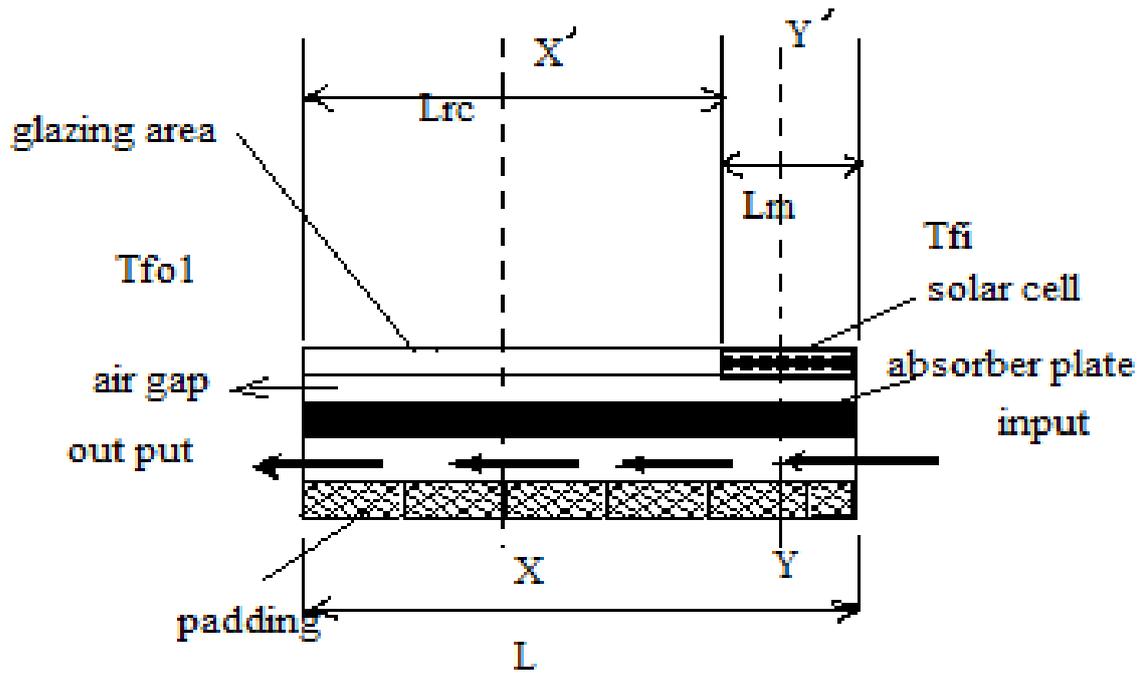


Fig. 3.4b Sectioned view

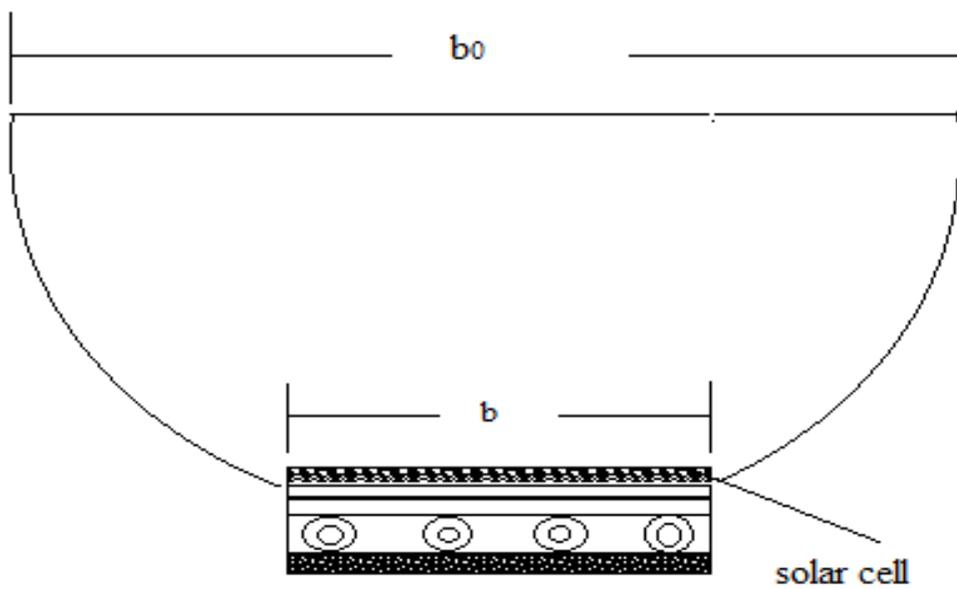


Fig. 3.4c Cut section Y-Y elevation

Table 3.4

Different parameters used in calculations [46 and 62]

Parameters	Numerical values	Parameters	Numerical values
α_g	0.050	A_m	0.6050
α_b	0.80	A_c	1.3950
α_{bf}	0.90	L_p	0.0020
α_c	0.90	K_m	64.0 W/mK
α_p	0.80	K_p	64.0 W/mK
B	0.890	L_i	0.10 m
K_g	0.780 W/m K	h_i	5.7 W/m ² K
K_b	0.035 W/m K	h_0	9.5 W/m ² K
K_p	0.166 W/m K	U_{tcp}	5.58 W/m ² K
L_g	0.004	U_{tca}	9.20 W/m ² K
L_c	0.005	U_{tpa}	4.74 W/m ² K
L_i	0.1	U_{Lm}	7.58 W/m ² K
β_0	0.0045/K	U_{LC}	4.52 W/m ² K
X	0.33m	PF ₁	0.378
Σ	5.67010^{-8} (W/m ² K ⁴)	PF ₂	0.934
τ_g	0.95	PF _c	0.955
F'	0.968	ϵ_g	0.95
η_0	0.15	ϵ_{bf}	0.95
Nanoparticles thermal properties used (Metallic CuO)			
Metallic NPs	Nanoparticles density (kg/m ³)	Specific heat C_p	heat conductivity k_p (W/m K)
CuO	6.31×10^3	550	17.6
Technical specifications of active solar distiller unit (N-PVT-CPC-DSSS) [54]			
Active solar distiller unit (double slope)			
Components		Specifications	
Length		2.0 m	
Width		1.0 m	

Glass inclined	15°		
Low side high	0.20 m		
Body's Material	GRP		
Stand's material	G. I.		
Cover's matter	glass		
Orientation	east to west		
Glass cover thickness	0.004 m		
Conductivity of glass K_g	0.816 W/mK		
Insulation thickness	0.10 m		
Insulation thermal conductivity	0.166 W/mK		
PVT-CPC collector [46]			
Components	Specifications	Components	Specifications
Collectors and types	N = 4, Tube and plate type	Area of aperture	2.0 m ²
Collector's receiver area	1.0 m × 1.0 m	Module area	0.50 m × 2.0 m
Thickness of collector plate	0.002 m	Receiver area	0.750 m × 2.0m
Thickness of C_u tube	0.00056 m	Module receiving area	0.250 m × 1.0 m
Each C_u tubes length	1.0 m	Collector receiving area	0.750 m × 1.0 m
K_i	0.1660 W/mK	F'	0.9680
FF	0.80	ρ	0.840
Insulation thickness	0.10 m	τ_g	0.950
CPC angle with horizontal	30°	α_c	0.90
Glass thickness on CPC	0.004 m	β_c	0.890
Under glass collector effective area	0.75 m ²	α_p	0.80
Pipe dia	0.0125 m	Under PV module effective area of collector	0.25 m ²
D. C motor	V, 24 W		

3.1b.2 Thermal modeling

The mathematical formulation is expressed in the balancing equations for various unit elements of taking all types of heat transfer. Following assumptions are considered to elements

of developed the characteristic equation [62]:

- i. Solar still is in quasi-steady-state (N-PVT-CPC-DS-HE).
- ii. Neglect the ohmic losses from solar cells.
- iii. Solar distiller unit is vapor leak proof.
- iv. Water level is stable.
- v. Condensation is film-wise over the entire surface of the glass.

3.1b.2.1 Governing equations of energy for various parts of the distiller unit of active double slope [54]:

a. East face

$$\alpha_g I_{SE} A_{gE} + h_{1wE} (T_w - T_{giE}) \frac{A_b}{2} - h_{EW} (T_{giE} - T_{giW}) A_{gE} = U_{cgaE} (T_{giE} - T_a) A_{gE} \quad (3.21)$$

b. West face

$$\alpha_g I_{SW} A_{gW} + h_{1wW} (T_w - T_{giW}) \frac{A_b}{2} + h_{EW} (T_{giE} - T_{giW}) A_{gW} = U_{cgaW} (T_{giW} - T_a) A_{gW} \quad (3.22)$$

On solving Equation (3.21) and (3.22)

$$T_{giE} = \frac{A_1 + A_2 T_w}{P} \quad (3.23)$$

$$T_{giW} = \frac{B_1 + B_2 T_w}{P} \quad (3.24)$$

$$T_{goE} = \frac{\frac{K_g}{L_g} T_{giE} + h_{1gE} T_a}{\frac{K_g}{L_g} + h_{1gE}} \quad (3.25)$$

$$T_{goW} = \frac{\frac{K_g}{L_g} T_{giW} + h_{1gW} T_a}{\frac{K_g}{L_g} + h_{1gW}} \quad (3.26)$$

The unknown terms, A_1 , A_2 , B_1 , B_2 , and P in Equation 3.23, 3.24, 3.25 and 3.26 are mentioned in Appendix A,

c. Basin liner

$$\alpha_b(I_{SE} + I_{SW}) + 2h_{bw}(T_b - T_w) + 2h_{ba}(T_b - T_a) \quad (3.27)$$

a. Water equation

$$m_f C_f \frac{dT_w}{dt} = \alpha_w(I_{SE} + I_{SW}) \frac{A_b}{2} + 2h_{bw}(T_b - T_w) \frac{A_b}{2} - h_{1wE}(T_w - T_{giE}) \frac{A_b}{2} - h_{1wW}(T_w - T_{giW}) \frac{A_b}{2} + Q_{uN} \quad (3.28)$$

b. Energy balance for heat exchanger immersed in basin water (BF/NF) of solar distiller unit can be written as:

$$m_f C_f \frac{dT_w}{dx} d_x = - (2\pi r_{11} U)(T_{HE} - T_w) d_x \quad (3.29)$$

Applying the boundary conditions T_w at $(x = 0) = T_{woN}$ and T_w at $(x = L) = T_{wi}$ on solving,

$$T_{wi} = T_{HE} \left[1 - \exp\left(\frac{-(2\pi r_{11} UL)}{m_f C_f}\right) \right] + T_{woN} \exp\left(\frac{-(2\pi r_{11} UL)}{m_f C_f}\right) \quad (3.30)$$

$$\text{Where } U = \left[\frac{1}{h_{bf}} + \left(\frac{r_{11}}{k_1}\right) \ln\left(\frac{r_{22}}{r_{11}}\right) \left(\frac{1}{h_{bf}}\right) \right]^{-1}$$

f. Energy balance for N-PVT-CPC water collectors is as

$$T_{woN} = \left[\frac{(AF_R(\alpha\tau))_1(1-K_p^N)}{m_f C_f(1-K_p)} \right] I_b + \left[\frac{(AF_R(UL))_1(1-K_p^N)}{m_f C_f(1-K_p)} \right] T_a + T_{wi} K_m^N \quad (3.31)$$

By solving the Equation 10 and 11 we get

$$T_{woN} = \left[\left[\frac{(AF_R(\alpha\tau))_1(1-K_p^N)}{m_f C_f(1-K_p)} \left(\frac{1}{(1-e^z K_m^N)} \right) \right] I_b + \left[\frac{(AF_R(UL))_1(1-K_p^N)}{m_f C_f(1-K_p)} \left(\frac{1}{(1-e^z K_m^N)} \right) \right] T_a + T_{HE} \left(\frac{(1-e^z) K_m^N}{(1-e^z K_m^N)} \right) \right] \quad (3.32)$$

Now heat energy gain is computed using the following relation N-PVT-CPC-DS-HE

$$Q_{uN} = m_f C_f (T_{woN} - T_{wi}) \quad (3.33)$$

From Equations (3.32) and (3.33), the water output temperature of N-PVT-CPC collector is

$$T_{HE} > T_{wi} > T_w$$

$$Q_{uN} = \left[\left(\frac{(AF_R(\alpha\tau)1)(1-K_p^N)}{(1-K_p)} \right) \left(\frac{1}{(1-e^z K_m^N)} \right) I_b + \left(\left(\frac{(AF_R(UL)1)(1-K_p^N)}{(1-K_p)} \right) \left(\frac{1}{(1-e^z K_m^N)} \right) \right) T_a + m_f C_f (T_{HE} \left(\frac{(1-e^z) K_m^N}{(1-e^z K_m^N)} \right) - T_{wi}) \right] \quad (3.34)$$

$$Q_{uN} = [D_1 I_b + D_2 T_a + D_3] \quad (3.35)$$

Where the unknown terms D_1 , D_2 and D_3 are given in appendix

By putting T_{giE} , T_{giW} , $2h_{bw}(T_b - T_w)$, and Q_{uN} from Equations (3.23), (3.24) and (3.30) in Equation (3.16)

$$\frac{dT_w}{dt} = -\frac{T_w}{m_f C_f} \left[2h_{bw} \frac{A_b}{2} + h_{1wE} \left(1 - \frac{A_1 + A_2}{P} \right) \frac{A_b}{2} + h_{1wW} \left(1 - \frac{B_1 + B_2}{P} \right) \frac{A_b}{2} - D_3 \right] + \left[\frac{I_b}{m_f C_f} (2h_{bw} + D_1) \frac{A_b}{2} + \frac{\{(\alpha_w(I_{SE} + I_{SW}) \frac{A_b}{2}) + D_2 T_a\}}{m_f C_f} \right] \quad (3.36)$$

$$\frac{dT_w}{dt} = -a_2 T_w + f_2(t)$$

Or

$$\frac{dT_w}{dt} + a_2 T_w = f_2(t) \quad (3.37)$$

Where

$$a_2 = \frac{1}{m_f C_f} \left[2h_{bw} \frac{A_b}{2} + h_{1wE} \left(1 - \frac{A_1 + A_2}{P} \right) \frac{A_b}{2} + h_{1wW} \left(1 - \frac{B_1 + B_2}{P} \right) \frac{A_b}{2} - D_3 \right]$$

$$f_2(t) = \frac{I_b}{m_f C_f} (2h_{bw} + D_2) \frac{A_b}{2} + \frac{\{(\alpha_w(I_{SE} + I_{SW}) \frac{A_b}{2}) + D_2 T_a\}}{m_f C_f}$$

$$\frac{dT_w}{dt} = \frac{f_2(t)}{a_2} (1 - e^{-a_2 \Delta t}) + T_{w0} e^{-a_2 \Delta t} \quad (3.38)$$

Where

T_{w0} is temperature of basin water at $t = 0$

$f_2(t)$ is mean value of $f_2(t)$ at $t = 0$ and t

By using the following Table 3.1, Table 3.2, and Table 3.3 for thermophysical properties and heat transfer coefficient from Table-3.4, and the per hour temperature variation of basefluid and CuO nanoparticles (BF/NF) [37] of the distiller unit can be obtained by Equation-3.18 on substituting T_{giE} , T_{giW} and T_w in equation

$$\eta_{gth} = \frac{h_{1wE}(T_w - T_{giE}) + h_{1wW}(T_w - T_{giW})(A_b)}{I_{SE}(t)A_{gE} + I_{SW}(t)A_{gW}} \quad (3.39)$$

$$\eta_{gth} = \frac{A_b}{P} \left\{ \frac{[h_{1wE}(P - A_2) + h_{1wW}(P - B_2)(T_w)] - [h_{1wE}(A_1) + h_{1wW}(B_1)]}{I_{SE}(t)A_{gE} + I_{SW}(t)A_{gW}} \right\} \quad (3.40)$$

$$\eta_{gth} = \frac{A_b}{P(I_{SE}(t)A_{gE} + I_{SW}(t)A_{gW})} \{ [h_{1wE}(E_1 - E_2)A_{gE} + h_{1wW}(E_1' - E_2')A_{gW}] + \left[\frac{f_2(t)}{a_2} (1 - e^{-a_2 \Delta t}) + T_{w0} e^{-a_2 \Delta t} \right] - [K_{1E}' I_{SE}(t) + K_{1W}' I_{SW}(t) + T_w(H_1 + H_2 + H_3 + H_4)] \} \quad (3.41)$$

Unknown expressions are mentioned in Appendix-A

On substituting $f_2(t)$, a_2 in Equation (3.41)

$$\eta_{gth} = \frac{A_b}{P} \left(\frac{e^{-a_2 \Delta t}}{(I_{SE}(t)A_{gE} + I_{SW}(t)A_{gW})} \right) \left\{ \left\{ \left[\frac{h_{1wE}(E_1 - E_2)A_{gE} + h_{1wW}(E_1' - E_2')A_{gW}}{H_{11} + H_{33}} \right] \{ [(\alpha_w + 2\alpha_b h_1)P + K_{1E}' I_{SE}(t) + [(\alpha_w + 2\alpha_b h_1)P + K_{1W}'] I_{SW}(t) + D_2 I_C(t)] (e^{-a_2 \Delta t} - 1) \} (K_{1E}' I_{SE}(t) + K_{1W}' I_{SW}(t)) \right\} e^{-a_2 \Delta t} \right\} + H_{11} (T_{w0} - T_a) \} \quad (3.42)$$

$$\eta_{gth} = \frac{A_b}{P} \left(\frac{e^{-a_2 \Delta t}}{(I_{SE}(t)A_{gE} + I_{SW}(t)A_{gW})} \right) \left[z_{22} \{ [(\alpha_w + 2\alpha_b h_1)P + K_{1E}'] I_{SE}(t) + [(\alpha_w + 2\alpha_b h_1)P + K_{1W}'] I_{SW}(t) + D_2 I_C(t) \} (e^{-a_2 \Delta t} - 1) - (K_{1E}' I_{SE}(t) + K_{1W}' I_{SW}(t)) e^{-a_2 \Delta t} + H_{11} (T_{w0} - T_a) \right]$$

$$\eta_{gth} = F' [(\alpha \tau)_{eff} + \frac{(T_{w0} - T_a)}{I_C(t)} (U_{eff})] \quad (3.43)$$

As an Equation (3.43) corresponds to thermal energy instantaneous efficiency (η_{gth}) of active double slope solar distiller with helically coiled heat exchanger (N-PVT-CPC-DS-HE)

Where

$$H_{11}' = H_1 + H_2 + H_3 + H_4 = U_{\text{eff}}$$

$$H_{33}' = U_b A_b - D_1$$

$$z_{22} = \left[\frac{h_{1wE}(E_1 - E_2)A_{gE} + h_{1wW}(E_1' - E_2')A_{gW}}{H_{11}' + H_{33}'} \right]$$

$$F' = \left(\frac{A_b}{P} \right) e^{-a_2 \Delta t}$$

$$\begin{aligned} (\alpha\tau)_{\text{eff}} = & \left[\frac{1}{(I_{SE}(t)A_{gE} + I_{SW}(t)A_{gW})} \right] \{ z_{22} \{ [(\alpha_w + 2\alpha_b h_1)P + K_{1E}'] I_{SE}(t) \\ & + [(\alpha_w + 2\alpha_b h_1)P + K_{1W}'] I_{SW}(t) + D_2 I_C(t)(e^{-a_2 \Delta t} - 1) \} \\ & - (K_{1E}' I_{SE}(t) + K_{1W}' I_{SW}(t)) e^{-a_2 \Delta t} \} \} \end{aligned}$$

Later an equation for the instantaneous loss thermal energy efficiency can be calculated by substituting Equation (3.37).

$$\frac{dT_w}{dt} + a_2 T_w = f_2(t)$$

Following relation can be taken from [70]

$$\eta_{\text{Lth}} = \frac{m_f C_f (T_w - T_{w0})}{(I_{SE}(t)A_{gE} + I_{SW}(t)A_{gW})}$$

$$\begin{aligned} \eta_{\text{Lth}} = & \left(\frac{m_f C_f}{(I_{SE}(t)A_{gE} + I_{SW}(t)A_{gW})} \right) \left(\frac{1}{(H_{11}' + H_{33}')} \right) \{ [(\alpha_w + 2\alpha_b h_1)P + K_{1E}'] I_{SE}(t) + [(\alpha_w + 2\alpha_b h_1)P + \\ & K_{1W}'] I_{SW}(t) + D_2 I_C(t) \} (1 - e^{-a_2 \Delta t}) + (H_{11}' + H_{33}') (T_{w0} - T_a) (e^{-a_2 \Delta t} - 1) \} \quad (3.44) \end{aligned}$$

$$\eta_{\text{Lth}} = F_L' [(\alpha\tau)_{\text{Leff}} - U_{\text{Leff}}' \frac{(T_{w0} - T_a)}{I(t)}] \quad (3.45)$$

Where

$$F_L = \frac{m_f C_f}{(H_{11} + H_{33})}$$

$$(\alpha\tau)_{Leff} = [(\alpha_w + 2\alpha_b h_1)P + K_{1E}]I_{SE}(t) + [(\alpha_w + 2\alpha_b h_1)P + K_{1W}]I_{SW}(t) + D_2 I_C(t) \{1 - e^{-a_2 \Delta t}\}$$

$$U_{Leff} = (H_{11} + H_{33})(e^{-a_2 \Delta t} - 1)$$

$$H_{33} = U_b A_b - D_1$$

The energy and exergy analysis has been done, respectively, based on the thermodynamics laws for the given entities. Per hour variation in thermal energy ($E_{hourlyEn}$) and thermal exergy ($E_{hourlyEx}$) of the proposed system can be taken using following relations [46, 47]:

$$E_{hourlyEn} = [h_{1wE}(T_w - T_{giE}) + h_{1wW}(T_w - T_{giW})]A_b \quad (3.46)$$

$$E_{hourlyEx} = \{h_{1wE}[(T_w - T_{giE}) - (T_a + 273) \ln\left(\frac{T_w + 273}{T_{giE} + 273}\right)] + h_{1wW}[(T_w - T_{giW}) - (T_a + 273) \ln\left(\frac{T_w + 273}{T_{giW} + 273}\right)]\}A_b \quad (3.47)$$

$$\eta_{hourlyEn} = \left\{ \frac{M_w L_v}{A_c I_C(t) + A_s I_s(t) 3600} \right\} 100 \quad (3.48)$$

$$\eta_{hourlyEx} = \left(\frac{100}{0.933 A_s I_s(t)} \right) \{h_{1wE}[(T_w - T_{giE}) - (T_a + 273) \ln\left(\frac{T_w + 273}{T_{giE} + 273}\right)] + h_{1wW}[(T_w - T_{giW}) - (T_a + 273) \ln\left(\frac{T_w + 273}{T_{giW} + 273}\right)]\}A_b \quad (3.49)$$

The constant 0.933 expresses the exchange constant for solar radiation of exergy, per hour water generation of the proposed system that can calculate by the mentioned equation.

$$M_w = \frac{q_{ew}}{L_v} 3600 = \frac{h_{ew}(T_w - T_g)}{L_v} 3600 \quad (3.50)$$

Where, the latent heat of vaporization is expressed as [47]:

$$L_v = 3.162510^6 + [1 - (7.61610^{-4} T_v)] \quad \text{for } T_v > 70 \text{ }^\circ\text{C}$$

$$L_v = 2.493510^6 [1 - (9.477910^{-4} T_v) + 1.313210^{-7} (T_v^2) - 4.797410^{-3} (T_v^3)]$$

For $T_v < 70 \text{ }^\circ\text{C}$

Hourly changes in basin water temperatures (Eqs. 3.37), thermal energy (Eqs. 3.46), thermal exergy (Eqs. 3.47), and output (Eqs. 3.50) of the proposed water system loaded nanoparticles have been obtained using thermal transfer relationships [16, 25], relationship for thermophysical properties of vapor, basefluid [31-34] and Nanoparticles (Table 3.10) [37- 42].

3.1b.2.2 Procedure to be adopted

Step I.

The initial values of temperature of the heat exchanger, basin fluid temperature, input and output temperature of collector, etc., are taken equilibrium to ambient temperature. Based on initial input, the output temperatures have been computed using properties of thermo-physical for base fluid from (Table-3.2) and CuO nanoparticles from (Table-3.9). The relevant equations have been used to assess the temperature of water of double slope solar still (Eqs. 3.38), collector outlet fluid temp (Eqs.3.31), and fluid temp in the heat exchanger (Eqs. 3.30).

Step II.

The heat transfer coefficients of collectors of double slope distiller unit using a helically coiled heat exchanger (N-PVT-CPC-DS-HE) and internal heat transfer coefficient have been calculated and compared using relations as given in (Table-3.10).

Step III.

Eqs. 3.46, Eqs. 3.47, and Eqs. 3.50 have been used for thermal energy, thermal exergy, and productivity, respectively, and results are compared for the mass of 100 kg and 280 kg of basin fluid.

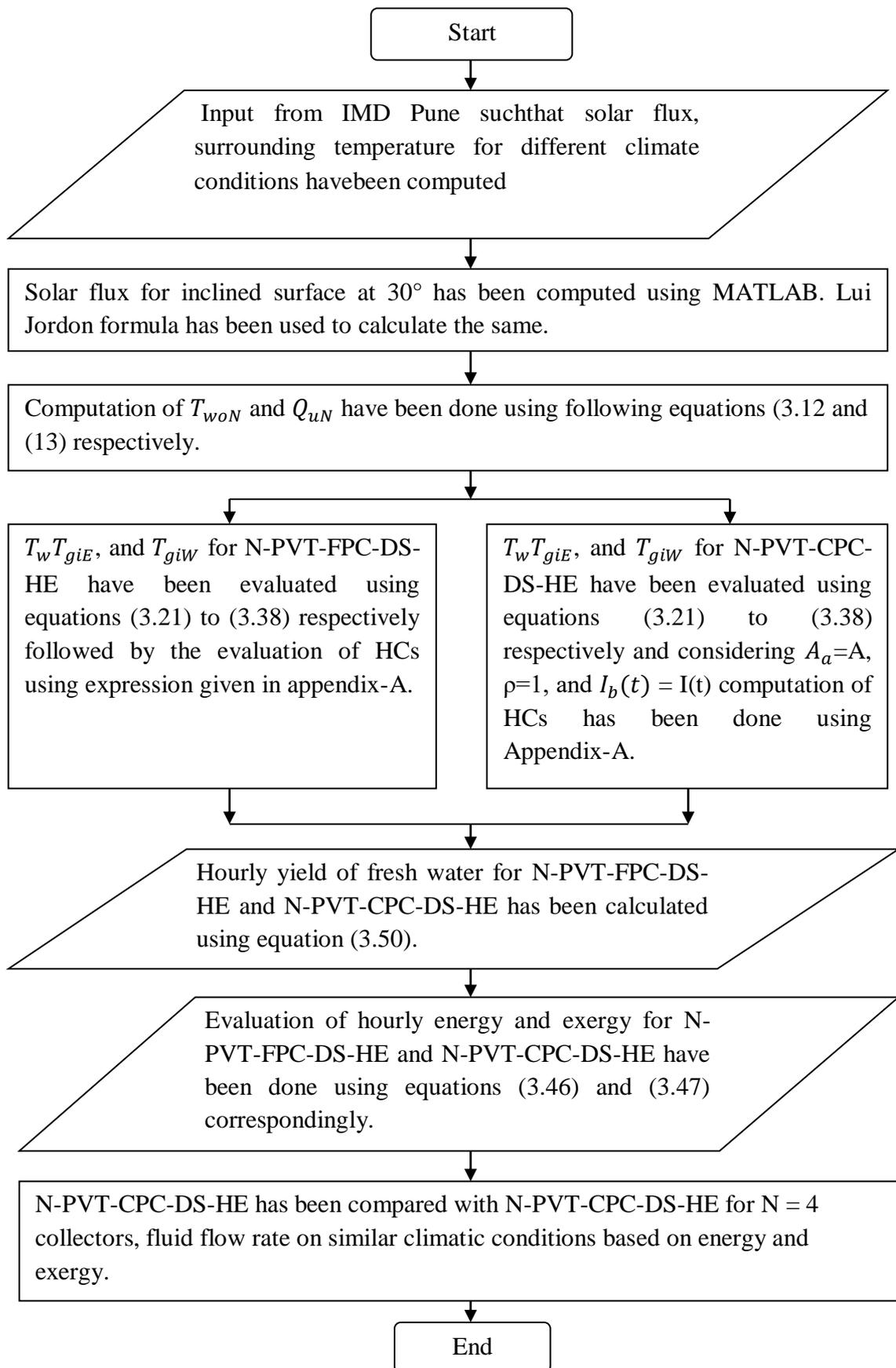


Fig.3.5 Flow chart of procedure adopted

3.2 Energy matrices and life cycle cost analysis of 25% PVT incorporating N- CPC-HE active solar distiller unit (single and double)

3.2a Energy matrices and life cycle cost analysis of single slope solar distiller -

Effect of energy matrices and life cycle cost analysis of 25% partly covered N-PVT-CPC active single slope solar distiller with helically coiled heat exchanger using CuO Nanoparticles”.

3.2a.1 Analysis

3.2a.1.1 Energy analysis

The amount of thermal energy is utilized to distillate by solar energy at an interval. Energy and exergy have been computed for given parameters of the system based on thermodynamics laws, respectively. The proposed system per hour thermal energy ($E_{hourly\ en}$) can be obtained using Equations (3.51, 3.52).

Where the unknown terms as T_w , T_{gi} , T_{go} , C_1 and S are given in appendix-A

$$E_{hourly\ En} = h_{1w}(T_w - T_{gi})A_b \quad (3.51)$$

$$\eta_{hourly\ En} = \left\{ \frac{M_w L_v}{A_c I_C(t) + A_s I_s(t) 3600} \right\} 100 \quad (3.52)$$

The annual energy of both the systems and annual yield is given in Table 3.5, 3.6a, 3.6b, 3.7, and 3.8.

Table 3.5

Annual energy system-A (N-PVT-CPC-SS-HE)

Month													Monthly Energy
	Type (a)			Type (b)			Type (c)			Type (d)			
Jan	448.93	3	1346.79	395.62	8	3164.96	106.9	11	1175.88	35.37	9	318.34	6005.98
Feb	438.44	3	1315.33	420.3	4	1681.21	127.59	12	1531.05	40.91	9	368.15	4895.74
Mar	551.16	5	2755.79	566.19	6	3397.13	243.01	12	2916.1	136.89	8	1095.14	10164.17
Apr	718.31	4	2873.23	712.87	7	4990.08	347.53	14	4865.49	299.98	5	1499.9	14228.7
May	768.14	4	3072.55	615.57	9	5540.09	455.99	12	5471.82	315.08	6	1890.49	15974.95
Jun	754.69	3	2264.08	580.79	4	2323.14	359.84	14	5037.81	207.17	6	1243	10868.04
Jul	579.87	2	1159.73	474.8	3	1424.4	344.31	10	3443.09	77.23	17	1312.85	7340.07
Aug	522.82	2	1045.65	470.49	3	1411.48	260.34	7	1822.38	157.41	19	2990.74	7270.25

Sep	720.67	7	5044.69	527.87	3	1583.62	380.82	10	3808.18	205.58	10	2055.76	12492.24
Oct	502.57	5	2512.83	366.57	10	3665.73	260.91	13	3391.87	124.17	3	372.52	9942.96
Nov	454.71	6	2728.25	299.15	10	2991.48	118.9	12	1426.83	105.66	2	211.33	7357.89
Dec	433.97	3	1301.9	301.83	7	2112.78	139.48	13	1813.21	42.53	8	340.27	5568.16
												Annually	112109.1

Table 3.6a

Annual energy system-C (N-PVT-FPC-DS-HE) East side

Month	Whether conditions												Monthly Energy
	Type (a)			Type (b)			Type (c)			Type (d)			
Jan	233.8	3	701.27	222.38	8	1779	80.52	11	885.71	26.89	9	242.05	3608.07
Feb	255.2	3	765.52	243.79	4	975.18	86.66	12	1039.95	28.26	9	254.32	3034.97
Mar	253.6	5	1267.8	224.35	6	1346.1	148.1	12	1777.04	88.32	8	706.54	5097.5
Apr	248.6	4	994.35	254.39	7	1780.7	195.6	14	2737.98	170.6	5	852.81	6365.86
May	255.7	4	1022.9	304.57	9	2741.1	240.2	12	2881.93	171.7	6	1030.04	7675.95
Jun	313.9	3	941.79	299.04	4	1196.2	202.7	14	2837.04	118.6	6	711.63	5686.64
Jul	273.1	2	546.13	271.7	3	815.11	191.3	10	1912.99	62.82	17	1067.92	4342.15
Aug	235.6	2	471.17	250.11	3	750.32	148.4	7	1038.51	91.13	19	1731.52	3991.52
Sep	62.87	7	440.08	81.36	3	244.07	212.9	10	2129.06	112.8	10	1127.89	3941.1
Oct	83.39	5	416.95	152.37	10	1523.7	136.8	13	1777.98	70.73	3	212.2	3930.86
Nov	116	6	695.99	155.22	10	1552.3	71.68	12	860.12	63.5	2	127.01	3235.36
Dec	230.1	3	690.37	170.56	7	1193.9	91.6	13	1190.78	29.23	8	233.85	3308.93
Annual Energy Eastside												54218.9	

Table 3.6b

Annual energy system-C (N-PVT-FPC-DS-HE) West side

Month	Whether conditions												Monthly Energy
	Type (a)			Type (b)			Type (c)			Type (d)			
Jan	232.73	3	698.19	222.15	8	1777.24	66.39	11	730.29	26.84	9	241.6	3447.32
Feb	254.29	3	762.86	243.01	4	972.02	86.48	12	1037.71	28.17	9	253.56	3026.15
Mar	251.95	5	1259.8	222.97	6	1337.79	147.42	12	1768.98	88.08	8	704.64	5071.18
Apr	247.33	4	989.33	253.2	7	1772.39	195.09	14	2731.23	170.1	5	850.5	6343.45
May	254.4	4	1017.6	303.29	9	2729.57	239.46	12	2873.47	171.15	6	1026.9	7647.53
Jun	313.24	3	939.72	298.66	4	1194.63	202.41	14	2833.7	118.42	6	710.54	5678.6
Jul	271.81	2	543.62	271.03	3	813.1	190.9	10	1908.96	62.51	17	1062.6	4328.31
Aug	234.88	2	469.75	248.32	3	744.96	147.88	7	1035.13	90.77	19	1724.6	3974.39
Sep	61.15	7	428.02	80.07	3	240.2	212.26	10	2122.57	112.32	10	1123.2	3913.99
Oct	82	5	409.98	151.41	10	1514.15	136.01	13	1768.17	70.36	3	211.08	3903.37
Nov	114.65	6	687.88	153.74	10	1537.37	71.3	12	855.56	63.18	2	126.37	3207.18
Dec	229.47	3	688.42	171.39	7	1199.75	91.35	13	1187.54	29.14	8	233.08	3308.8
Annual Energy Westside												53850.3	

Table 3.7

Daily, monthly and annually yield system-A (N-PVT-CPC-SS-HE)

Month	Whether conditions												Monthly Energy
	Type (a)			Type (b)			Type (c)			Type (d)			
Jan	14.05	3	42.14	12.56	8	100.5	3.86	11	42.42	1.25	9	11.26	196.32
Feb	13.37	3	40.1	14.24	4	56.97	4.62	12	55.42	1.45	9	13.08	165.56
Mar	17.01	5	85.05	17.48	6	104.9	8.91	12	106.87	4.95	8	39.63	336.46
Apr	21.9	4	87.6	21.72	7	152.05	11.32	14	158.45	10.02	5	50.08	448.18
May	23.45	4	93.81	18.9	9	170.13	14	12	167.95	10.61	6	63.65	495.54
Jun	23.03	3	69.08	17.78	4	71.1	11.42	14	159.83	7.56	6	45.39	345.4
Jul	17.73	2	35.46	14.53	3	43.6	10.91	10	109.13	2.78	17	47.32	235.5
Aug	16.05	2	32.1	14.31	3	42.93	9.57	7	67	5.72	19	108.6	250.7
Sep	22.19	7	155.3	16.17	3	48.5	11.96	10	119.59	7.52	10	75.2	398.63
Oct	15.32	5	76.58	11.36	10	113.64	8.38	13	108.95	4.5	3	13.51	312.68
Nov	14.25	6	85.48	9.95	10	99.47	4.31	12	51.76	3.82	2	7.65	244.36
Dec	13.8	3	41.4	9.47	7	66.26	5.07	13	65.97	1.51	8	12.11	185.74
Annual Yield (kg)												3615.06	

Table 3.8

Daily, monthly and annually yield system-C (N-PVT-FPC-DS-HE)

Month	Whether conditions												Monthly yield
	Type (a)			Type (b)			Type (c)			Type (d)			
Jan	13.98	3	41.93	13.44	8	107.54	5.32	11	58.5	1.91	9	17.15	225.12
Feb	15.21	3	45.62	14.48	4	57.91	6.29	12	75.45	2.01	9	18.07	197.04
Mar	14.24	5	71.22	12.18	6	73.06	10.87	12	130.4	6.4	8	51.23	325.91
Apr	14.68	4	58.72	13.58	7	95.08	12.13	14	169.88	11.25	5	56.23	379.91
May	14.83	4	59.32	17.61	9	158.53	14.38	12	172.53	10.96	6	65.74	456.12
Jun	18.17	3	54.5	17.63	4	70.51	12.61	14	176.53	8.67	6	52.02	353.55
Jul	15.37	2	30.74	16.3	3	48.89	11.96	10	119.57	4.54	17	77.13	276.33
Aug	13.66	2	27.32	14.62	3	43.86	9.77	7	68.37	6.62	19	125.82	265.37
Sep	3.09	7	21.61	4.86	3	14.57	12.76	10	127.56	8.25	10	82.53	246.27
Oct	4.6	5	23.02	8.53	10	85.26	8.18	13	106.37	5.13	3	15.4	230.04
Nov	5.87	6	35.22	9.56	10	95.59	5.2	12	62.46	4.6	2	9.2	202.46
Dec	14.13	3	42.39	10.63	7	74.39	6.68	13	86.87	2.08	8	16.66	220.32
Annual Yield (kg)												3378.45	

3.2a.1.2 Exergy analysis

The second law of thermodynamics based exergy analysis finds magnitudes, location, and causes of inefficiencies, while some limitations can be overcome by advanced exergy analysis.

Exergy can be evaluated by using the concept of entropy [14]. The following expression for hourly gain for N identical PVT-CPC active double slope with helically coiled heat exchanger solar distiller can be written as:

Exergy gain per hour

$$E_{hourlyEx} = h_{1w}[(T_w - T_{go}) - (T_a + 273) \ln\left(\frac{T_w+273}{T_{gi}+273}\right)]A_b \quad (3.53)$$

$$\eta_{hourlyEx} = \left[\left(\frac{100}{0.933A_s I_s(t)}\right) \left\{h_{1w}[(T_w - T_{gi}) - (T_a + 273) \ln\left(\frac{T_w+273}{T_{gi}+273}\right)] A_b\right\}\right] \quad (3.54)$$

The value 0.933 shows the conversion factor of solar radiation into exergy. Annual exergy is given in Table 3.12, 3.13, and Table 3.14 shows an annual comparative analysis of thermal energy, exergy, and yield.

Table 3.9

Per day, monthly and per annum thermal exergy of system-A (N-PVT-CPC-SS-HE)

Month	Whether Conditions												Monthly exergy
	Type (a)		Type (b)		Type (c)		Type (d)						
Jan	1.61	3	4.83	1.38	8	11	0.18	11	2.01	0.02	9	0.19	18.05
Feb	1.61	3	4.83	1.5	4	5.98	0.22	12	2.66	0.03	9	0.24	13.71
Mar	2	5	10	2.12	6	12.8	0.5	12	6	0.18	8	1.44	30.18
Apr	2.68	4	10.71	2.7	7	18.9	0.75	14	10.51	0.59	5	2.93	43.07
May	2.79	4	11.16	1.91	9	17.2	1.11	12	13.31	0.55	6	3.27	44.9
Jun	2.71	3	8.14	1.79	4	7.14	0.76	14	10.69	0.26	6	1.58	27.56
Jul	1.92	2	3.84	1.39	3	4.16	0.76	10	7.65	0.05	17	0.8	16.45
Aug	1.78	2	3.56	1.53	3	4.58	0.52	7	3.64	0.2	19	3.82	15.59
Sep	2.81	7	19.68	1.98	3	5.95	0.94	10	9.42	0.29	10	2.86	37.91
Oct	1.95	5	9.73	1.17	10	11.7	0.66	13	8.6	0.15	3	0.44	30.45
Nov	1.62	6	9.73	0.74	10	7.38	0.18	12	2.11	0.14	2	0.28	19.5
Dec	1.37	3	4.12	0.94	7	6.6	0.28	13	3.7	0.03	8	0.27	14.69
Annual Exergy (kWh)													312.07

Table 3.10

Per day, per month and per annum thermal exergy for system-C (N-PVT-FPC-DS-HE)

Month	Whether Conditions				Monthly Exergy
	Type (a)	Type (b)	Type (c)	Type (d)	

Jan	2.06	3	6.18	1.81	8	14.5	0.31	11	3.45	0.043	9	0.39	24.52
Feb	2.19	3	6.57	2.05	4	8.2	0.37	12	4.48	0.046	9	0.41	19.66
Mar	2.31	5	11.57	2.25	6	13.49	0.73	12	8.73	0.292	8	2.34	36.13
Apr	2.46	4	9.86	2.58	7	18.05	0.97	14	13.57	0.78	5	3.9	45.38
May	2.51	4	10.02	2.22	9	19.95	1.35	12	16.16	0.689	6	4.13	50.26
Jun	2.91	3	8.72	2.16	4	8.63	1	14	14.04	0.36	6	2.16	33.56
Jul	2.17	2	4.35	1.79	3	5.38	0.98	10	9.8	0.124	17	2.1	21.63
Aug	1.91	2	3.82	1.88	3	5.65	0.69	7	4.83	0.278	19	5.29	19.59
Sep	1.26	7	8.81	1.19	3	3.57	1.22	10	12.16	0.37	10	3.7	28.24
Oct	1.39	5	6.93	1.34	10	13.43	0.86	13	11.21	0.212	3	0.64	32.21
Nov	1.3	6	7.82	0.94	10	9.44	0.27	12	3.22	0.216	2	0.43	20.91
Dec	1.71	3	5.14	1.31	7	9.17	0.46	13	5.97	0.062	8	0.5	20.78
Annual Exergy (kWh)													352.86

Table 3.11

Annual thermal energy, annual thermal exergy and annual yield obtained from system-A (N-PVT-CPC-SS-HE) and system-C (N-PVT-FPC-DS-HE)

Outputs	NPVTCPCSSHE	NPVTFPCDSHE	
Overall thermal exergy (kWh)	312.07	352.86	
Yield (kg)	3615.06	3378.4	
	South side	East side	West side
Overall thermal energy (kWh)	112109.1	54218.92	53850.28

3.2a.2 Matrices analysis

The energy matrices become important if the construction energy is lower to produce. Energy matrices inform about the payback time of energy (EPT), payback factor of energy (EPF) and efficiency of life cycle cost (LCCE) based on energy and exergy [80].

3.2a.2.1 Payback time of energy (EPT) [80]

The time duration is needed to recover total exhausted energy in manufacturing material can be expressed as:

$$EPT_{(e)} = \frac{\text{Embodied Energy } (E_{in})}{\text{Annual energy output } (E_{out})} \quad (3.55)$$

$$EPT_{(ex)} = \frac{\text{Embodied Energy } (E_{in})}{\text{Annual exergy output } (E_{out})} \quad (3.56)$$

3.2a.2.2 Payback factor of energy (EPF) [80]

It is reciprocal of EPT and the superior value of EPF on an annual basis to express the overall performance of solar still. It can be expressed as:

$$EPF_{(e)} = \frac{\text{Overall Energy Output } (E_{out})}{\text{Embodied Energy } (E_{in})} \quad (3.57)$$

$$EPF_{(ex)} = \frac{\text{Overall Exergy Output } (E_{out})}{\text{Embodied Energy } (E_{in})} \quad (3.58)$$

3.2a.2.3 Lifecycle cost Efficiency (LCCE) [80]

$$LCCE_{(e)} = \frac{E_{out} \times n - E_{in}}{E_{sol} \times n} \quad (3.59)$$

Where, Energy out (E_{out}), energy input (E_{in}), solar energy (E_{sol}) in (kWh), and n is life span in years. The equations have been estimated for the proposed systems. The embodied energy plays an important role in different components of any system. The embodied energy of different parts (fiber reinforced plastic body, glass cover, PV module, FPC, CPC heat exchanger, and CuO nanoparticles) of the proposed system is presented in Table 3.12, Table 3.13, capital investment Table 3.14, Table 3.15, and LCCE in Table 3.16 and Table 3.17 respectively.

Table 3.12

Embodied energy of various components of system-A (N-PVT-CPC-SS-HE) and system-C (N-PVT-FPC-DS-HE)

Name of component	Embodied energy (kWh)	
	N-PVT-CPC-SS-HE	N-PVT-FPC-DS-HE
FRP body of SS	1737.79	1352.51

FPC (N=4)	3279.41	2209.92
PV (glass-glass)	980	980
Copper heat exchanger	25.83	25.83
Nanoparticles (CuO)	17.82	17.82
Others	20	20
Total EE of system	6060.85	4606.08

Table 3.13

Embodied energy of various components of system-A (N-PVT-CPC-SS-HE) and system-B (N-PVT-CPC-DS-HE)

Name of component	Embodied Energy (kWh)	
	N-PVT-CPC-SS-HE	N-PVT-CPC-DS-HE
FRP body	1737.79	1483.9
FPC/CPC (N=4)	3279.41	3279.41
PV (glass-glass)	980	980
Copper heat exchanger	25.83	25.83
Nanoparticles (CuO)	17.82	17.82
Others	20	20
Total EE of system	6060.85	5806.96

Table 3.14

Capital investment and cost of different components of system-A (N-PVT-CPC-SS-HE) and system-C (N-PVT-FPC-DS-HE)

Parameters	N-PVT-FPC-DS-HE		N-PVT-CPC-SS-HE	
	Cost		Cost	
	₹	\$	₹	\$
FRP body	10200	139.135	13693	186.78
Glass cover 2.05	1600	21.825	1600	21.825
Iron stand	1000	13.641	1000	13.641
Inlet /outlet nozzle	200	2.728	200	2.728
Iron clamp	250	3.410	250	3.410
Gaskets	200	2.728	200	2.728
Silicon gel	200	2.728	200	2.728
PVT-FPC (N=4) 8500	34000	463.784		0.000

PVT-CPC (N=4) 9000		0.000	36000	491.06
Motor and pump	1200	16.369	1200	16.369
Helically coiled heat exchanger	466.25	6.360	466.25	6.360
Fabrication and other cost	6000	81.844	6000	81.844
100 gm CuO nanoparticles	7425	101.282	7425	101.282
Total cost	62741.25	855.83	68234.25	930.75

Table 3.15

Capital investment and cost of different components of system-A (N-PVT-CPC-SS-HE) and system-B (N-PVT-CPC-DS-HE)

Parameters	N-PVT-CPC-SS-HE		N-PVT-CPC-DS-HE	
	Cost		Cost	
	₹	\$	₹	\$
FRP body	13693	186.78	10200	139.135
Glass cover 2.05	1600	21.825	1600	21.825
Iron stand	1000	13.641	1000	13.641
Inlet /outlet nozzle	200	2.728	200	2.728
Iron clamp	250	3.410	250	3.410
Gaskets	200	2.728	200	2.728
Silicon gel	200	2.728	200	2.728
PVT-CPC (N=4) 9000	36000	0.000	36000	491.06
Motor and pump	1200	16.369	1200	16.369
Helically coiled heat exchanger	466.25	6.360	466.25	6.360
Fabrication and other costs	6000	81.844	6000	81.844
100 gm CuO nanoparticles	7425	101.282	7425	101.282
Total cost of	68234.25	930.75	64741.25	883.11

Table 3.16

Embodied energy (E_{in}), the conversion efficiency of the life cycle (LCCE), energy payback factor (EPF), and energy payback time for (N-PVT-FPC-DS-HE) and (N-PVT-CPC-SS-HE) for 30 years

S.No.	Parameters	NPVT-FPC-DS-HE	NPVT-CPC-SS-HE
1	Annual yield	3378.4	3615.05
2	Latent heat	2260	2260
3	Year	30	30
4	Energy output over life	63626.53	68083.44
5	Mean solar intensity	401.8	401.8
6	Area	5.05	5.05

7	Month	12	12
8	Annual solar energy	24349.08	24349.08
9	Solar energy over life	730472.4	730472.4
10	Embodied energy	4606.08	6060.85
11	Annual energy out	2120.88	2269.44
12	Exergy	352.86	312.02
13	(EPT)e	2.17	2.67
14	(EPT)ex	13.05	19.42
15	(EPF)e	0.46	0.37
16	(EPF)ex	0.07661	0.05148
17	(LCCE)e	0.08080	0.08491
18	(LCCE)ex	0.0081861	0.004517282

Table 3.17

Embodied energy (E_{in}), the conversion efficiency of the life cycle (LCCE), energy payback factor (EPF), and energy payback time for (N-PVT-FPC-DS-HE) and (N-PVT-CPC-SS-HE) for 50 years

S.No.	Parameters	NPVT-FPC-DS-HE	NPVT-CPC-SS-HE
1	Annual yield	3378.400	3615.050
2	Latent heat	2260	2260
3	Year	50	50
4	Energy output over life	106044.222	113472.403
5	Mean solar intensity	401.800	401.800
6	Area	5.050	5.050
7	Month	12.000	12.000
8	Annual solar energy	24349.080	24349.080
9	Solar energy over life	1217454	1217454
10	Embodied energy	4606.080	6060.850
11	Annual energy out	2120.884	2269.448
12	Exergy	352.860	312.020
13	(EPT)e	2.172	2.671
14	(EPT)ex	13.054	19.425
15	(EPF)e	0.460	0.374
16	(EPF)ex	0.077	0.051
17	(LCCE)e	0.083	0.088
18	(LCCE)ex	0.011	0.008

3.2b Energy matrices and life cycle cost analysis of active solar distillers –energy matrices and life cycle cost analysis effect on 25% partly covered N-PVT-CPC active double slope solar distiller with helically coiled heat exchanger using CuO nanoparticles”.

3.2b.1 Analysis

3.2b.1.1 Energy analysis

The amount of thermal energy is utilized to distillate by solar energy at an interval. Energy and exergy analysis have been determined for given parameters of the system based on thermodynamics laws, respectively. The proposed system per hour thermal energy ($E_{\text{hourly en}}$) can be obtained using the following Equations (3.60, 3.61).

$$E_{\text{hourly En}} = [h_{1wE}(T_w - T_{giE}) + h_{1wW}(T_w - T_{giW})](A_b) \quad (3.60)$$

$$\eta_{\text{hourly En}} = \left\{ \frac{M_w L_v}{A_c I_C(t) + A_s I_s(t) 3600} \right\} 100 \quad (3.61)$$

The annual energy of both the systems and annual yield is given in Table 3.18a, 3.18b, 3.19a, 3.19b, 3.20, and 3.21.

Table 3.18a

Annual energy system-A (N-PVT-CPC-DS-HE), Eastside

Month	Whether condition												Monthly Energy
	Type (a)			Type (b)			Type (c)			Type (d)			
Jan	316.11	3	948.34	266.54	8	2132.32	86.96	11	956.52	29.42	9	264.8	4301.98
Feb	259.09	3	777.28	254.47	4	1017.89	92.93	12	1115.18	32.57	9	293.09	3203.43
Mar	269.82	5	1349.12	244.92	6	1469.5	171.57	12	2058.84	101.96	8	815.68	5693.13
Apr	240.79	4	963.18	238.95	7	1672.67	239.56	14	3353.84	205.08	5	1025.38	7015.07
May	208.59	4	834.36	315.71	9	2841.35	283.76	12	3405.15	217.99	6	1307.94	8388.8
Jun	53.96	3	161.88	389.71	4	1558.85	242.26	14	3391.65	150.28	6	901.69	6014.07
Jul	401.14	2	802.27	325.19	3	975.57	228.12	10	2281.24	60.26	17	1024.35	5083.44
Aug	348.21	2	696.42	299.35	3	898.06	174.28	7	219.93	111.02	19	2109.41	4923.82
Sep	71.37	7	499.59	136.28	3	408.83	228.26	10	2282.55	143.84	10	1438.37	4629.35
Oct	115.03	5	575.17	167.09	10	1670.87	154.85	13	2013.05	84.01	3	252.03	4511.12
Nov	167.72	6	1006.32	208.41	10	2084.07	81.62	12	979.49	74.45	2	148.9	4218.77
Dec	278.08	3	834.24	187.04	7	1309.29	96.56	13	1255.31	32.4	8	259.2	3658.04
Annual Energy Eastside in (kg)													61641.04

Table 3.18b

Annual energy system-A (N-PVT-CPC-DS-HE) west side

Month	Whether conditions												Monthly Energy
	Type (a)			Type (b)			Type (c)			Type (d)			
Jan	318.49	3	955.47	265.7	8	2125.47	71.2	11	783.21	29.36	9	264.24	4128.4
Feb	258.35	3	775.06	253.7	4	1014.88	92.73	12	1112.71	32.47	9	292.23	3194.89
Mar	268.24	5	1341.18	243.4	6	1460.34	171.17	12	2054	101.7	8	813.61	5669.13
Apr	239.36	4	957.44	237.7	7	1663.85	238.96	14	3345.39	204.57	5	1022.84	6989.52
May	207.25	4	829.01	314.5	9	2830.88	282.93	12	3395.12	217.37	6	1304.2	8359.21
Jun	52.97	3	158.91	388.9	4	1555.44	241.69	14	3383.62	149.91	6	899.45	5997.43
Jul	395.57	2	791.14	324.3	3	972.77	227.52	10	2275.23	59.94	17	1018.99	5058.13
Aug	346.35	2	692.71	296.4	3	889.3	173.73	7	1216.1	110.6	19	2101.35	4899.46
Sep	69.35	7	485.46	134.5	3	403.6	227.4	10	2274	143.33	10	1433.27	4596.34
Oct	113.38	5	566.89	166	10	1659.99	153.99	13	2001.84	83.54	3	250.63	4479.35
Nov	166.18	6	997.08	207.8	10	2078.31	81.37	12	976.39	74.14	2	148.29	4200.07
Dec	277.17	3	831.52	186.5	7	1305.31	96.28	13	1251.69	32.29	8	258.29	3646.82
Annual Energy in west side in (kg)												61218.8	

Table 3.19a

Annual energy system-C (N-PVT-FPC-DS-HE) East side

Month	Whether conditions												Monthly Energy
	Type (a)			Type (b)			Type (c)			Type (d)			
Jan	233.8	3	701.27	222.38	8	1779	80.52	11	885.71	26.89	9	242.05	3608.07
Feb	255.2	3	765.52	243.79	4	975.18	86.66	12	1039.95	28.26	9	254.32	3034.97
Mar	253.6	5	1267.8	224.35	6	1346.1	148.1	12	1777.04	88.32	8	706.54	5097.5
Apr	248.6	4	994.35	254.39	7	1780.7	195.6	14	2737.98	170.6	5	852.81	6365.86
May	255.7	4	1022.9	304.57	9	2741.1	240.2	12	2881.93	171.7	6	1030.04	7675.95
Jun	313.9	3	941.79	299.04	4	1196.2	202.7	14	2837.04	118.6	6	711.63	5686.64
Jul	273.1	2	546.13	271.7	3	815.11	191.3	10	1912.99	62.82	17	1067.92	4342.15
Aug	235.6	2	471.17	250.11	3	750.32	148.4	7	1038.51	91.13	19	1731.52	3991.52
Sep	62.87	7	440.08	81.36	3	244.07	212.9	10	2129.06	112.8	10	1127.89	3941.1
Oct	83.39	5	416.95	152.37	10	1523.7	136.8	13	1777.98	70.73	3	212.2	3930.86
Nov	116	6	695.99	155.22	10	1552.3	71.68	12	860.12	63.5	2	127.01	3235.36
Dec	230.1	3	690.37	170.56	7	1193.9	91.6	13	1190.78	29.23	8	233.85	3308.93
Annual Energy Eastside												54218.9	

Table 3.19b

Annual energy system-C (N-PVT-FPC-DS-HE) West side

Month	Whether conditions												Monthly Energy
	Type (a)			Type (b)			Type (c)			Type (d)			
Jan	232.73	3	698.19	222.15	8	1777.24	66.39	11	730.29	26.84	9	241.6	3447.32
Feb	254.29	3	762.86	243.01	4	972.02	86.48	12	1037.71	28.17	9	253.56	3026.15
Mar	251.95	5	1259.8	222.97	6	1337.79	147.42	12	1768.98	88.08	8	704.64	5071.18
Apr	247.33	4	989.33	253.2	7	1772.39	195.09	14	2731.23	170.1	5	850.5	6343.45
May	254.4	4	1017.6	303.29	9	2729.57	239.46	12	2873.47	171.15	6	1026.9	7647.53
Jun	313.24	3	939.72	298.66	4	1194.63	202.41	14	2833.7	118.42	6	710.54	5678.6
Jul	271.81	2	543.62	271.03	3	813.1	190.9	10	1908.96	62.51	17	1062.6	4328.31
Aug	234.88	2	469.75	248.32	3	744.96	147.88	7	1035.13	90.77	19	1724.6	3974.39
Sep	61.15	7	428.02	80.07	3	240.2	212.26	10	2122.57	112.32	10	1123.2	3913.99
Oct	82	5	409.98	151.41	10	1514.15	136.01	13	1768.17	70.36	3	211.08	3903.37
Nov	114.65	6	687.88	153.74	10	1537.37	71.3	12	855.56	63.18	2	126.37	3207.18
Dec	229.47	3	688.42	171.39	7	1199.75	91.35	13	1187.54	29.14	8	233.08	3308.8
Annual Energy Westside													53850.3

Table 3.20

Daily, monthly and annually yield system-A (N-PVT-CPC-DS-HE)

Month	Whether conditions												Monthly Yield
	Type (a)			Type (b)			Type (c)			Type (d)			
Jan	20.03	3	60.08	16.42	8	131.39	5.71	11	62.79	2.08	9	18.72	272.99
Feb	15.37	3	46.11	15.19	4	60.75	6.72	12	80.7	2.31	9	20.8	208.36
Mar	15.55	5	77.74	13.72	6	82.31	11.66	12	139.91	7.37	8	58.99	358.95
Apr	14.41	4	57.62	14.66	7	102.65	15.11	14	211.51	13.37	5	66.85	438.62
May	12.27	4	49.08	19.22	9	172.99	17.21	12	206.48	14.07	6	84.4	512.95
Jun	5.34	3	16.03	23.8	4	95.19	15.13	14	211.79	10.97	6	65.81	388.83
Jul	24.33	2	48.66	19.82	3	59.47	14.4	10	143.96	4.33	17	73.69	325.79
Aug	21.38	2	42.76	17.78	3	53.33	11.54	7	80.77	8.06	19	153.09	329.96
Sep	3.95	7	27.68	8.23	3	24.69	14.22	10	142.2	10.51	10	105.12	299.7
Oct	6.64	5	33.22	9.86	10	98.65	9.36	13	121.74	6.08	3	18.25	271.86
Nov	9.6	6	57.59	13.87	10	138.66	5.92	12	71	5.38	2	10.76	278.02
Dec	17.7	3	53.11	11.55	7	80.87	7.02	13	91.28	2.3	8	18.42	243.68
Annual Yield (kg)													3929.68

Table 3.21

Daily, monthly and annually yield system-C (N-PVT-FPC-DS-HE)

Month	Whether conditions												Monthly yield
	Type (a)			Type (b)			Type (c)			Type (d)			
Jan	13.98	3	41.93	13.44	8	107.54	5.32	11	58.5	1.91	9	17.15	225.12
Feb	15.21	3	45.62	14.48	4	57.91	6.29	12	75.45	2.01	9	18.07	197.04
Mar	14.24	5	71.22	12.18	6	73.06	10.87	12	130.4	6.4	8	51.23	325.91

Apr	14.68	4	58.72	13.58	7	95.08	12.13	14	169.88	11.25	5	56.23	379.91
May	14.83	4	59.32	17.61	9	158.53	14.38	12	172.53	10.96	6	65.74	456.12
Jun	18.17	3	54.5	17.63	4	70.51	12.61	14	176.53	8.67	6	52.02	353.55
Jul	15.37	2	30.74	16.3	3	48.89	11.96	10	119.57	4.54	17	77.13	276.33
Aug	13.66	2	27.32	14.62	3	43.86	9.77	7	68.37	6.62	19	125.82	265.37
Sep	3.09	7	21.61	4.86	3	14.57	12.76	10	127.56	8.25	10	82.53	246.27
Oct	4.6	5	23.02	8.53	10	85.26	8.18	13	106.37	5.13	3	15.4	230.04
Nov	5.87	6	35.22	9.56	10	95.59	5.2	12	62.46	4.6	2	9.2	202.46
Dec	14.13	3	42.39	10.63	7	74.39	6.68	13	86.87	2.08	8	16.66	220.32
Annual Yield (kg)													3378.45

3.2b.1.2 Exergy analysis

In exergy analysis, second law of thermodynamics is followed to find magnitudes, location, and causes of inefficiencies, while some limitations can be overcome by advanced exergy analysis. Exergy can be evaluated by using the concept of entropy [70]. The following expression for hourly gain for N identical PVT-CPC active double slope with helically coiled heat exchanger solar distiller can be written as exergy gain per hour.

$$E_{\text{hourly Ex}} = \{h_{1wE}[(T_w - T_{giE}) - (T_a + 273) \ln\left(\frac{T_w+273}{T_{giE}+273}\right)] + h_{1wW}[(T_w - T_{giW}) - (T_a + 273) \ln\left(\frac{T_w+273}{T_{giW}+273}\right)]\}A_b \quad (3.62)$$

$$\eta_{\text{hourly Ex}} = \left(\frac{100}{0.933A_s I_s(t)}\right) \{h_{1wE}[(T_w - T_{giE}) - (T_a + 273) \ln\left(\frac{T_w+273}{T_{giE}+273}\right)] + h_{1wW}[(T_w - T_{giW}) - (T_a + 273) \ln\left(\frac{T_w+273}{T_{giW}+273}\right)]\}A_b \quad (3.63)$$

The value 0.933 shows the conversion factor of solar radiation into exergy. Annual exergy is given in Table 3.22, 3.23, and Table 3.24 shows an annual comparative analysis of thermal energy, exergy, and yield.

Table 3.22

Per day, monthly and annually thermal exergy of system-A (N-PVT-CPC-DS-HE)

Month	Whether conditions												Monthly Exergy
	Type (a)			Type (b)			Type (c)			Type (d)			
Jan	2.4	3	7.34	2.03	8	16.26	0.31	11	3.39	0.04	9	0.38	27.37

Feb	2.21	3	6.63	2.08	4	8.32	0.37	12	4.43	0.05	9	0.44	19.82
Mar	2.4	5	12.02	2.35	6	14.1	0.8	12	9.54	0.31	8	2.46	38.13
Apr	2.45	4	9.8	2.54	7	17.77	1.16	14	16.28	0.91	5	4.53	48.38
May	2.24	4	8.95	2.35	9	21.14	1.57	12	18.89	0.86	6	5.13	54.11
Jun	1.28	3	3.84	2.71	4	10.85	1.15	14	16.16	0.44	6	2.64	33.48
Jul	2.88	2	5.77	2.09	3	6.27	1.13	10	11.27	0.09	17	1.51	24.81
Aug	2.53	2	5.07	2.16	3	6.47	0.77	7	5.36	0.32	19	6.09	22.99
Sep	1.2	7	8.42	1.55	3	4.65	1.27	10	12.7	0.45	10	4.55	30.32
Oct	1.46	5	7.32	1.37	10	13.72	0.91	13	11.86	0.23	3	0.7	33.6
Nov	1.51	6	9.07	1.15	10	11.46	0.28	12	3.32	0.23	2	0.45	24.31
Dec	1.93	3	5.79	1.33	7	9.29	0.44	13	5.75	0.06	8	0.49	21.33
Annual Exergy (kWh)													378.65

Table 3.23

Per day, monthly and annually thermal exergy of system-C (N-PVT-FPC-DS-HE)

Month	Whether Conditions												Monthly Exergy
	Type (a)			Type (b)			Type (c)			Type (d)			
Jan	2.06	3	6.18	1.81	8	14.5	0.31	11	3.45	0.043	9	0.39	24.52
Feb	2.19	3	6.57	2.05	4	8.2	0.37	12	4.48	0.046	9	0.41	19.66
Mar	2.31	5	11.57	2.25	6	13.49	0.73	12	8.73	0.292	8	2.34	36.13
Apr	2.46	4	9.86	2.58	7	18.05	0.97	14	13.57	0.78	5	3.9	45.38
May	2.51	4	10.02	2.22	9	19.95	1.35	12	16.16	0.689	6	4.13	50.26
Jun	2.91	3	8.72	2.16	4	8.63	1	14	14.04	0.36	6	2.16	33.56
Jul	2.17	2	4.35	1.79	3	5.38	0.98	10	9.8	0.124	17	2.1	21.63
Aug	1.91	2	3.82	1.88	3	5.65	0.69	7	4.83	0.278	19	5.29	19.59
Sep	1.26	7	8.81	1.19	3	3.57	1.22	10	12.16	0.37	10	3.7	28.24
Oct	1.39	5	6.93	1.34	10	13.43	0.86	13	11.21	0.212	3	0.64	32.21
Nov	1.3	6	7.82	0.94	10	9.44	0.27	12	3.22	0.216	2	0.43	20.91
Dec	1.71	3	5.14	1.31	7	9.17	0.46	13	5.97	0.062	8	0.5	20.78
Annual Exergy (kWh)													352.86

Table 3.24

Annual thermal energy, annual thermal exergy and annual yield obtained from system-A(N-

PVT-CPC-DS-HE) and system-C(N-PVT-FPC-DS-HE)

Outputs	N-PVT-CPC-DS-HE	N-PVT-FPC-DS-HE
Overall thermal exergy (kWh)	378.65	352.86
Yield (kg)	3929.6	3378.4

	Eastside	Westside	Eastside	Westside
Overall thermal energy (kWh)	61641.04	61218.75	54218.92	53850.28

3.2b.2 Energy matrices

In this analysis, the energy payback time, energy payback factor and life cycle cost analysis based on energy and exergy have been carried out [64].

3.2b.2.1 Payback time of energy (EPT) [80]

Duration of time needed to regain total energy used in manufacturing material can be expressed as:

$$EPT_{(e)} = \frac{\text{Embodied Energy } (E_{in})}{\text{Annual energy output } (E_{out})} \quad (3.64)$$

$$EPT_{(ex)} = \frac{\text{Embodied Energy } (E_{in})}{\text{Annual exergy output } (E_{out})} \quad (3.65)$$

3.2b.2.2 Production factor of energy (EPF) [80]

It is reciprocal of EPT and the superior value of EPF on an annual basis to express the overall performance of solar still. It can be expressed as:

$$EPF_{(e)} = \frac{\text{Overall Energy Output } (E_{out})}{\text{Embodied Energy } (E_{in})} \quad (3.66)$$

$$EPF_{(ex)} = \frac{\text{Overall Exergy Output } (E_{out})}{\text{Embodied Energy } (E_{in})} \quad (3.67)$$

3.2b.2.3 Lifecycle cost efficiency (LCCE) [80]

$$LCCE_{(e)} = \frac{E_{out} \times n - E_{in}}{E_{sol} \times n} \quad (3.68)$$

Where, E_{out} - Energy out, E_{in} - Energy input, E_{sol} - solar energy (kWh), and n is life span in years. The equations have been estimated for the proposed systems. The role of embodied energy is very vital for components of any system. The embodied energy of different parts (fiber reinforced plastic body, glass cover, PV module, FPC, CPC heat exchanger, and CuO nanoparticles) of the proposed system is presented in Table 3.25, Table 3.26, Table 3.27, and Table 3.28 for double slope flat and CPC solar distiller, Table 3.29, and Table 3.30 is comparison between single and double slope solar distiller.

Table 3.25

Embodied Energy of different components of system-C (N-PVT-FPC-DS-HE) and system-A (N-PVT-CPC-DS-HE)

Name of components	Embodied energy (kWh)	
	N-PVT-FPC-DS-HE[61]	N-PVT-CPC-DS-HE
Fiber Reinforce Plastic body of DS	755.61	755.61
Galvanised Iron (angle Iron)	416.4	416.4
Cover of glass	180.5	180.5
FPC (N=4)	2209.92	-
CPC (N=4)	-	3279.41
Photovoltaic (glass-glass)	980	980
Copper made heat exchanger	25.83	25.83
Nanoparticles (CuO)	17.82	17.82
Others	20	20
Total EE of system	4606.08	5675.57

Table 3.26

Capital investment and cost of different components of flat plat double slope (N-PVT-FPC-DS-HE) and CPC double slope (N-PVT-CPC-DS-HE)

Parameters	N-PVT-FPC-DS-HE[61]	N-PVT-CPC-DS-HE
	Cost	Cost

	₹	\$	₹	\$
FRP body	10200	139.135	10200	139.135
Glass cover 2.05	1600	21.825	1600	21.825
Iron stand	1000	13.641	1000	13.641
Inlet /outlet nozzle	200	2.728	200	2.728
Iron clamp	250	3.410	250	3.410
Gaskets	200	2.728	200	2.728
Silicon gel	200	2.728	200	2.728
PVT-FPC (N=4) 8500	34000	463.784		0.000
PVT-CPC (N=4) 9000		0.000	36000	491.06
Motor and pump	1200	16.369	1200	16.369
Helically coiled heat exchanger	466.25	6.360	466.25	6.360
Fabrication and other cost	6000	81.844	6000	81.844
100 gms CuO nanoparticles	7425	101.282	7425	101.282
Total cost of	62741.25	855.83	64741.25	883.11

Table 3.27

Embodied energy (E_{in}), the conversion efficiency of the life cycle (LCCE), energy payback factor (EPF), and energy payback time for (N-PVT-FPC-DS-HE) and (N-PVT-CPC-DS-HE)

S.No.	Parameters	NPVT-FPC-DS-HE[61]	NPVT-CPC-DS-HE
1	Annual yield	3378.4	3929.6
2	Latent heat	2260	2260
3	Year	30	30
4	Energy output over life	63626.53	74007.46
5	Mean solar intensity	401.8	401.8
6	Area	5.05	5.05
7	Month	12	12
8	Annual solar energy	24349.08	24349.08
9	Solar energy over life	730472.4	730472.4
10	Embodied energy	4606.08	5806.96
11	Annual energy out	2120.88	2466.91
12	Exergy	352.86	378.65
13	(EPT)e	2.17177	2.35394
14	(EPT)ex	13.05356	15.33596
15	(EPF)e	0.46045	0.42482
16	(EPF)ex	0.07661	0.06521
17	(LCCE)e	0.08080	0.09336
18	(LCCE)ex	0.0081861	0.0076013

Table 3.28

Embodied energy (E_{in}), conversion efficiency of the life cycle (LCCE), energy payback factor (EPF), and Energy payback time for (N-PVT-FPC-DS-HE) and (N-PVT-CPC-DS-HE)

S.No.	Parameters	NPVT-FPC-DS-HE[61]	NPVT-CPC-DS-HE
1	Annual yield	3378.40	3929.60
2	Latent heat	2260.00	2260.00
3	Year	50	50
4	Energy output over life	106044.22	123345.78
5	Mean solar intensity	401.800	401.800
6	Area	5.050	5.050
7	Month	12.000	12.000
8	Annual solar energy	24349.08	24349.08
9	Solar energy over life	1217454	1217454
10	Embodied energy	4606.08	5806.96
11	Annual energy out	2120.88	2466.92
12	Exergy	352.86	378.65
13	(EPT) _e	2.172	2.354
14	(EPT) _{ex}	13.054	15.336
15	(EPF) _e	0.460	0.425
16	(EPF) _{ex}	0.077	0.065
17	(LCCE) _e	0.083	0.097
18	(LCCE) _{ex}	0.011	0.011

Table 3.29

Embodied energy (E_{in}), conversion efficiency of the life cycle (LCCE), energy payback factor (EPF), and Energy payback time for single slope (N-PVT-CPC-SS-HE) and double slope (N-PVT-CPC-DS-HE)

S.No.	Parameters	NPVT-CPC-SS-HE	NPVT-CPC-DS-HE
1	Annual yield	3615.05	3929.6
2	Latent heat	2260	2260
3	Year	30	30
4	Energy output over life	68083.44	74007.47
5	Mean solar intensity	401.8	401.8
6	Area	5.05	5.05
7	Month	12	12
8	Annual solar energy	24349.08	24349.08
9	Solar energy over life	730472.4	730472.4
10	Embodied energy	6060.85	5806.96
11	Annual energy out	2269.45	2466.92
12	Exergy	312.020	378.650

13	(EPT)e	2.671	2.354
14	(EPT)ex	19.43	15.34
15	(EPF)e	0.374	0.425
16	(EPF)ex	0.051	0.065
17	(LCCE)e	0.085	0.093
18	(LCCE)ex	0.005	0.008

Table 3.30

Embodied energy (E_{in}), the conversion efficiency of the life cycle (LCCE), energy payback factor (EPF), and energy payback time for single slope (N-PVT-CPC-SS-HE) and double slope (N-PVT-CPC-DS-HE)

S.No.	Parameters	NPVT-CPC-SS-HE	NPVT-CPC-DS-HE
1	Annual yield	3615.05	3929.60
2	Latent heat	2260	2260
3	Year	50	50
4	Energy output over life	113472.40	123345.78
5	Mean solar intensity	401.80	401.80
6	Area	5.05	5.05
7	Month	12.000	12.000
8	Annual solar energy	24349.08	24349.08
9	Solar energy over life	1217454	1217454
10	Embodied energy	6060.85	5806.96
11	Annual energy out	2269.45	2466.92
12	Exergy	312.020	378.650
13	(EPT)e	2.671	2.354
14	(EPT)ex	19.425	15.336
15	(EPF)e	0.374	0.425
16	(EPF)ex	0.051	0.065
17	(LCCE)e	0.088	0.097
18	(LCCE)ex	0.008	0.011

3.3 Environoeconomic and exergoeconomic analysis of active solar distillers

Economic, environ-economic, exergoeconomic study of various systems i.e. single and double slope active solar distiller incorporating 25% photovoltaic thermal compound parabolic concentrator (PVT-CPC) with a helically coiled heat exchanger (HE) using CuO nanoparticles

have been computed and compared with previous results, an active double slope incorporating photovoltaic thermal flat plate collector (PVT-FPC) with a helically coiled heat exchanger (HE) using nanofluid.

3.3a Economic analysis N-PVT-CPC collector active solar distiller with helically coiled heat exchanger (HE) using CuO nanoparticles-Economic analysis is necessary for the economic feasibility of the system. Total annual cost, factor of shrinking fund, and factor of capital recovery for system-A (N-PVT-CPC-SS-HE) and system-B (N-PVT-CPC-DS-HE)

3.3a.1 Capital cost

The fabrication cost of the system is given in Table 3.14 and 3.15

3.3a.2 life of the system

The lifetime of the system is taken 30 and 50 years.

3.3a.3 Salvage value (S)

$$S = 0.2 \times PCC \quad (3.69)$$

Where PCC is primary capital cost

Annual salvage cost (ASC)

$$ASC = S \times SFF \quad (3.70)$$

Where SFF is a factor of shrinking fund

3.3a.4 Maintenance cost annually (AMC)

$$AMC = 0.15 \times FAC \quad (3.71)$$

Where FAC is first annual cost

3.3a.5 Capital recovery factor (CRF)

It represents the present cost in total annual cost over life at a fixed rate of interest.

$$CRF = \frac{i \times (1+i)^n}{(1+i)^n - 1} \quad (3.72)$$

3.3a.6 Shrinking fund factor

$$SFF = \frac{i}{(1+i)^n - 1} \quad (3.73)$$

3.3a.7 First annually cost is obtained

$$FAC = PCC \times CRF \quad (3.74)$$

3.3a.8 Total annual cost obtained

$$TAC = FAC + AMC - ASC \quad (3.75)$$

3.3a.9 Cost of distillate per kg obtained

$$\text{Cost/kg} = \frac{TAC}{\text{yield in life}} \quad (3.76)$$

Table 3.31

Economic analysis of N-incorporating PVT-CPC active single slope solar distiller with helically coiled heat exchanger using CuO nanoparticles

NPVT-CPC-SS-HE					
i	0.01	0.03	0.05	0.07	0.1
n	30	30	30	30	30
(1+i) ⁿ	1.348	2.427	4.322	7.612	17.449
CRF	0.039	0.051	0.065	0.081	0.106
PCC	930.760	930.760	930.760	930.760	930.760
FAC	36.065	47.487	60.547	75.007	98.734
AMC	5.410	7.123	9.082	11.251	14.810
AMC life	162.293	213.690	272.463	337.530	444.304
S	186.152	186.152	186.152	186.152	186.152

SFF	0.029	0.021	0.015	0.011	0.006
ASC	5.352	3.913	2.802	1.971	1.132
ASC life	160.546	117.383	84.056	59.120	33.950
TAC	36.123	50.697	66.828	84.287	112.413
TAC life (\$)	37.813	143.793	248.954	353.416	509.089
TAC life (₹)	2772.071	10541.498	18250.844	25908.920	37321.303
yield in annual	3615.050	3615.050	3615.050	3615.050	3615.050
yield in life	108451.500	108451.500	108451.500	108451.500	108451.500
Cost(\$)/kg annual	0.010	0.014	0.018	0.023	0.031
Cost (₹)/kg annual	0.733	1.028	1.355	1.709	2.280
Cost in life (\$)/kg	0.000	0.001	0.002	0.003	0.005
Cost in life(₹)/kg	0.026	0.097	0.168	0.239	0.344

Table 3.32

Economic analysis of N-incorporating PVT-CPC active single slope solar distiller with helically coiled heat exchanger using CuO nanoparticles.

N-PVT-CPC-SS-HE					
i	0.01	0.03	0.05	0.07	0.1
n	50	50	50	50	50
(1+i)^n	1.645	4.384	11.467	29.457	117.391
CRF	0.026	0.039	0.055	0.072	0.101
PCC	930.760	930.760	930.760	930.760	930.760
FAC	23.746	36.174	50.984	67.443	93.876
AMC	3.562	5.426	7.648	10.116	14.081
AMC life	178.097	271.308	382.380	505.820	704.068
S	186.152	186.152	186.152	186.152	186.152
SFF	0.016	0.009	0.005	0.002	0.001
ASC	2.888	1.650	0.889	0.458	0.160
ASC life	144.386	82.516	44.460	22.895	7.997
TAC	24.420	39.950	57.742	77.101	107.797
TAC life (\$)	57.457	224.966	388.904	550.368	789.946
TAC life (₹)	4212.147	16492.282	28510.553	40347.471	57910.976
yield in annual	3615.050	3615.050	3615.050	3615.050	3615.050
yield in life	180752.500	180752.500	180752.500	180752.500	180752.500
Cost(\$)/kg annual	0.007	0.011	0.016	0.021	0.030
cost (₹)/kg annual	0.495	0.810	1.171	1.564	2.186
Cost life (\$)/kg	0.000	0.001	0.002	0.003	0.004
cost in life(₹)/kg	0.023	0.091	0.158	0.223	0.320

Table 3.33

Economic analysis of N-PVT-FPC collector active solar distiller (double slope) with helically coiled heat exchanger using CuO nanoparticles

N-PVT-FPC-DS-HE					
i	0.01	0.03	0.05	0.07	0.1
n	30	30	30	30	30
(1+i) ⁿ	1.348	2.427	4.322	7.612	17.449
CRF	0.039	0.051	0.065	0.081	0.106
PCC	754.550	754.550	754.550	754.550	754.550
FAC	29.237	38.497	49.085	60.806	80.042
AMC	4.386	5.774	7.363	9.121	12.006
AMC life	131.568	173.235	220.881	273.629	360.189
S	150.910	150.910	150.910	150.910	150.910
SFF	0.029	0.021	0.015	0.011	0.006
ASC	4.338	3.172	2.271	1.598	0.917
ASC life	130.151	95.160	68.142	47.928	27.523
TAC annum	29.285	41.099	54.176	68.330	91.131
TAC life (\$)	30.654	116.571	201.823	286.508	412.709
TAC life (₹)	2247.267	8545.799	14795.624	21003.884	30255.693
Yield in annual	3378.400	3378.400	3378.400	3378.400	3378.400
Yield in life	101352.000	101352.000	101352.000	101352.000	101352.000
Cost (\$)/kg annual	0.009	0.012	0.016	0.020	0.027
Cost (₹)/kg annual	0.635	0.892	1.176	1.483	1.978
Cost/l life (\$)	0.000	0.001	0.002	0.003	0.004
Cost in life(₹)/kg	0.022	0.084	0.146	0.207	0.299

Table 3.34

Economic analysis of N-PVT-FPC collector active solar distiller (double slope) with helically coiled heat exchanger using CuO nanoparticles

N-PVT-FPC-DS-HE					
i	0.01	0.03	0.05	0.07	0.10
n	50	50	50	50	50
(1+i) ⁿ	1.645	4.384	11.467	29.457	117.391
CRF	0.026	0.039	0.055	0.072	0.101
PCC	754.550	754.550	754.550	754.550	754.550
FAC	19.251	29.326	41.332	54.675	76.103
AMC	2.888	4.399	6.200	8.201	11.415
AMC life	144.380	219.945	309.988	410.059	570.775

S	150.910	150.910	150.910	150.910	150.910
SFF	0.016	0.009	0.005	0.002	0.001
ASC	2.341	1.338	0.721	0.371	0.130
ASC life	117.051	66.895	36.043	18.561	6.483
TAC annum	19.797	32.387	46.811	62.505	87.389
TAC life (\$)	46.579	182.376	315.277	446.173	640.395
TAC life (₹)	3414.710	13369.989	23112.980	32708.952	46947.362
Yield in annual	3378.400	3378.400	3378.400	3378.400	3378.400
Yield in life	168920.000	168920.000	168920.000	168920.000	168920.000
Cost (\$)/kg annual	0.006	0.010	0.014	0.019	0.026
Cost (₹)/kg annual	0.430	0.703	1.016	1.356	1.896
Cost/l life (\$)	0.000	0.001	0.002	0.003	0.004
Cost in life(₹)/kg	0.020	0.079	0.137	0.194	0.278

Table 3.35

Economic analysis of N-PVT-CPC collector active solar distiller (double slope) with helically coiled heat exchanger using CuO nanoparticles

N-PVT-CPC-DS-HE					
i	0.01	0.03	0.05	0.07	0.1
n	30	30	30	30	30
$(1+i)^n$	1.348	2.427	4.322	7.612	17.449
CRF	0.039	0.051	0.065	0.081	0.106
PCC	847.309	847.309	847.309	847.309	847.309
FAC	32.832	43.229	55.119	68.282	89.882
AMC	4.925	6.484	8.268	10.242	13.482
AMC life	147.742	194.531	248.034	307.267	404.469
S	169.462	169.462	169.462	169.462	169.462
SFF	0.029	0.021	0.015	0.011	0.006
ASC	4.872	3.562	2.551	1.794	1.030
ASC life	146.151	106.859	76.519	53.820	30.906
TAC annum	32.885	46.151	60.836	76.730	102.334
TAC life (\$)	34.423	130.901	226.633	321.729	463.444
TAC life (₹)	2523.530	9596.358	16614.492	23585.952	33975.113
Yield in annual	3929.600	3929.600	3929.600	3929.600	3929.600
Yield in life	117888.000	117888.000	117888.000	117888.000	117888.000
Cost (\$)/kg annual	0.008	0.012	0.015	0.020	0.026
Cost (₹)/kg annual	0.613	0.861	1.135	1.431	1.909
Cost/l life (\$)	0.000	0.001	0.002	0.003	0.004
Cost in life(₹)/kg	0.021	0.081	0.141	0.200	0.288

Table 3.36

Economic analysis of N-PVT-CPC collector active solar distiller (double slope) with helically coiled heat exchanger using CuO nanoparticles

N-PVT-CPC-DS-HE					
i	0.01	0.03	0.05	0.07	0.1
n	50	50	50	50	50
(1+i) ⁿ	1.645	4.384	11.467	29.457	117.391
CRF	0.026	0.039	0.055	0.072	0.101
PCC	847.309	847.309	847.309	847.309	847.309
FAC	21.617	32.931	46.413	61.396	85.459
AMC	3.243	4.940	6.962	9.209	12.819
AMC life	162.129	246.983	348.096	460.469	640.942
S	169.462	169.462	169.462	169.462	169.462
SFF	0.016	0.009	0.005	0.002	0.001
ASC	2.629	1.502	0.809	0.417	0.146
ASC life	131.441	75.118	40.474	20.843	7.280
TAC annum	22.231	36.368	52.565	70.188	98.132
TAC life (\$)	52.305	204.796	354.035	501.022	719.121
TAC life (₹)	3834.491	15013.600	25954.326	36729.958	52718.736
Yield in annual	3929.600	3929.600	3929.600	3929.600	3929.600
Yield in life	196480.000	196480.000	196480.000	196480.000	196480.000
Cost (\$)/kg annual	0.006	0.009	0.013	0.018	0.025
Cost (₹)/kg annual	0.415	0.678	0.981	1.309	1.831
Cost/l life (\$)	0.000	0.001	0.002	0.003	0.004
Cost in life(₹)/kg	0.020	0.076	0.132	0.187	0.268

Table3.37

The total annual cost, factor of shrinking fund, and factor of capital recovery, and distillate cost per annum in \$/kg and ₹/kg for system-A(N-PVT-CPC-SS-HE), system-B (N-PVT-CPC-DS-HE), and system-C (N-PVT-FPC-DS-HE) [64].

	Years (n)	I (%)	S(\$)	CRF	SFF	Cost of water (in kg)/annum		TAC (\$)
						(\$/kg)	(₹/ kg)	
System (A) N-PVT-CPC-SS-HE	30	5	186.15	0.0650	0.0150	0.0184	1.355	248.95
		7	186.15	0.0805	0.0105	0.0233	1.709	353.41
		10	186.15	0.1060	0.0060	0.0310	2.279	509.09
	50	5	186.15	0.0547	0.0047	0.0159	1.170	388.90
		7	186.15	0.0724	0.0024	0.0213	1.563	550.36

		10	186.15	0.1008	0.0008	0.0298	2.186	789.94
System (B) N-PVT-CPC-DS-HE	30	5	169.46	0.0650	0.0150	0.0154	1.134	226.63
		7	169.46	0.0805	0.0105	0.0195	1.431	321.72
		10	169.46	0.1060	0.0060	0.0260	1.909	463.44
	50	5	169.46	0.0547	0.0047	0.0133	0.980	354.03
		7	169.46	0.0724	0.0024	0.0178	1.309	501.02
		10	169.46	0.1008	0.0008	0.0249	1.830	719.12
System (C) N-PVT-FPC-DS-HE (Previous system)	30	5	150.91	0.0650	0.0150	0.0160	1.175	201.82
		7	150.91	0.0805	0.0105	0.0202	1.482	286.50
		10	150.91	0.1060	0.0060	0.0269	1.977	412.70
	50	5	150.91	0.0547	0.0047	0.0138	1.015	315.27
		7	150.91	0.0724	0.0024	0.0185	1.356	446.17
		10	150.91	0.1008	0.0008	0.0258	1.896	640.39

As per previous studies the systems have been tested for 30 and 50 years, but practically it is not feasible. Therefore in present study, the energy payback and life cycle analysis have been computed for 15 and 30 years.

Table 3.38

The total annual cost, factor of shrinking fund, and factor of capital recovery, and distillate cost per annum in \$/kg and ₹/ kg)for system-A (N-PVT-CPC-SS-HE), system-B (N-PVT-CPC-DS-HE), and system-C (N-PVT-FPC-DS-HE) [64].

	Years (n)	I (%)	S(\$)	CRF	SFF	Cost of water (in kg)/annum		TAC (\$)
						(\$/kg)	(₹/ kg)	
System (A) N-PVT-CPC-SS-HE	15	5	186.15	0.0963	0.0463	0.0261	1.916	162.031
		7	186.15	0.1097	0.0397	0.0304	2.233	221.007
		10	186.15	0.1314	0.0314	0.0373	2.734	309.820
	20	5	186.15	0.0802	0.0302	0.0222	1.627	186.152
		7	186.15	0.0943	0.0243	0.0266	1.956	260.612
		10	186.15	0.1174	0.0174	0.0338	2.483	372.304
System (B) N-PVT-CPC-DS-HE	15	5	176.62	0.0963	0.0463	0.0228	1.672	153.736
		7	176.62	0.1097	0.0397	0.0265	1.949	209.693
		10	176.62	0.1314	0.0314	0.0325	2.387	293.959
	20	5	176.62	0.0802	0.0302	0.0193	1.420	176.622
		7	176.62	0.0943	0.0243	0.0232	1.708	247.270
		10	176.62	0.1174	0.0174	0.0295	2.167	353.244
System (C)	15	5	171.16	0.0963	0.0463	0.0257	1.885	148.987

N-PVT-FPC-DS-HE (Previous system)	7	171.16	0.1097	0.0397	0.0299	2.197	203.215	
	10	171.16	0.1314	0.0314	0.0367	2.690	284.878	
	20	5	171.16	0.0802	0.0302	0.0218	171.166	
		7	171.16	0.0943	0.0243	0.0262	1.925	239.632
		10	171.16	0.1174	0.0174	0.0333	2.443	342.332

3.3b Environ-economic analysis 25% partially covered (N-PVT-CPC-HE) active solar distiller (single and double slope)– Numerical formulation of environmental cost, like carbon credits, CO₂ mitigated per annum are given as [80]:

3.3b.1 CO₂ Emission

The electrical generation intensity is equal to meanCO₂that is approximately 0.98 kg of CO₂/kWh.

$$\text{CO}_2\text{emission per year} = \frac{\text{Embodied energy} \times 0.98}{\text{life time}} \quad (3.77)$$

For Indian conditions

$$\text{CO}_2\text{emission per year} = \frac{\text{Embodied energy} \times 1.58}{\text{life time}} \quad (3.78)$$

3.3b.2 CO₂ mitigation

It can be calculated per kWh and represented by equation:

$$\text{CO}_2 \text{ mitigation per year} = (E_{\text{out}} \times n) \times 1.58 \quad (3.79)$$

Total CO₂mitigation is computed by equation:

$$\text{Total mitigation over life} = (E_{\text{out}} \times n) \times 1.58 / 1000 \quad (3.80)$$

3.3b.3 Carbon credit earned

$$\text{The carbon credit earned} = \text{Net mitigation of over life} \times D \quad (3.81)$$

Where D is change from 5\$ to 20\$/ton of CO₂ mitigation

3.3c Exergoeconomic analyses of 25% partly covered (N-PVT-CPC-HE) active solar distiller (single and double slope)- Second law of thermodynamics is used with a combination of cost analysis. Many authors have researched exergoeconomic analysis loss of energy per unit cost with the motto of exergy loss has to minimize.

3.3c.1 Parameter (R_{ex}) is used to express the exergoeconomic Tiwari et al. [50]

$$R_{ex} = \frac{L_{ex,annm}}{TAC} \quad (3.82)$$

Where, $L_{ex,annual}$ based on exergy loss, and the term TAC the total annual cost. The rate of exergy loss is expressed as:

Table 3.39

Exergoeconomic analyses of N-PVT-CPC collector active solar distiller (single slope) with a helically coiled heat exchanger using CuO nanoparticles for 30 years

Rate of Interest	0.01	0.03	0.05	0.07	0.1
Annual Exergy	312.00	312.00	312.00	312.00	312.00
Rex in (\$)	8.637	6.154	4.669	3.702	2.775
Rate of (\$)	73.310	73.310	73.310	73.310	73.310
Rex in (kWh/₹)	0.117	0.083	0.063	0.050	0.037
Mw/Year	3615.050	3615.050	3615.050	3615.050	3615.050
Sell price in (₹)	5.000	5.000	5.000	5.000	5.000
Annual productivity (np%)	682.546	486.340	368.949	292.524	219.334
Present value	138.110	76.692	43.071	24.454	10.668

Table 3.40

Exergoeconomic analyses of N-PVT-CPC collector active solar distiller (double slope) with a helically coiled heat exchanger using CuO nanoparticles for 30 years

Rate of Interest	0.01	0.03	0.05	0.07	0.1
Annual Exergy	378.650	378.650	378.650	378.650	378.650
Rex in (\$)	11.048	7.872	5.972	4.735	3.550
Rate of (\$)	73.310	73.310	73.310	73.310	73.310
Rex in (kWh/₹)	0.149	0.106	0.081	0.064	0.048
Mw/Year	3929.600	3929.600	3929.600	3929.600	3929.600
Sell price in (₹)	5.000	5.000	5.000	5.000	5.000
Annual productivity (np%)	781.968	557.181	422.691	335.134	251.283
Present value	131.040	72.766	40.866	23.202	10.122

Table 3.41

Exergoeconomic analyses of N-PVT-FPC collector active solar distiller (double slope) with a helically coiled heat exchanger using CuO nanoparticles for 30 years

Rate of Interest	0.01	0.03	0.05	0.07	0.1
Annual Exergy	352.850	352.850	352.850	352.850	352.850
Rex in (\$)	10.623	7.569	5.742	4.553	3.414
Rate of (\$)	73.310	73.310	73.310	73.310	73.310
Rex in (kWh/₹)	0.143	0.102	0.077	0.061	0.046
Mw/Year	3378.400	3378.400	3378.400	3378.400	3378.400
Sell price in (₹)	5.000	5.000	5.000	5.000	5.000
Annual productivity (np%)	693.711	494.295	374.984	297.309	222.922
Present value	126.992	70.518	39.604	22.486	9.809

Table 3.42

Exergoeconomic analyses of N-PVT-CPC collector active solar distiller (single slope) with a helically coiled heat exchanger using CuO nanoparticles for 50 years

Rate of Interest	0.01	0.03	0.05	0.07	0.1
Annual Exergy	312.000	312.000	312.000	312.000	312.000
Rex in (\$)	12.776	7.810	5.403	4.047	2.894
Rate of (\$)	73.310	73.310	73.310	73.310	73.310
Rex in (kWh/₹)	0.172	0.105	0.073	0.055	0.039
Mw/Year	3615.050	3615.050	3615.050	3615.050	3615.05
Sell price in (₹)	5.000	5.000	5.000	5.000	5.000
Annual productivity (np%)	1009.643	617.165	426.998	319.786	228.725
Present value	113.188	42.463	16.233	6.319	1.586

Table 3.43

Exergoeconomic analyses of N-PVT-CPC collector active solar distiller (double slope) with a helically coiled heat exchanger using CuO nanoparticles for 50 years

Rate of Interest	0.01	0.03	0.05	0.07	0.1
Annual Exergy	378.650	378.650	378.650	378.650	378.650
Rex in (\$)	16.342	9.989	6.911	5.176	3.702
Rate of (\$)	73.310	73.310	73.310	73.310	73.310
Rex in (kWh/₹)	0.221	0.135	0.093	0.070	0.050
Mw/Year	3929.600	3929.600	3929.600	3929.600	3929.600

Sell price in (₹)	5.000	5.000	5.000	5.000	5.000
Annual productivity (np%)	1156.710	707.063	489.196	366.367	262.042
Present value	107.393	40.289	15.402	5.996	1.505

Table 3.44

Exergoeconomic analyses of N-PVT-FPC collector active solar distiller (double slope) with a helically coiled heat exchanger using CuO nanoparticles for 50 years

Rate of Interest	0.01	0.03	0.05	0.07	0.1
Annual Exergy	352.850	352.850	352.850	352.850	352.850
Rex in (\$)	15.714	9.606	6.646	4.977	3.560
Rate of (\$)	73.310	73.310	73.310	73.310	73.310
Rex in (kWh/₹)	0.212	0.130	0.090	0.067	0.048
Mw/Year	3378.400	3378.400	3378.400	3378.400	3378.400
Sell price in (₹)	5.000	5.000	5.000	5.000	5.000
Annual productivity (np%)	1026.159	627.261	433.984	325.017	232.467
Present value	104.076	39.044	14.926	5.811	1.458

RESULTS AND DISCUSSION

4.1 Discussion of results

Annual energy, exergy, energy matrices, enviroeconomic, exergoeconomic parameters for active single and double slope as per methodology adopted in previous chapter have been computed using MATLAB program. Outcomes are discussed in this chapter in detail.

4.1a **Energy and exergy analyses of 25% incorporating PVT-CPC active solar distiller unit (single slope)** - Hourly variation in solar intensity in W/m^2 and ambient temperature has been represented in Fig. 4.1. Mean velocity of air is 4.02 m/s.

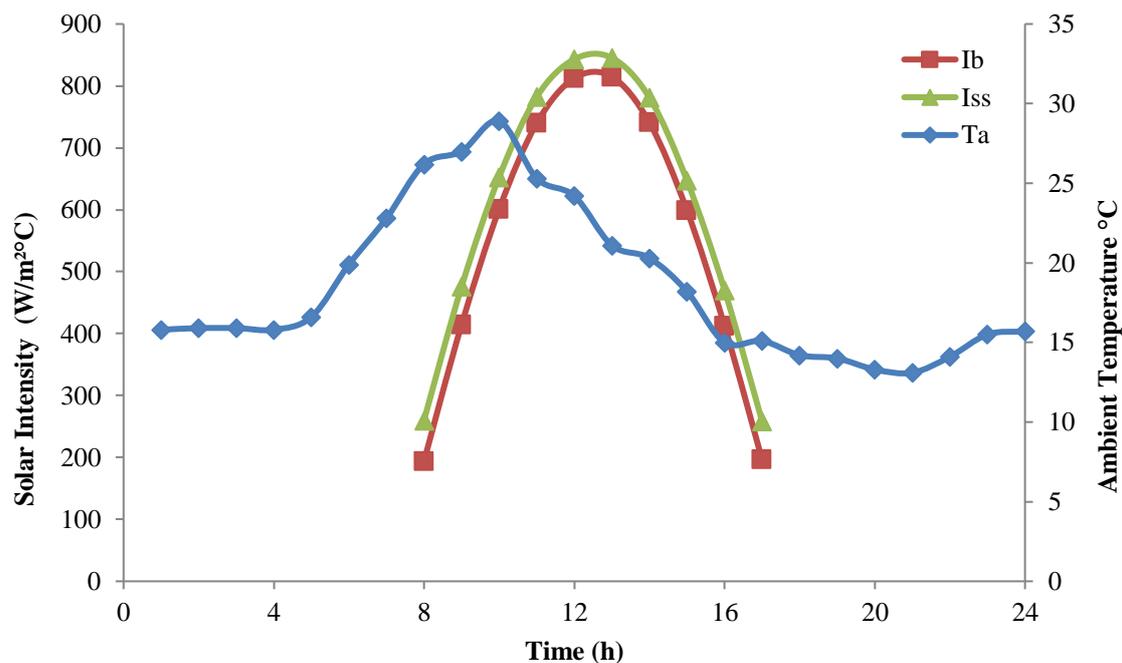


Fig. 4.1 Ambient temperature and solar radiation of typical day in May

Fig. 4.2 shows the per hour variation in basin water temperature in $^{\circ}\text{C}$ for the proposed system at $N = 4$, and the fluid flow rate is 0.02kg/s water depth 0.14 m for a-type days month wise. The amount of basin water temperature (T_w) is lower than the N^{th} collector's outlet

temperature (T_{woN}). It happens because basin water is fed to the first collector through the D. C. motor pump. Later on, inside temperature of glass is lower than basin water temperature due to the glass surface being in contact with the atmosphere. Hence its heat losses are due to convection and radiation followed by conduction.

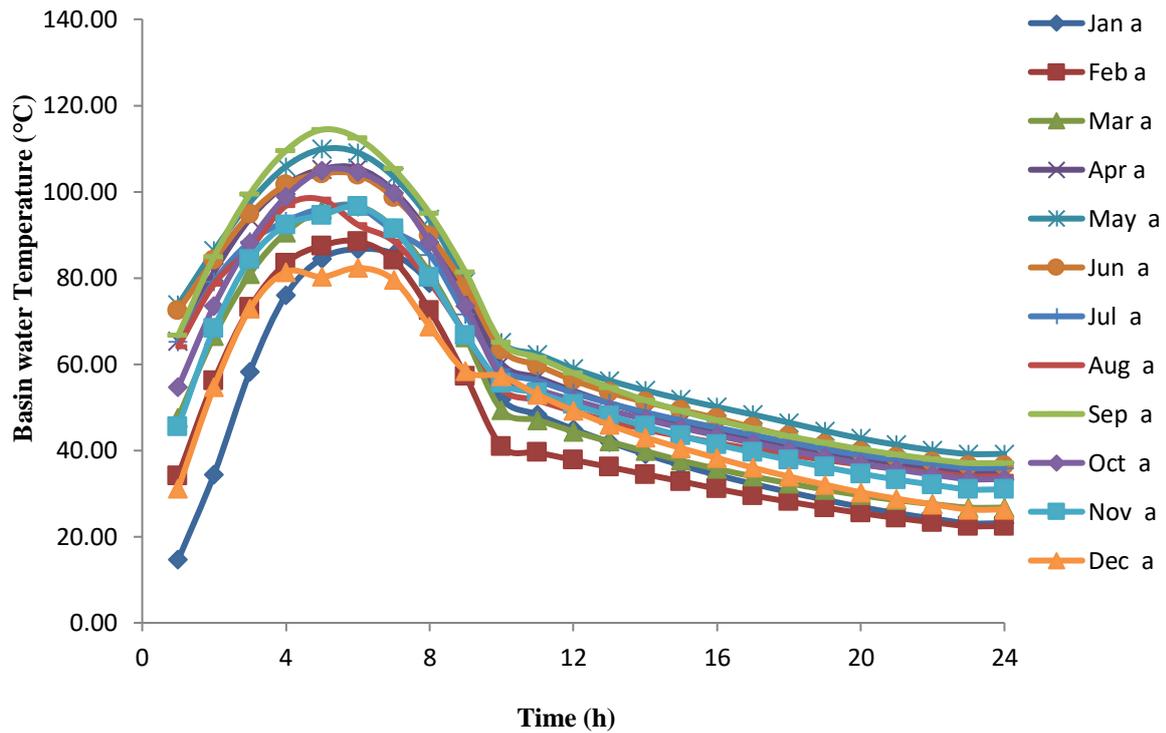


Fig. 4.2 per hour variation in temperature of basin water in °C for a-Type days

Fig. 4.3 shows the monthly variation in basin water temperature in °C vs. yield in kg for the proposed system at $N = 4$; fluid flow rate is 0.02 kg/s water depth 0.14 m. Yield rises with rising temperature. March, April, and May have a higher value corresponding to a rise in basin water temperature in the summer season. An almost similar pattern follows in August, September, and October. The maximum yield occurs in May, corresponding to maximum basin water temperature, and minimum yield occurs in December, corresponding to minimum temperature.

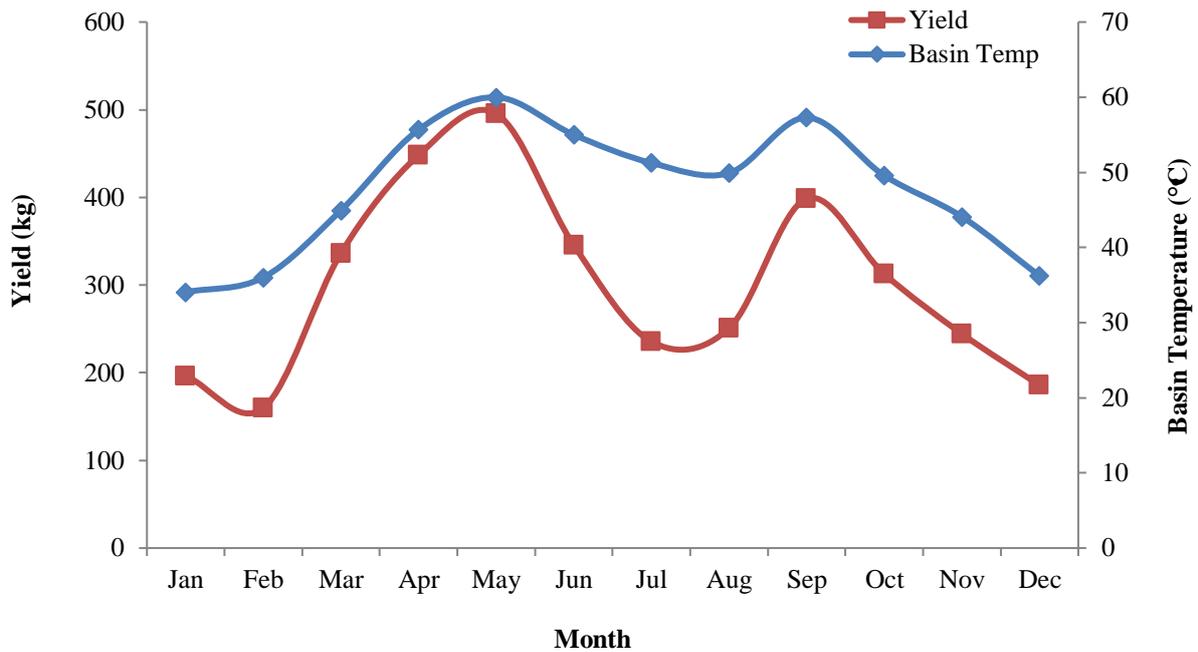


Fig. 4.3 Monthly variation in mean basin water temperature vs yield

Fig. 4.4 shows per hour variation in collector outlet temperature (T_{woN}) in °C for the proposed system at $N = 4$; the fluid flow is 0.02 kg/s and water depth 0.14 m for month-wise. Maximum temperature occurs in the daytime from 12.00 pm to 3.00 pm and minimum in after all. Maximum collector outlet temperature (T_{woN}) in °C is in March and the minimum in December.

Fig. 4.5 shows the comparison temperature of collector outlet (T_{woN}) in °C vs. yield in kg for the proposed system at $N = 4$; the fluid flow is 0.02 kg/s and the water depth 0.14 m. It is found that the value of yield rises with rising collector outlet temperature. Summer season, March, April, and May, has a higher value corresponding to a rise in collector outlet temperature, and almost similar patterns follow in August, September, and October. Maximum yield occurs in May, corresponding to maximum collector outlet temperature and low yield value in July, August, summer, and December, and January in the winter season. Minimum yield occurs in December, corresponding to minimum temperature.

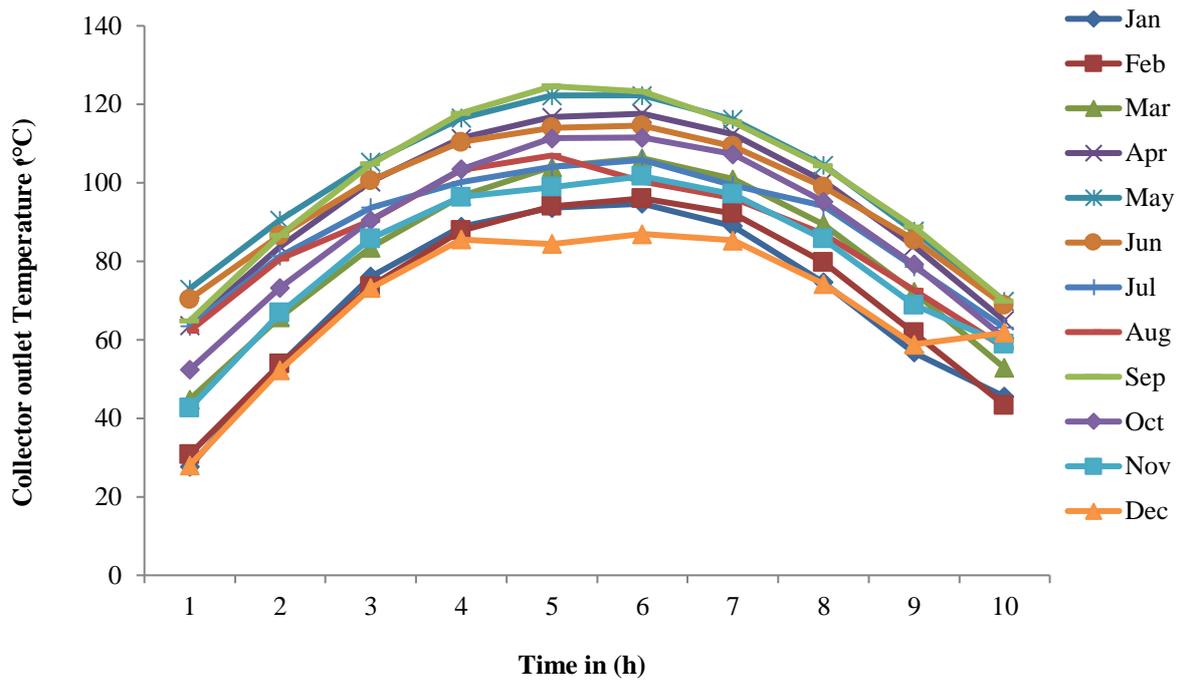


Fig. 4.4 Hourly variation in collector outlet water temperature month-wise in a-Type days

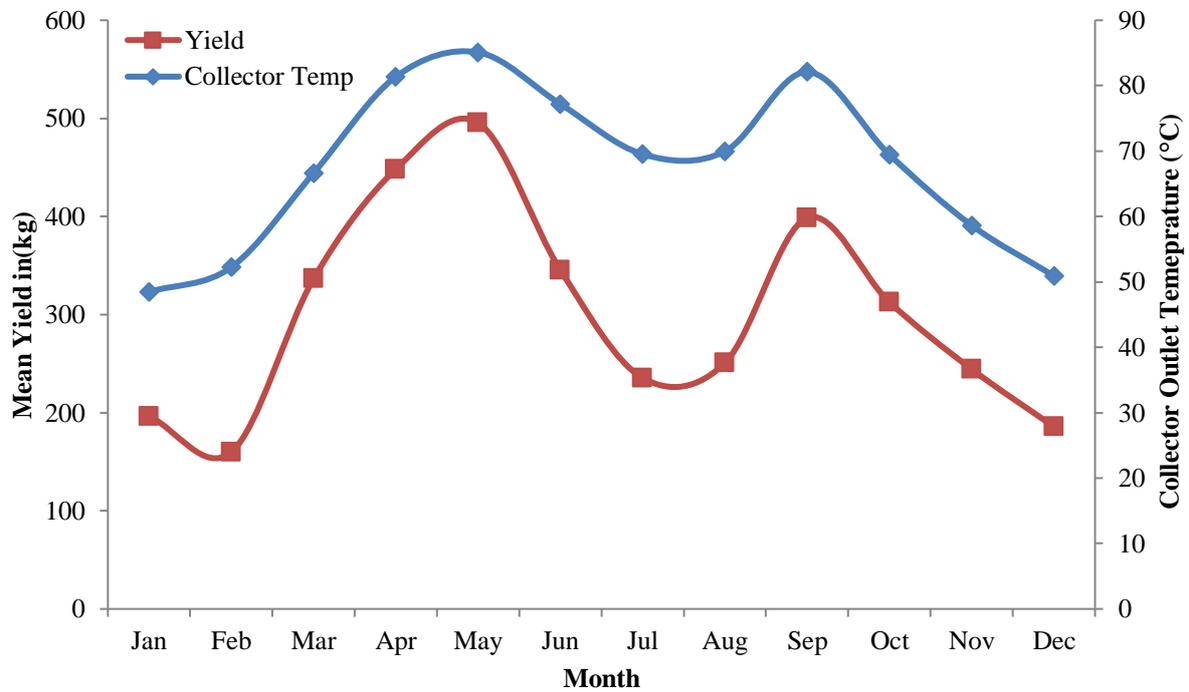


Fig. 4.5 Monthly variation in mean collector outlet water temperature vs yield

Fig. 4.6 shows per hour variation in inside glass temperature (T_{gi}) in $^{\circ}\text{C}$ for the proposed system at $N = 4$; the fluid flow rate is 0.02 kg/s and water depth 0.14 m for month-wise. The graph follows almost the same pattern for all months. The inside glass temperature is always lower than the basin water temperature. It happens due to the glass surface in contact with ambient air; therefore, heat losses occur. Here, the rate of evaporation matters by temperature differences between basin water (T_w) vs inside glass temperature (T_{gi}). Evaporative heat transfer coefficient is inversely proportional to $(T_w - T_{gi})$, while convective and radiative heat transfer coefficient is responsible for heat loss. Therefore high yield is possible when the evaporative heat transfer coefficient is high.

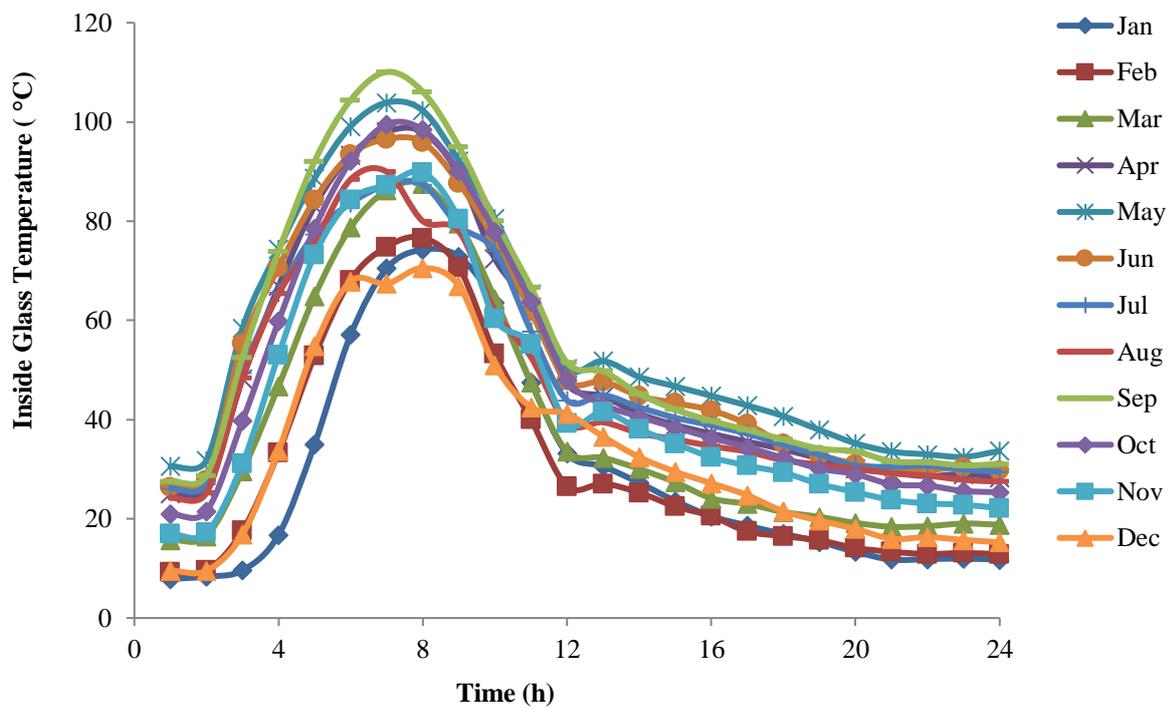


Fig. 4.6 per hour variation of inside glass temperature month-wise in a -Type days

Fig. 4.7 illustrates per hour variation of different temperatures of the proposed system at $N = 4$, the flow rate is 0.02 kg/s , and the water depth 0.14 m for type-a days in May. Basin water temperature (T_w) is lower than the collector outlet temperature (T_{woN}) in $^{\circ}\text{C}$. The output of the

basin is fed input to the first collector with the help of a pump, and then the input of the second collector is the output of the first collector, followed by all four collectors. The output of the fourth collector outlet is fed to basin of distiller unit. Further, inside glass temperature is lower than basin water temperature (T_w). It is due to the glass surface in contact with the atmosphere. Hence its heat losses are due to convection and radiation followed by conduction. Solar cells are attached to the collector top surface, so their temperature also reduces due to convection by ambient air. Peak power of photovoltaic in case of partly covered (N-PVT-CPC-SS-HE) with single slope still using heat exchanger kept same. The electrical exergy is the same for active double slope solar distiller using a heat exchanger (N-PVT-FPC-DS-HE).

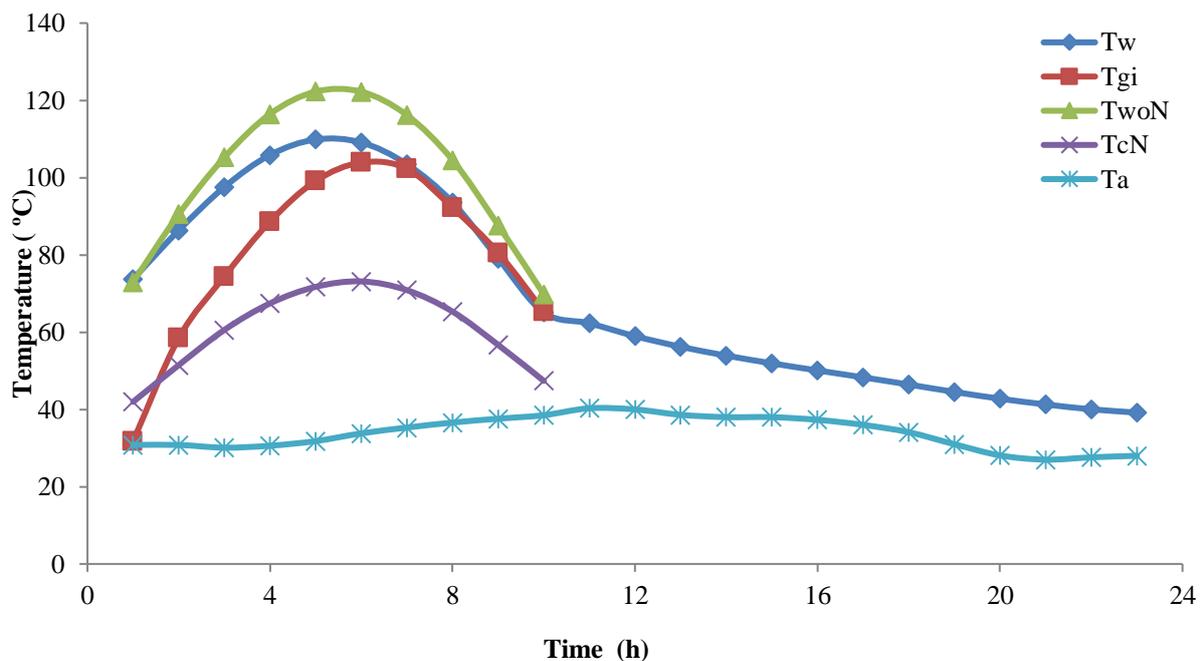


Fig. 4.7 Per hour variation of temperatures (T_w , T_{gi} , T_{woN} , T_{cN} and T_a) in May for a-Type days

Fig. 4.8 shows the variation of average thermal exergy of the proposed system at $N = 4$, the fluid flow is 0.02 kg/s, and the water depth 0.14m. It is clear from the figure that May has the highest value and pre-monsoon in March, April, and May. The thermal exergy increases with basin water temperature and post-monsoon in September and October. While in other

months it is decreasing and in February it has the lowest value. As the trend of the graph shows, the thermal exergy decreases with decreases in basin water temperature. It increases vice versa, which is apparent from April and September to an optimum level.

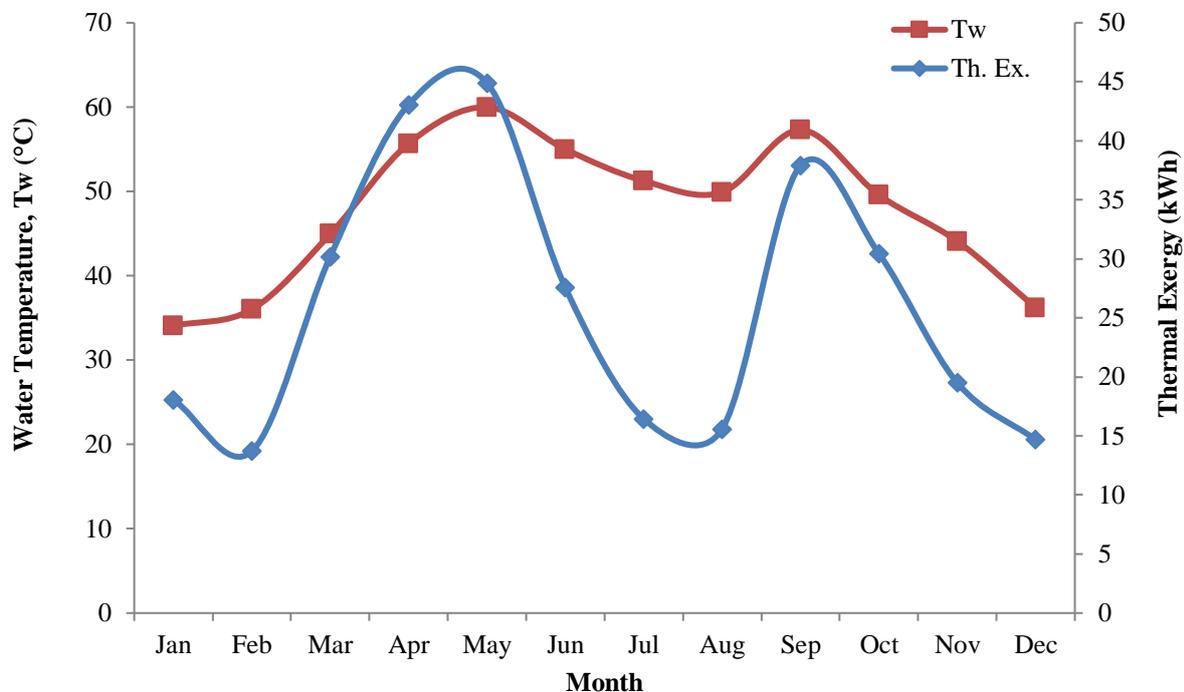


Fig. 4.8 Average thermal exergy vs T_w month wise

Fig. 4.9 shows the electrical exergy of the proposed system (system-A) at $N = 4$; the fluid flow is 0.02 kg/s and the depth of water 0.14m. The graph represents thermal exergy for month-wise for the same basin area compared to the previous research. The result shows that the influence of CuO nanoparticles in the helically coiled heat exchanger does not affect electricity generation due to photovoltaic thermal attached to the system. The average electrical exergy for the proposed system is significantly higher than the already existing system. The results appear- as: 11.22 kWh/month, 12.38 kWh/month, and 12.08 kWh/month 12.38 kWh/month (maximum) and 6.93kWh/month (minimum), which depend on the covering of the photovoltaic thermal system, which is 25% in the previous and the proposed system. These results can be further improved by increasing the coverage area by 50%, 75%, and 100%. The

proposed system can generate a sufficient amount of electricity used to operate the pump's motor to circulate water, and the rest can be stored for further use when there is no sunlight. So this system is called self-sustainable.

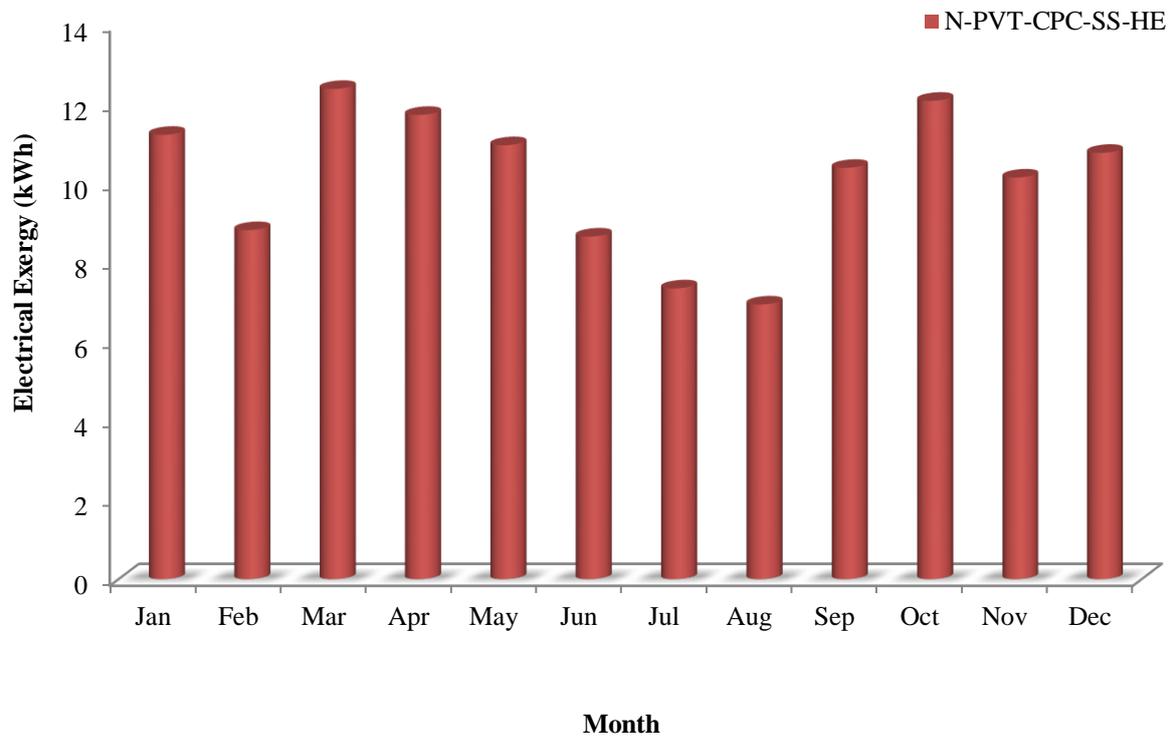


Fig.4.9 Mean electrical exergy month-wise

Fig. 4.10 represents the average value of potable water generation month-wise in kg for the proposed system at $N = 4$; the fluid flow is 0.02 kg/s and water depth 0.14 m . It is observed that the average yield of proposed system is higher than previous system, which occurs due to a higher amount of radiant energy permitted to fall on partly covered N identical photovoltaic compound parabolic concentrator collector's receiver surface. Therefore, the amount of heat added to the proposed system (N-PVT-CPC-SS-HE) is higher than the previous system (N-PVT-FPC-DS-HE).

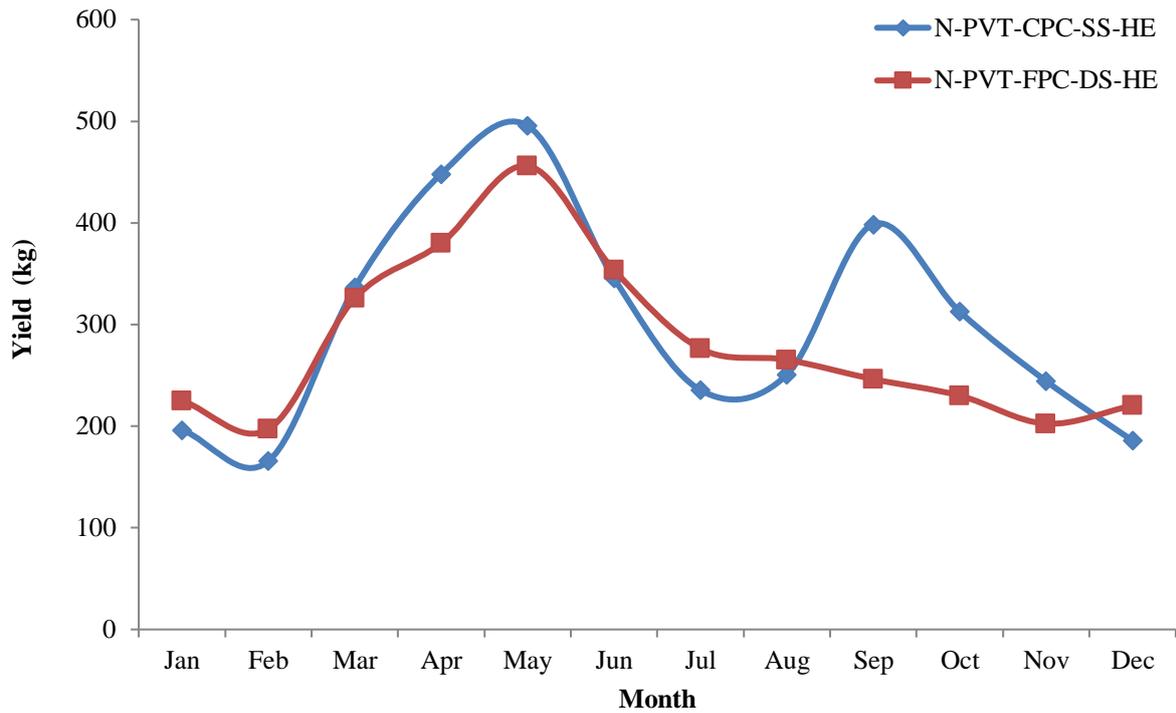


Fig. 4.10 Monthly variation in average yield in kg

Fig. 4.11 compares the present research to previous research [62]. The comparison reveals that the performance of the proposed system is much better than previous research. The proposed system uses CuO nanoparticles, annual yield in kg 3615.05 kg, and previous system [62] analyzed CuO , Al_2O_3 , TiO_2 nanofluids, water, and annual yield 3250.99, 3084.4, 2863.33, and 2735.11 kg, respectively. The enhancement in the percentage of the proposed system yield with the previous system is 11.19, 17.2, 26.25, and 32.17%, respectively. Table 3.5 shows the numerical representation in comparative form for a proposed and previous system based on yield.

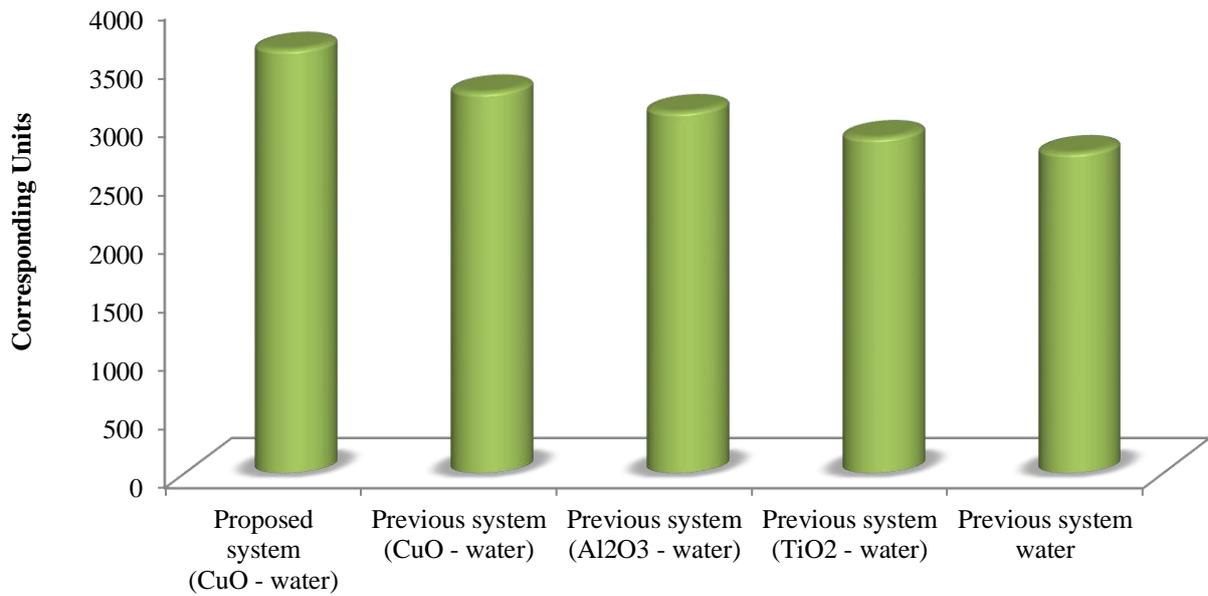


Fig. 4.11 Comparative analysis of proposed and previous system

Table 4.1

Enhancement in the daily thermal energy and thermal exergy of proposed and previous systems using CuO nanoparticles

System descriptions	Outputs				Enhancement %			
	CuO+Water	Al ₂ O ₃ +Water	TiO ₂ +Water	Water	CuO+Water	Al ₂ O ₃ +Water	TiO ₂ +Water	Water
Proposed system (N-PVT-CPC-SS-HE)								
Daily thermal energy (kWh)	15.99	-	-	-	16.75	51.13	61.82	80.67
Daily thermal exergy (kWh)	1.068	-	-	-	23.16	3.9	16.08	20
Previous system (N-PVT-FPC-DS-HE)								
Daily thermal energy (kWh)	13.7	10.58	9.88	8.85				
Daily thermal exergy (kWh)	1.39	1.11	0.92	0.89				

It is found that enhancement daily in thermal energy of the proposed system with CuO nanoparticles than the previous system with various nanofluids CuO, Al₂O₃, TiO₂, and water are found 16.75%, 51.13%, 61.82%, and 80.67% more significant correspondingly. The thermal exergy of the proposed system with CuO nanoparticles is more significant than the previous system with various nanofluids 16.08% for TiO₂, and 20% greater for water and 23.16%, 3.93% less for CuO, Al₂O₃ respectively.

Table 4.2

Enhancement in annual yield, obtained by proposed system and previous systems using CuO nanoparticles

System descriptions	Outputs				Enhancement %			
	CuO+Water	Al ₂ O ₃ +Water	TiO ₂ +Water	Water	CuO+Water	Al ₂ O ₃ +Water	TiO ₂ +Water	Water
Proposed system (N-PVT-CPC-SS-HE)								
Annual yield in kg	3615	-	-	-	11.19	17.2	26.25	32.17
Previous system (N-PVT-FPC-DS-HE)								
Annual yield in kg	3251	3084	2863	2735				

The enhancement in yield of the proposed system is obtained for CuO nanoparticles greater than the previous system with CuO 11.19%, Al₂O₃ 17.2%, TiO₂ 26.25%, and water 32.17%. The electrical exergy is almost the same as the previous system.

4.1b Energy and exergy analyses of 25% incorporating PVT-CPC active solar distiller unit (double slope) - Hourly variation of temperature in different sections of Nth double slope photovoltaic compound parabolic concentrator collector with helically coiled heat exchanger (N-PVT-CPC-DS-HE) proposed system (system-B) and (N-PVT-FPC-DS-HE) previous system (system-C) both systems are presented in Fig. 3.4 and Fig. 3.2. In these systems, the different temperatures of the proposed system are higher compared to the previous system.

Fig.4.12 shows the positive increment in basin water temperature for the proposed system by 5.97 °C/day for the same basin area compared to the previous research. The increasing trend of graph continuous up to May and the gap between the proposed and existing work is almost uniform. Hence, the influence of CuO nanoparticles in the helically coiled heat exchanger increases basin water temperature. The average daily basin water temperature for the proposed system is extensively enhanced than the previous system, i.e., 47.30 °C/day and 42.99 °C/day, respectively. The higher temperature is due to external thermal energy from PVT-CPC.

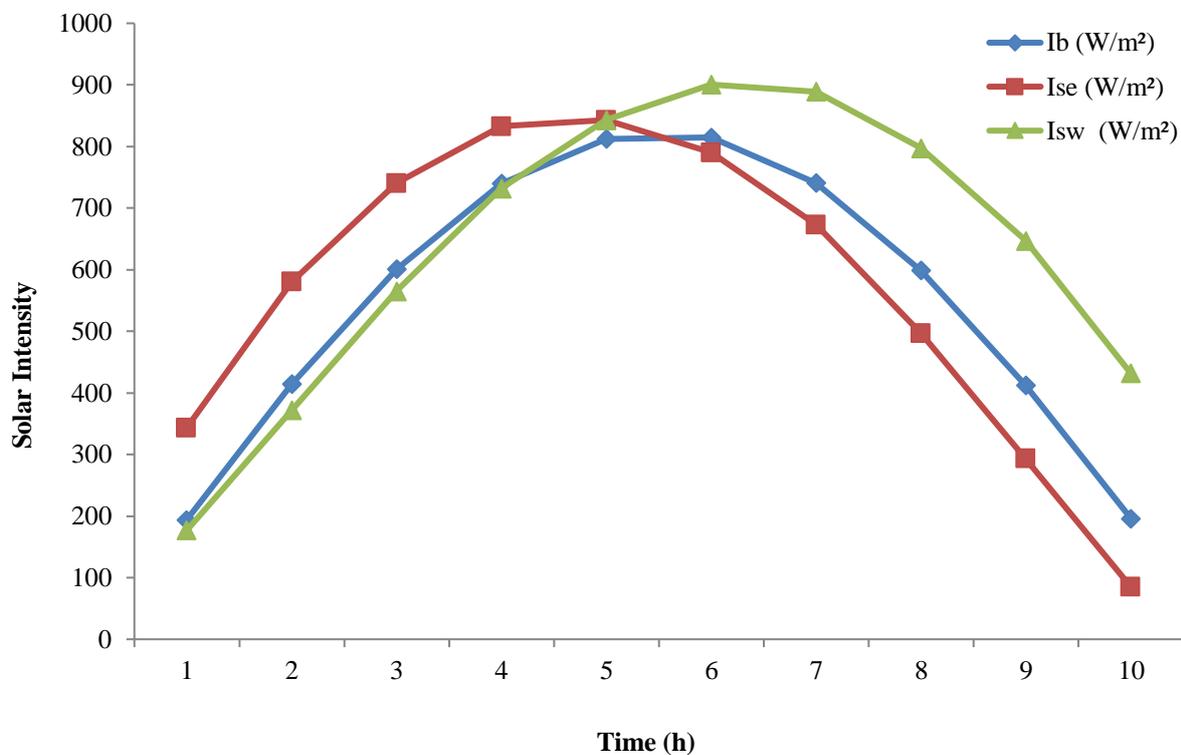


Fig.4.12 Per hour variation of solar radiation for New Delhi climatic conditions

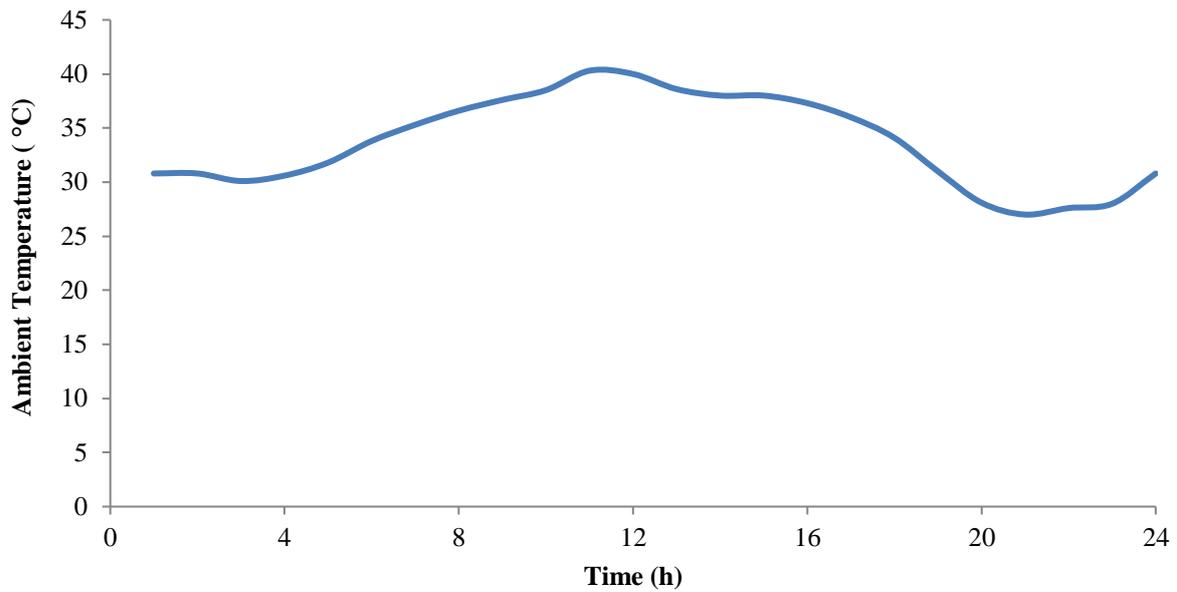


Fig.4.13 Per hour variation of ambient temperature in May for a-Type days

Fig. 4.14 shows the positive increment in basin water temperature for the proposed system by 5.97 °C/day for the same basin area compared to the previous research. The increasing trend of graph continuous up to May and the gap between the proposed and existing work is almost uniform. Hence, external thermal energy from PVT-CPC and influence of CuO nanoparticles in the helically coiled heat exchanger increases the temperature and conducts through it the basin water in an efficient manner. Average basin water temperature for the proposed system is extensively enhanced than the previous system, i.e., 47.30 °C /day and 42.99 °C /day, respectively.

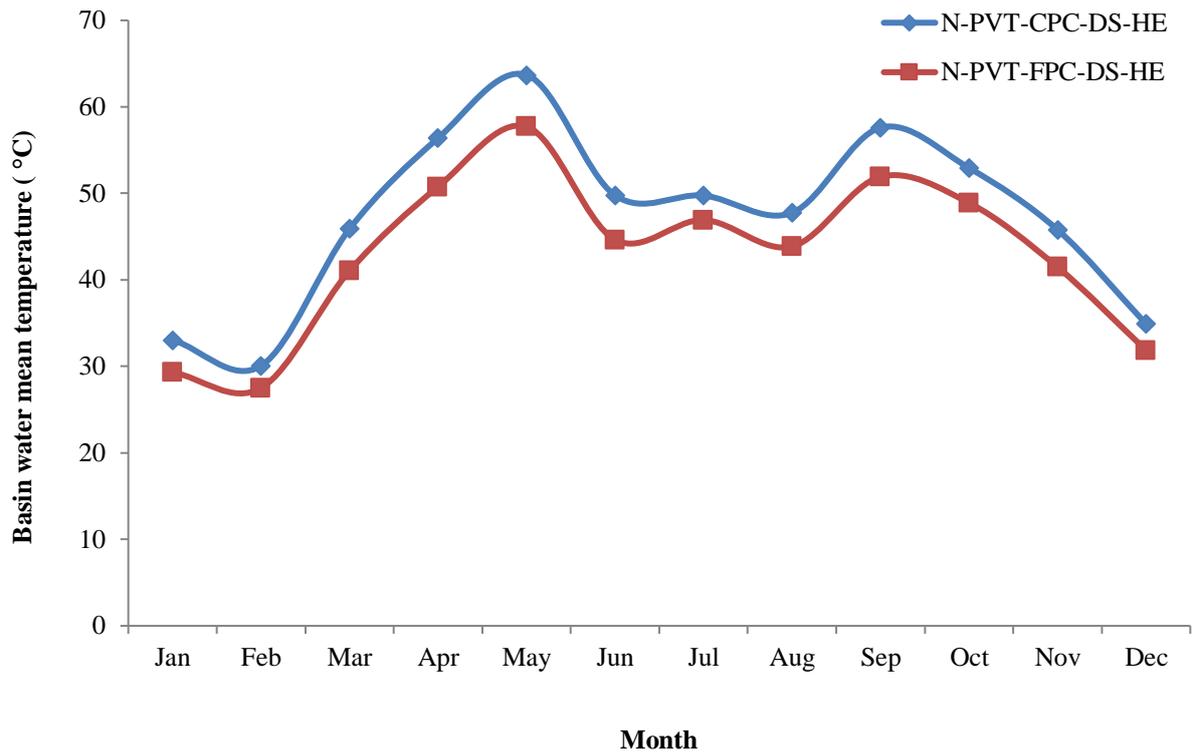


Fig.4.14 Monthly variation in temperature of basin water

Eastside inner glass temperature of proposed system is shown in Fig. 4.15; about 4.37°C/day increment is noticed for the same basin area compared to the previous research in May Inner glass temperature is increasing up to May, and also uniform gap between proposed and existing system is observed. Therefore, it is concluded that CuO nanoparticles in the helically coiled heat exchanger also influence inner glass temperature. The average inner glass temperature of the proposed unit is more extensively enhanced than the already existing system, and results appear as: 40.02°C/day and 37.24°C/day, respectively.

Similar trends were observed for westside inner glass temperature, as shown in Fig. 4.16. Maximum difference in westside inner glass temperature is 4.37 °C/day in May. average temperatures of proposed and previous systems are 39.96 °C/day and 37.23 °C/day, respectively.

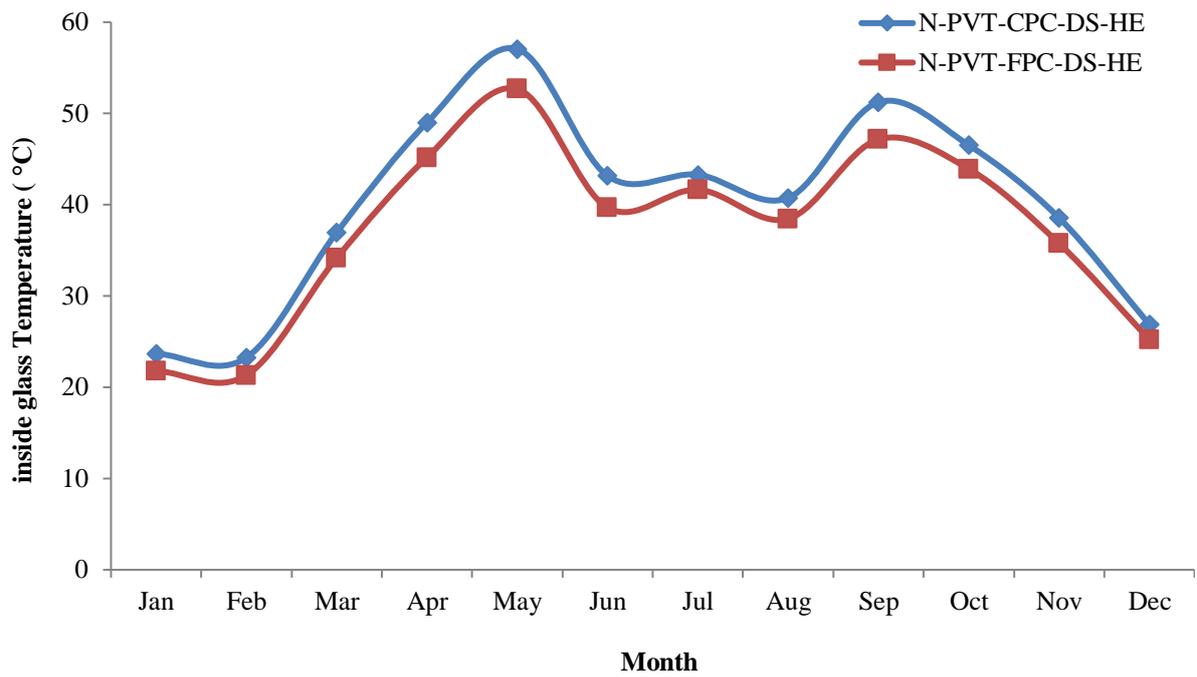


Fig.4.15 per month inside glass temperature variation in Eastside

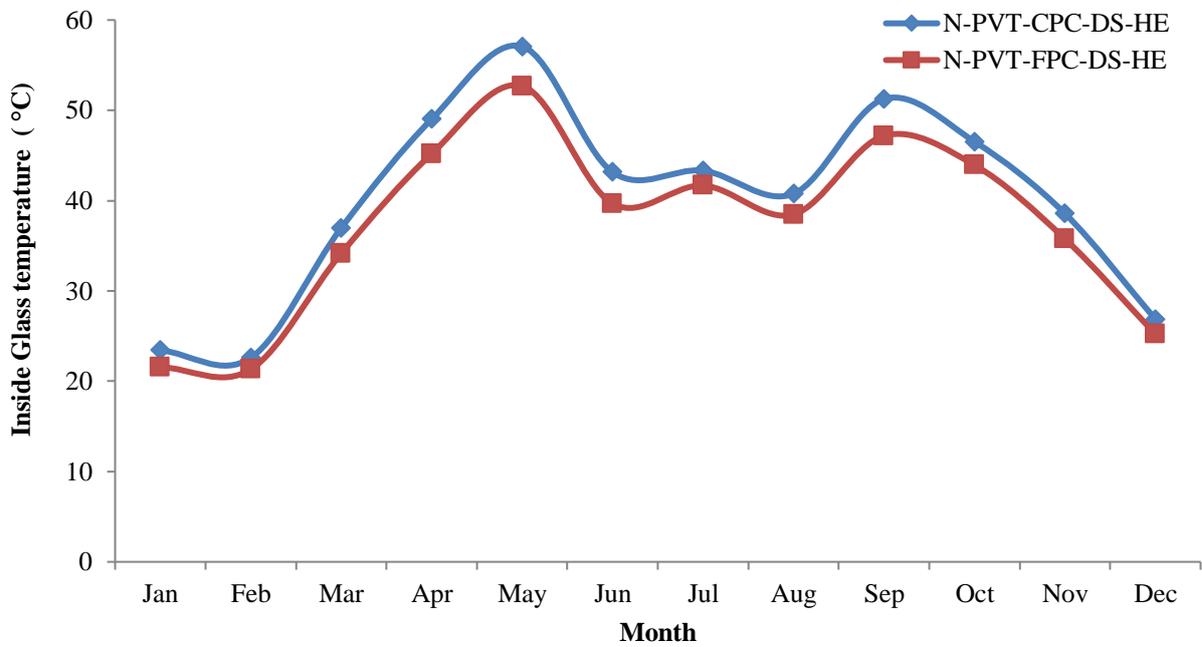


Fig.4.16 per month inside glass temperature variation in Westside

Fig. 4.17 shows the addition in heat energy on the east side for the proposed system 22.99 (kW/m²/day) compared to the earlier research for the same basin area for eastside. The daily average heat energy in basin water of proposed system is 165.7 kW/m²/day and 145.7 kW/m²/day in proposed and previous system correspondingly. Uniform gap between monthly average heat energy is maintained due to CuO nanoparticles in the helically coiled heat exchanger

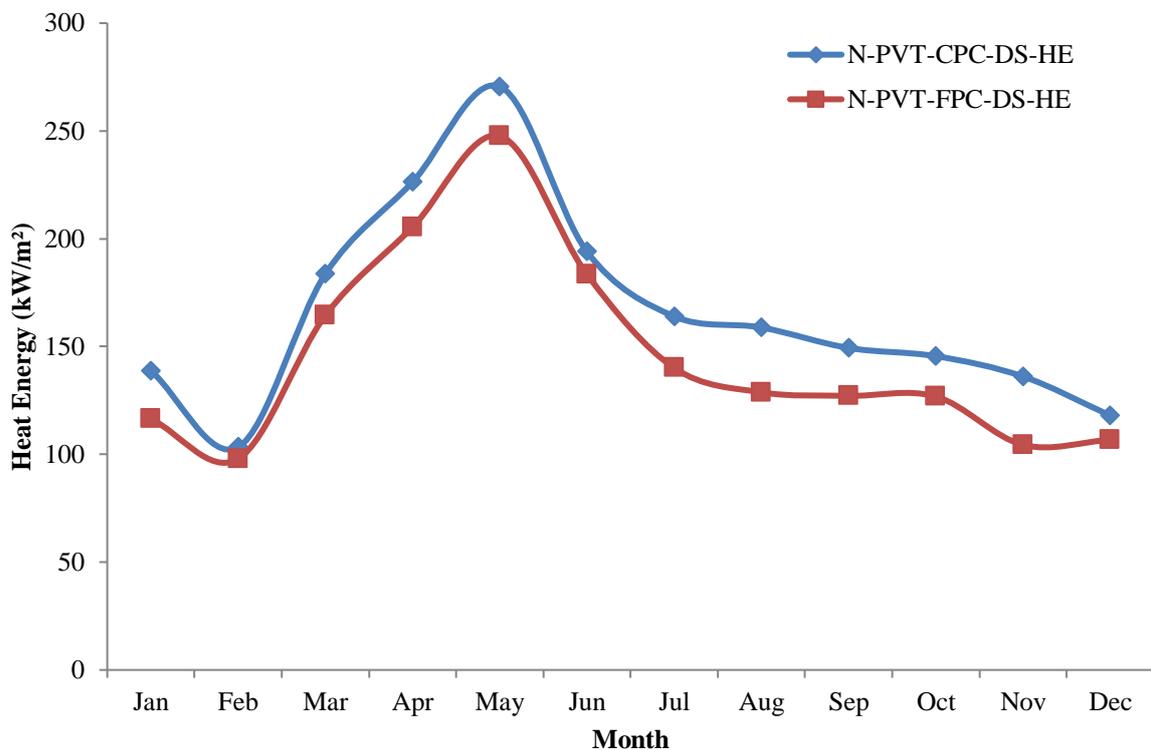


Fig.4.17 Monthly variation of heat energy (East side)

A similar tendency is observed in the westside basin heat energy (Fig. 4.18). In this case additional 22.95 kW/m²/day heat energy is noticed compared to the earlier research for the same basin area. It is also evident that there is significant heat gain to water by implementing CPC compared to FPC. Differences between prior work to existing work with a uniform gap

and Maximum and minimum average daily heat energy is 164.56kW/m²/day and 144.75kW/m²/day, respectively.

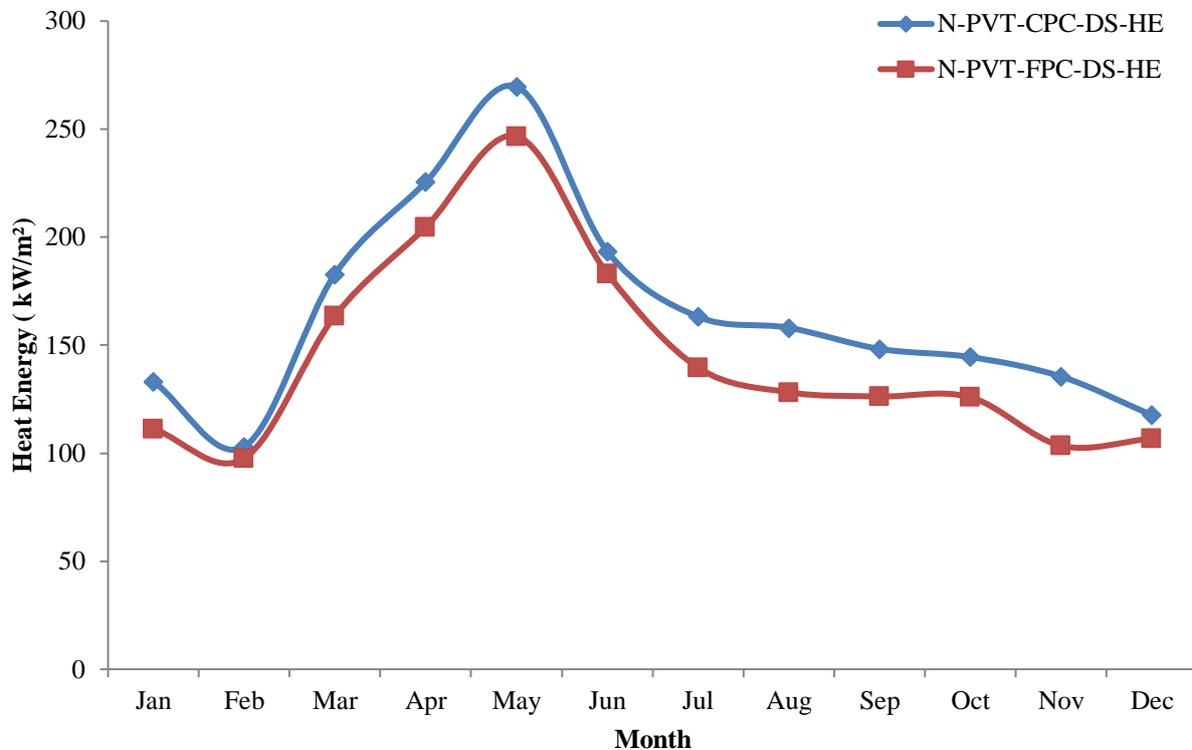


Fig.4.18 Monthly variation of heat energy in kW/m²(West side)

Fig. 4.19 shows the constructive augmentation in coefficient of heat transfer Eastside for the proposed system by 17.32 W/m²°C/day for the same basin area compared to the previous research. The increasing trend of the graph is continuous up to May and Fig. 4.19 shows the generalized gap between proposed and previous work is almost uniform. This increment is due to introducing CPC place of FPC. The average heat transfer coefficient for the proposed system is more extensively enhanced than the already existing unit, and results appear as: 37.52 W/m²°C per day and 30.54 W/m²°C per day, correspondingly.

Fig. 4.20 shows similar trend is noticed in the Westside for the proposed system by 17.31 W/m²°C/day for the same basin area is compared to the previous researcher. Average heat transfer coefficient basis for the proposed unit is extensively enhanced than the already existing

unit, and results appear as: 37.47 W/m²°C per day and 30.49 W/m²°C per day, correspondingly.

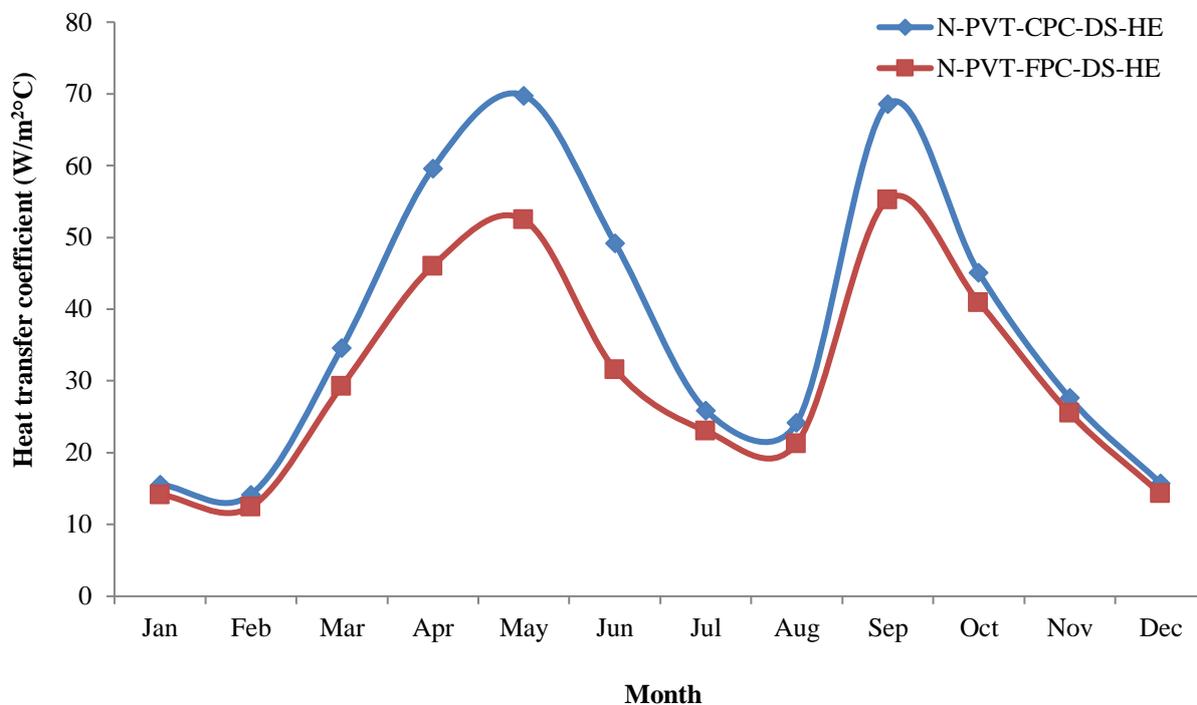


Fig.4.19 Monthly variation in heat transfer coefficient (East side)

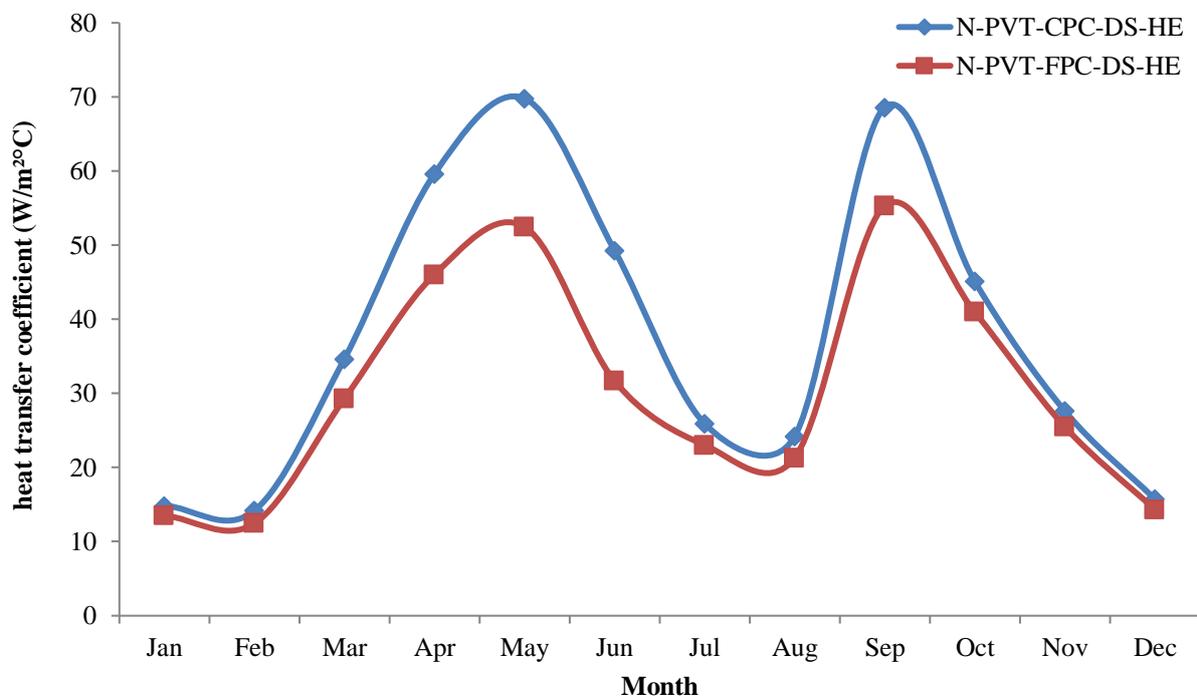


Fig.4.20 Monthly variation in heat transfer coefficient (west side)

Fig. 4.21 shows the electrical exergy for the proposed system for the same basin area compared to the previous research. Hence it can be predicted that the influence of CuO nanoparticles in the helically coiled heat exchanger does not affect electricity generation due to photovoltaic thermal attached to the system. The average electrical exergy daily for the proposed system appears- as: 11.22 kWh/month, 12.38 kWh/month, and 12.08 kWh/month 12.38 kWh/month (maximum) and 6.93kWh/month (minimum), which depend on the covering of the photovoltaic thermal system, which is 25% in the previous and the proposed system. These results can be further improved by increasing the coverage area by 50%, 75%, and 100%. The proposed system can generate a sufficient amount of electricity used to operate the pump's motor to circulate water, and the rest can be stored for further use when there is no sunlight. So this system is called self-sustainable.

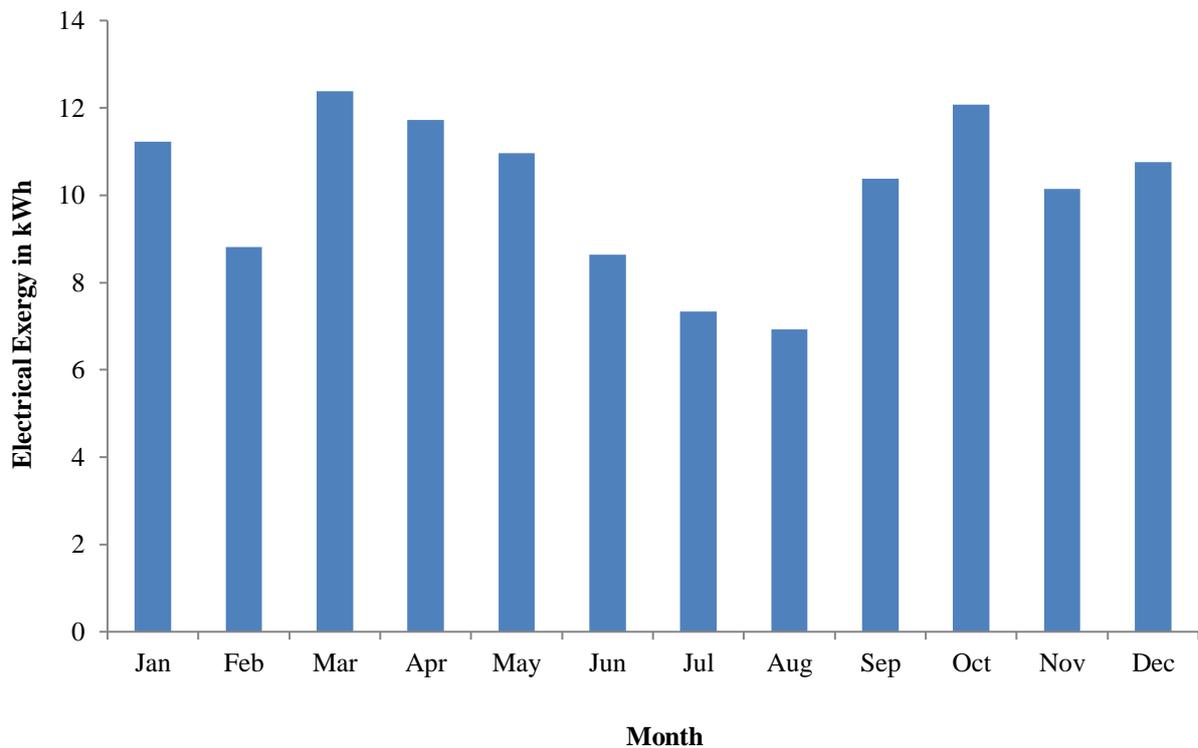


Fig.4.21 Mean electrical exergy

Fig. 4.22 shows the positive increment in thermal exergy for the proposed system 0.16 (kWh/day) for the same basin area compared to the previous research. Average thermal exergy

for the proposed unit is extensively enhanced than the already existing unit, and results appear as: 1.31kWh/day and 1.22 kWh/day, respectively.

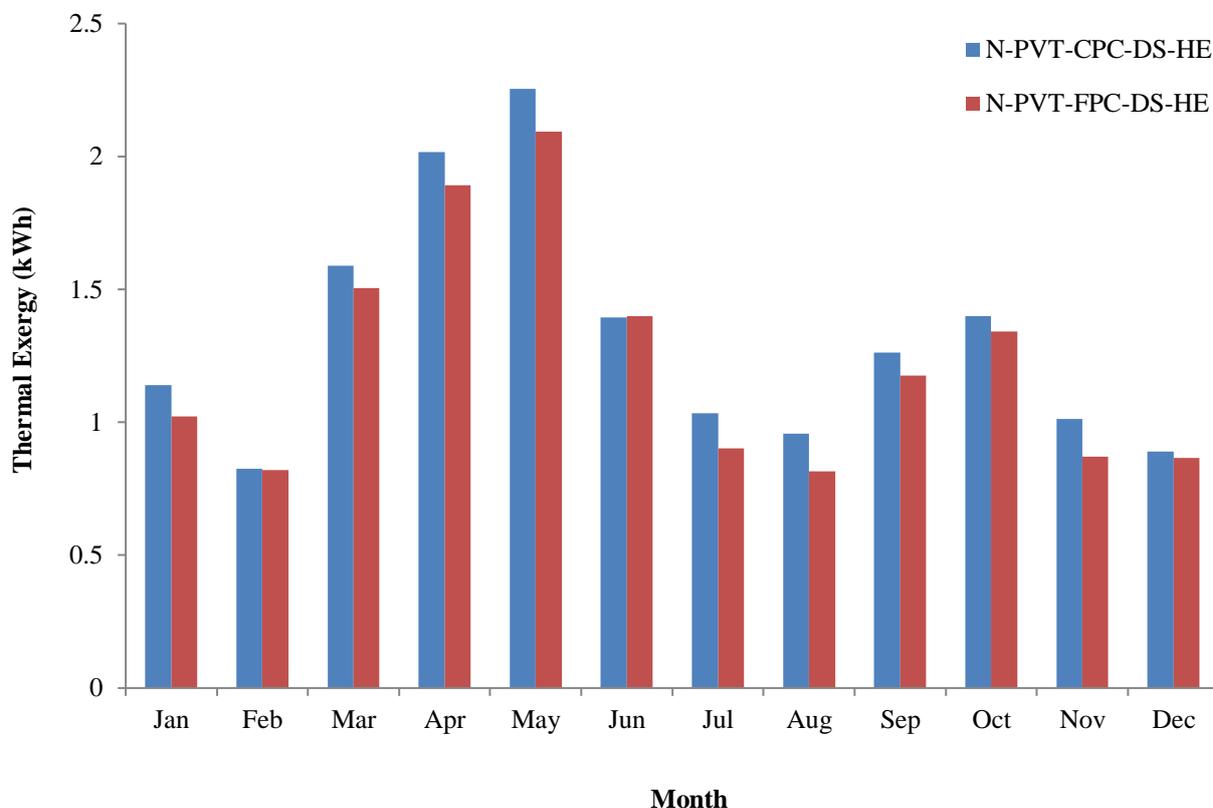


Fig.4.22 Monthly average variation in thermal exergy

Fig. 4.23 shows the positive increment in daily yield for the proposed system by 2.43 kg/day for the same basin area compared to the previous research. The daily average yield for the proposed unit is extensively enhanced than the already existing unit, and results appear as: 10.56 kg/day and 9.08 kg/day, respectively.

As the previous research has low value of yield, thermal energy and thermal exergy in case of FPC while the proposed research has CPC there is a countable increment in yield, thermal energy and thermal exergy, respectively. Remarkable enhancement is seen.

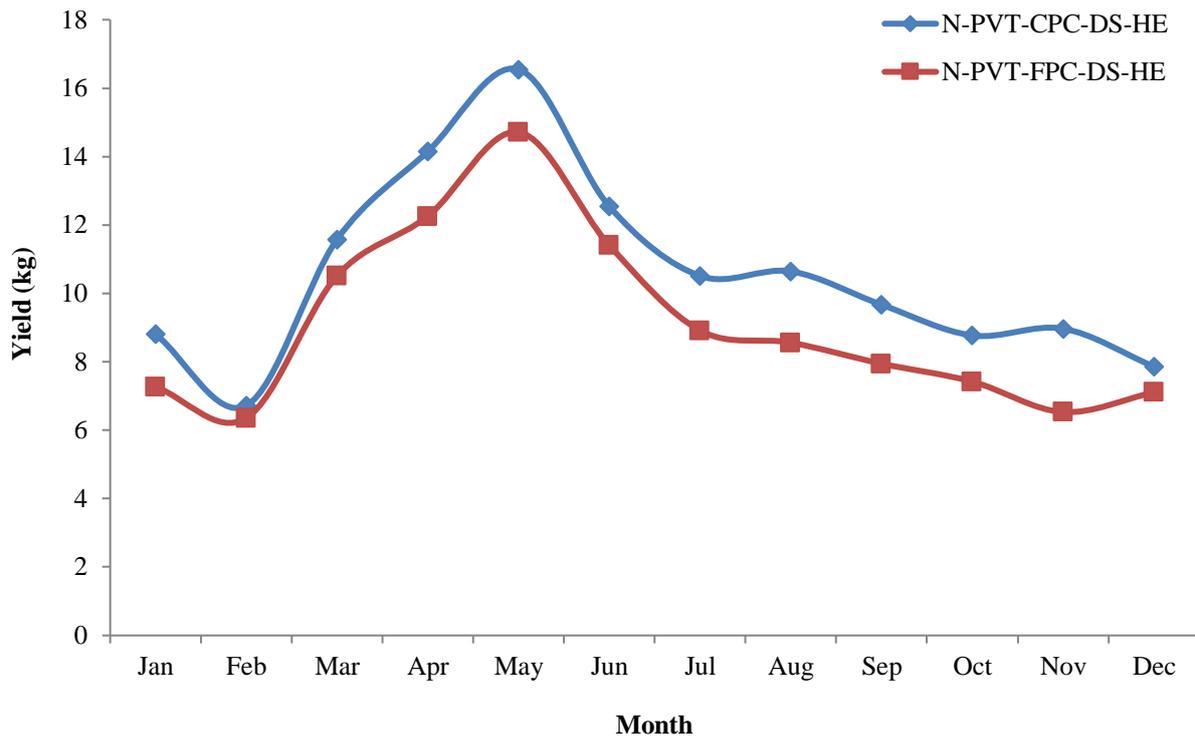


Fig.4.23 Daily yield of the proposed system

Table 4.3

Enhancement in average daily yield, average thermal energy and average thermal exergy of proposed system over the previous research

Parameters	Thermal energy, exergy and daily yield			Enhancement (%)		
	Thermal energy (kW/m ²)	Thermal exergy (kW/m ²)	Daily yield (kg)	Thermal energy	Thermal exergy	Daily yield (kg)
Proposed System	165.13	1.31	10.56	13.68	8.22	16.31
Previous Research [62]	145.25	1.21	9.08			

4.2a Energy matrices and life cycle cost analysis of active solar distiller (single slope)

– Relevant data and equations for ambient temperature and radiant energy for New Delhi

climatic conditions have taken input to MATLAB software to compute thermal energy, thermal exergy, energy and exergy based EPT, EPF, and LCCE for the life span of 30 and 50 years, have been computed. Annual exergy for system-A and system C is 312.07 kWh and 352.86 kWh, respectively. The amount of energy matrices based on energy and exergy for proposed system-B is better than system-C. EPT based on energy and exergy is 5.60% and 12.91% higher, respectively. EPF based on energy and exergy is relatively more minor: 5.93% and 14.82%, respectively. LCCE based on energy and exergy is appreciably greater than system-C: 13.63% and 5.20% for 30 and 50 years of life considered, respectively. Cost of distillate reduces more for system-A than system C. The distillate cost on an annual basis and life span basis for system-A is 1.59₹/kg and 0.288 ₹/kg, respectively, and for system-C 1.83 ₹/kg and 0.298 ₹/kg, respectively.

Fig. 4.1 represents the per hour variation of solar intensity and ambient temperature. The mean solar intensity is 401.8 kW for 275 clear days in a year in the meteorological conditions of New Delhi. The preliminary asset cost for establishments is \$930.76 and \$855.83 with corresponding embodied energies, i.e., 6060.85 kWh and 4606.08 kWh for system-A and system-C, respectively. Although system-A has improved distillate output by 7.0% compared to system-C, it has considerably more embodied energy. Also, the EPF of system-A is relatively less than system C, but its LCCE is appreciably greater than system C for 30 and 50 years of life considered for both the systems, as represented in Table 3.19 and 3.20.

Table 3.15 and Table 3.16 present the computation of embodied energy (E_{in}) for system-A and system-C, respectively. Cost of different components, Table 3.17 represents based on energy and exergy for system-A and system-C the payback time of energy(EPT), payback factor of energy (EPF), and life cycle cost analysis (LCCE),for 280 kg mass of water, $N = 4$ based on energy and exergy. The embodied energy of system-A is higher than system-C because the requirement of material for system-A is more due to the shape of CPC's. The value

of EPT based on energy and exergy 22.96% and 48.08% higher than system-C because embodied energy of system-A is greater about 31.58%, and annual exergy is reduced by 11.52% than system-C. The energy payback factor (EPF) based on energy and exergy for system-A is 18.67% and 32.79% lower than system-C.

Table 3.19 represents the computation of the life cycle cost efficiency (LCCE) for system-A and system-C for 280 kg, 100 kg mass of water, $N = 4$, and a fluid flow of 0.02 kg/s, and 0.03 kg/s. based on energy and exergy LCCE for system-A is higher by 5.08 % because the annual energy overall is greater by about 7%, and embodied energy is higher by 31.58%.

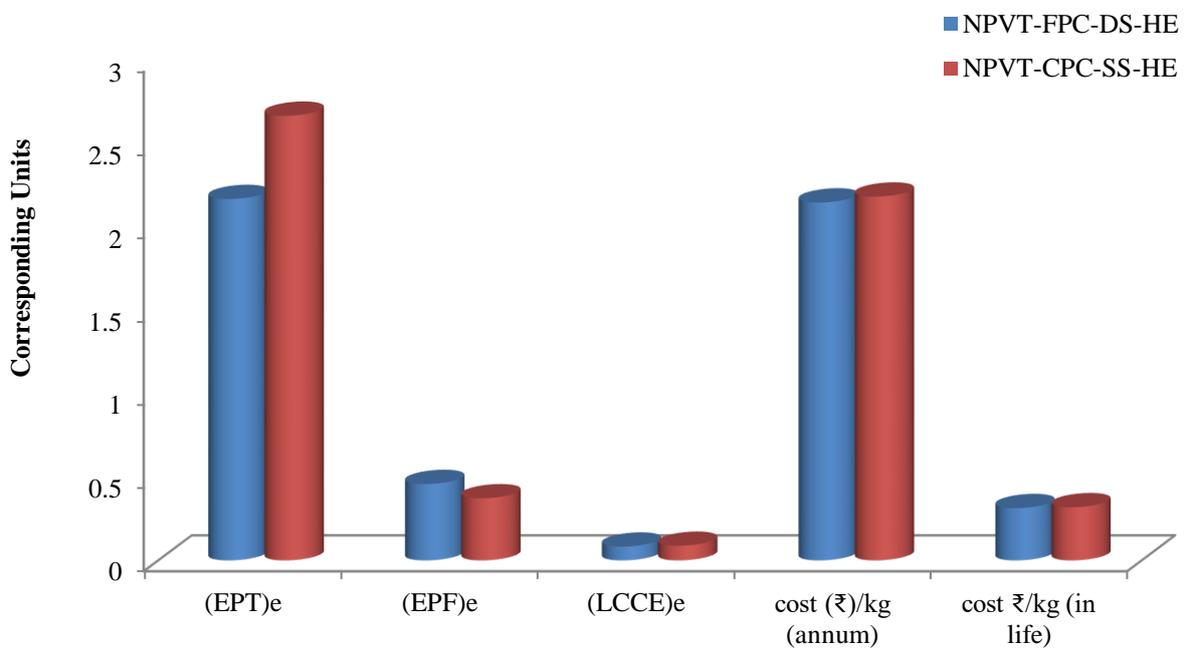


Fig.4.24 Energy matrices observations for the proposed systems based on energy

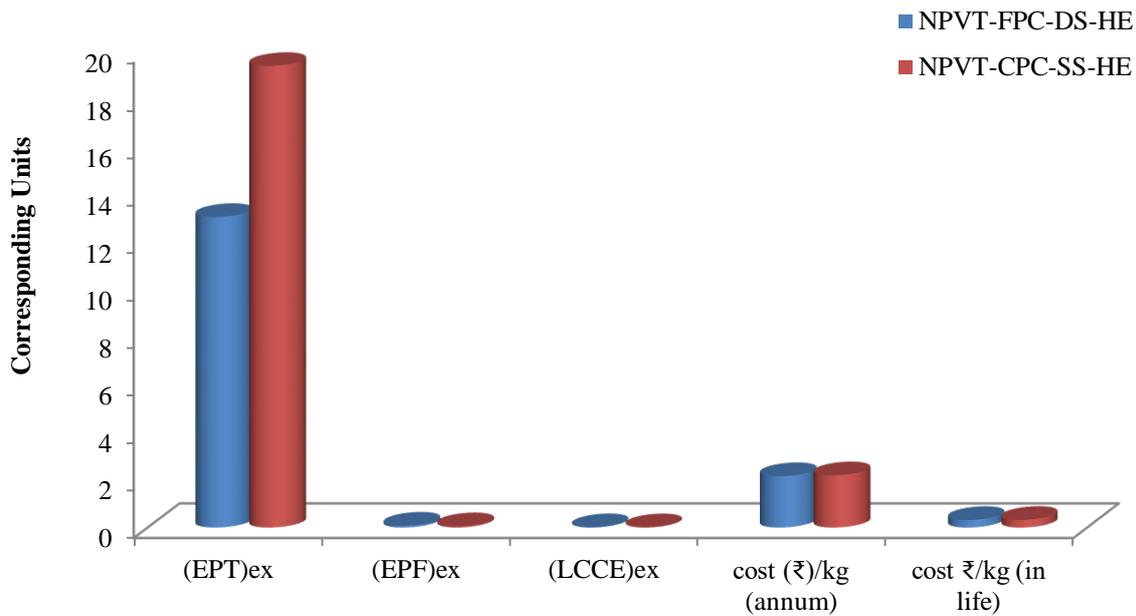
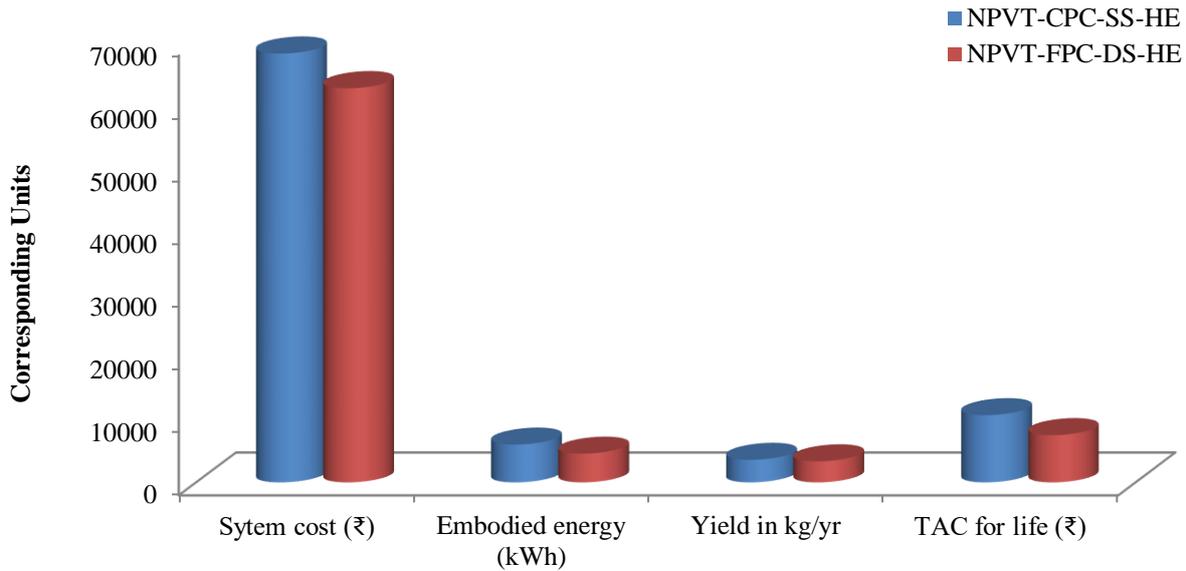


Fig.4.25 Energy matrices observations for the proposed systems based on exergy

Table 3.14 shows the capital investment for system-A and system-C. Economic observation of system-A and system-C has been computed based on 30 and 50 years for the interest rate of 5, 7, and 10%, respectively presented in Table 3.33, Table 3.34, Table 3.35, and Table 3.36. The value of TAC has been found minimum of 3% of the rate of interest as expected. The water generation cost has been computed and found to vary from 0.168 ₹/kg, 0.238 ₹/kg, and 0.344 ₹/kg for system-A, and 0.165 ₹/kg, 0.235 ₹/kg, and 0.338 ₹/kg for system-C respectively for the life span of 30 years, and from 0.157 ₹/kg, 0.223 ₹/kg, and 0.320 ₹/kg for system-A, and 0.155 ₹/kg, 0.219 ₹/kg, and 0.315 ₹/kg respectively for system-C for the life span of 50 years. The observation of water production cost has been made of system-C is lower than system-A. Fig. 4.26 shows the capital investment (₹), yield in kg per annum, embodied energy (kWh), and total annual cost (TAC) in (₹). This represents that the TAC is greater for system-A, than system-C while the yield of system-A is higher than system-C. Correspondingly, due to more components added, the cost of the distiller unit increases slightly for system-A.



Figs. 4.26 Economic observations for proposed system (system-A)

It costs \$ 930.67 due to the CPC attached to the flat plate collector as per the dollar rate (\$10.66). Therefore, even though it has more embodied energy, its overall economic establishment is more outstanding. Both the systems are self-sustainable and thus applicable for remote areas, especially solar-rich areas. System-A is eco-friendly and accelerates potable water production. This system can be commercialized based on investments. Economic studies based on design, material, and performance is required to fulfill the industrial and domestic potable water needs.

4.2b Energy matrices and life cycle cost analysis of active solar distiller (double slope) –Relevant data and equations for solar radiation and ambient temperature for climatic conditions New Delhi have been computed using MATLAB. The thermal energy, thermal exergy, payback time of energy (EPT), payback factor of energy (EPF), and life cycle cost efficiency (LCCE) for the life span of 30 and 50 years have been computed. The annual exergy for system-B and system C is 378.65 kWh and 352.86 kWh. The amount of energy matrices based on energy and exergy for proposed system-B is better than system C. EPT based on energy and exergy is 8.38% and 17.48% higher, respectively. EPF based on energy and exergy

is relatively more minor: 7.73% and 14.88%, respectively. LCCE based on energy and exergy is appreciably greater than system-B: 15.55%, 0.679% for 30 and 15.87%, 0.68 for 50 years of life considered, respectively. The cost of distillate reduces more for system-B than system C. The distillate cost on an annual basis and life span basis for system-B is 1.98₹/kg and 0.30 ₹/kg, respectively, and for system-C 2.44 ₹/kg and 0.338 ₹/kg, correspondingly.

Fig. 4.12 and Fig. 4.13 represent solar intensity and ambient temperature variations per hour. The mean solar intensity is 401.8 kW for 275 clear days in a year for the New Delhi meteorological conditions. The preliminary asset cost for establishments is \$883.11 and \$855.83 with corresponding embodied energies, i.e., 5675.57 kWh and 4606.08 kWh for system-B and system-C, respectively. Although system-B has improved distillate output by 16.31% compared to system-C, it has considerably more embodied energy. Also, the EPF of system-B is relatively less than system C, but its LCCE is appreciably greater than system C for 30 and 50 years of life considered for both the systems.

Table 3.27 presents the embodied energy (E_{in}) computation for system-B and system-C. Table 3.28 shows the cost of different components, and Table 3.29, Table 3.30, represent payback time of energy (EPT), payback factor of energy (EPF), and life cycle cost efficiency (LCCE) based on energy and exergy for system-B and system-C. Figs. 3.31 and Figs. 3.32 represents the EPT, EPF, LCCE, and cost analysis for 280 kg mass of water, $N=4$ based on energy and exergy. The embodied energy of system-A is higher than system-B because the requirement of material for system-A is more due to the shape of CPC's. The value of EPT based on energy and exergy 8.38% and 17.48% higher than system-B because embodied energy of system-A is greater than 26.07%, and yearly exergy is greater 7.3% than system-C. The energy payback factor (EPF) based on energy and exergy for system-A is 7.73% and 14.88% lower than system-B. Fig.4.27 and Fig. 4.28 show the life cycle cost efficiency (LCCE) for system-B and system-C for 280 kg, and 100 kg mass of water, $N=4$, and fluid

flow 0.02 kg/s, and 0.03 kg/s. It has been analyzed that LCCE based on energy and exergy for system-A is higher by 15.55% and 7.14%, respectively, because the energy is annually greater by 16.31%, and embodied energy is higher by 26.07%.

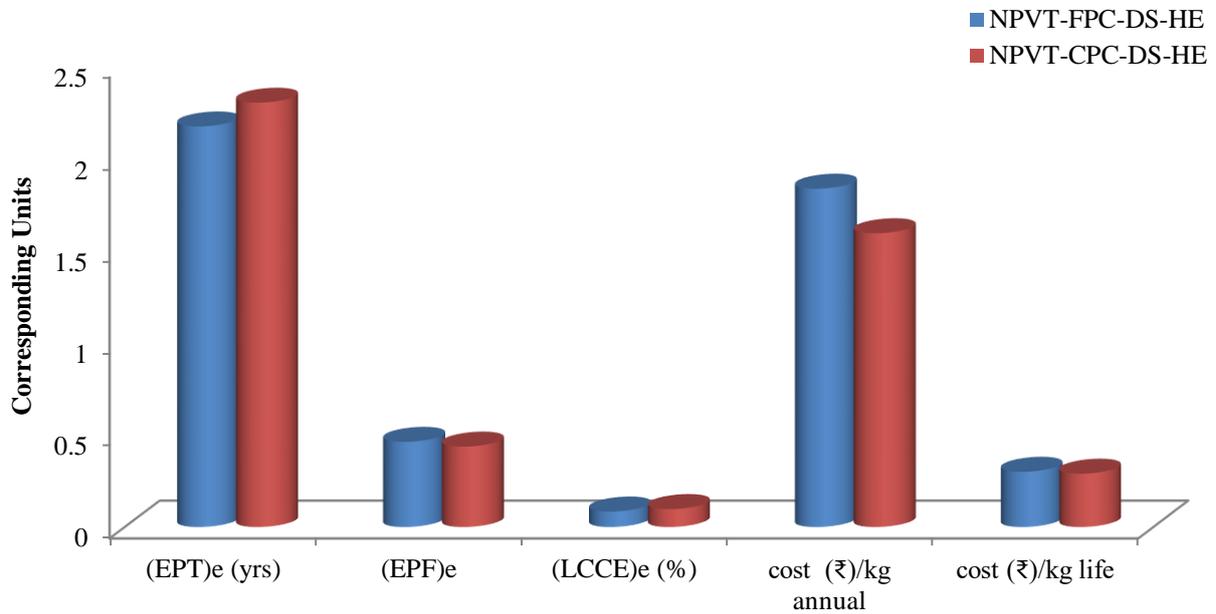


Fig.4.27 Energy matrices observations for the proposed systems based on energy

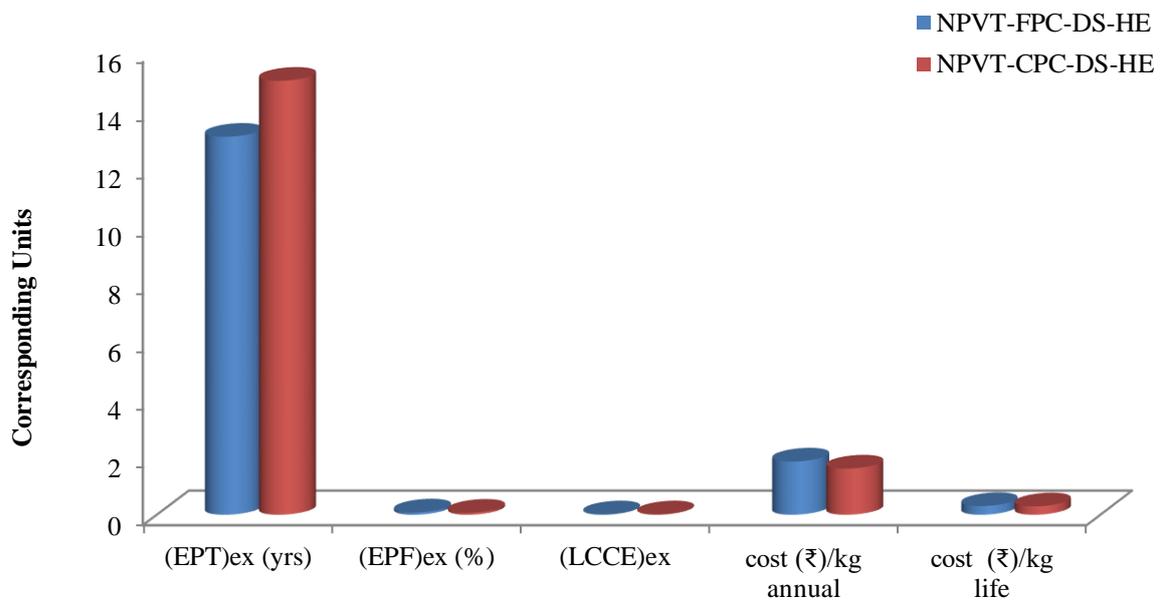
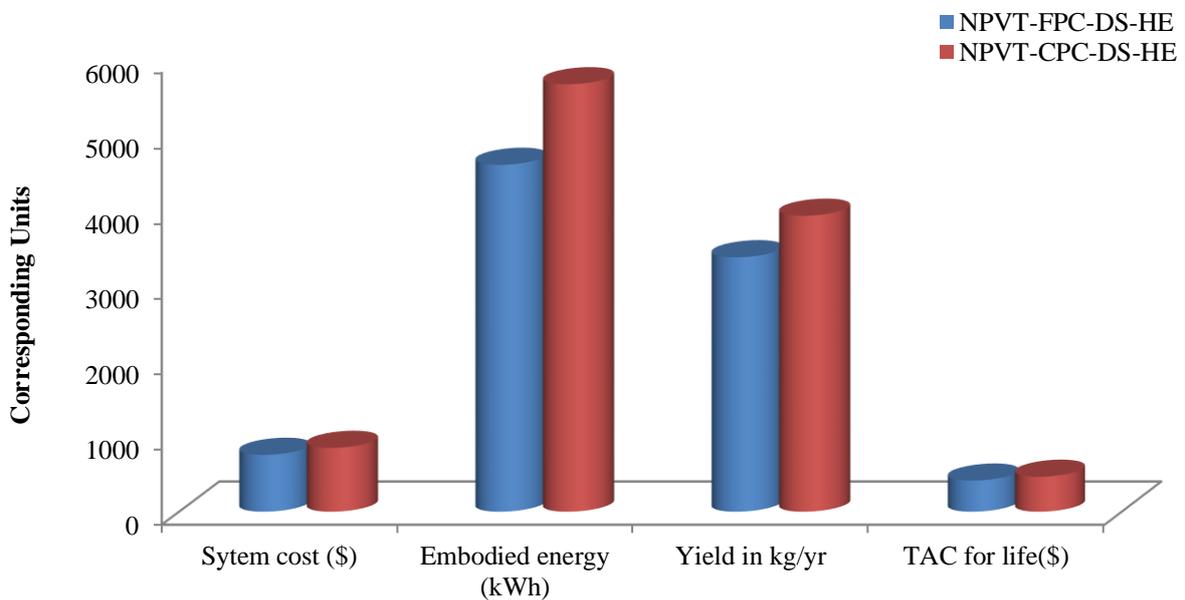


Fig.4.28 Energy matrices observations for the proposed systems based on exergy

Table 3.31, Table 3.32 Table 3.33, and Table 3.34 show the capital investment for system-A and system-B and TAC for both systems have been computed for 30 and 50 years for the interest rate of 5, 7, and 10%, respectively, as presented in Table 3.32, Table 3.33, Table 3.34, and Table 3.35. As expected, the lowest amount of TAC has been found on 5% interest rate. Water production cost varied from 0.146₹ to 0.30₹ for system-B, and from 0.165₹ to 0.338₹ for system-C, respectively; for system-B for life span of 30 years and from 0.137₹ to 0.279₹ for system-B, and from 0.155₹ to 0.315₹ for system-C, respectively; for system-B for 50 years at an interest rate of 5, 7, and 10%, respectively. The water production cost has been observed for system-B is lower than system-C. Figs.4.29 shows the capital investment, yield per kg in a year, embodied energy and total annual cost (TAC) in \$. This represents that the TAC for system-B is higher than system-C while the yield of system-B is higher than system-C.



Figs. 4.29 Economic observations for proposed system (system-A)

The cost of the distiller unit increases slightly for system-B due to more components added. It costs \$883.11 due to the CPC attached to the flat plate collector as per the dollar rate

(\$73.33). Therefore, even though it has more embodied energy, its overall economic establishment is more outstanding. Both the systems are self-sustainable and thus applicable for remote areas, especially solar-rich areas. System-B is eco-friendly and accelerates the production of potable water. This system can be commercialized based on investments. Economic studies based on design, material, and performance is required to fulfill the potable water needs of industrial and domestic.

4.3a Economic analysis of 25% partly incorporating (N-PVT-CPC-HE) active solar distiller (single and double slope) -As results are shown for 15, 20, 30, and 50 years in Table 3.42 and Table 3.43 found that the cost of distillate depends on rate of interest. Interest rate increases will increase price of distillate per annum, while system life increases will decrease the cost of distillate. For system-A at interest rate of 5, 7, and 10% for 15, 20, 30, 50 years the cost of distillate are 1.916, 2.233, and 2.734 (₹/ kg), and 1.627, 1.956, 2.483(₹/ kg), and 1.355, 1.709, and 2.279 (₹/ kg), and 1.170, 1.563, and 2.186 (₹/ kg) respectively. For system-B at interest rate of 5, 7, and 10% for 15, 20, 30, 50 years the cost of distillate are 1.672, 1.949, and 2.387 (₹/ kg), and 1.420, 1.708, 2.167(₹/ kg), and 1.134, 1.431, and 1.909 (₹/ kg), and 0.980, 1.309, and 1.830 (₹/ kg) respectively.

For system-C at interest rate of 5, 7, and 10% for 15, 20, 30, 50 years the cost of distillate are 1.885, 2.197, and 2.690 (₹/ kg), and 1.601, 1.935, 2.443(₹/ kg), and 1.175, 1.482, and 1.977 (₹/ kg), and 1.015, 1.356, and 1.896 (₹/ kg) respectively.

It is found that as per cost of distillate, system-B performance is better than system-A and system-C, and system-C is better than system-A.

4.3b Environ-economic analysis 25% partly incorporating (N-PVT-CPC-HE) active solar distiller (single and double slope) – Fig. 4.30 shows environ-economic analysis of system-A (N-PVT-CPC-SS-HE), system-B (N-PVT-CPC-DS-HE), and system-C (N-PVT-FPC-DS-HE) [64] for 15 years.

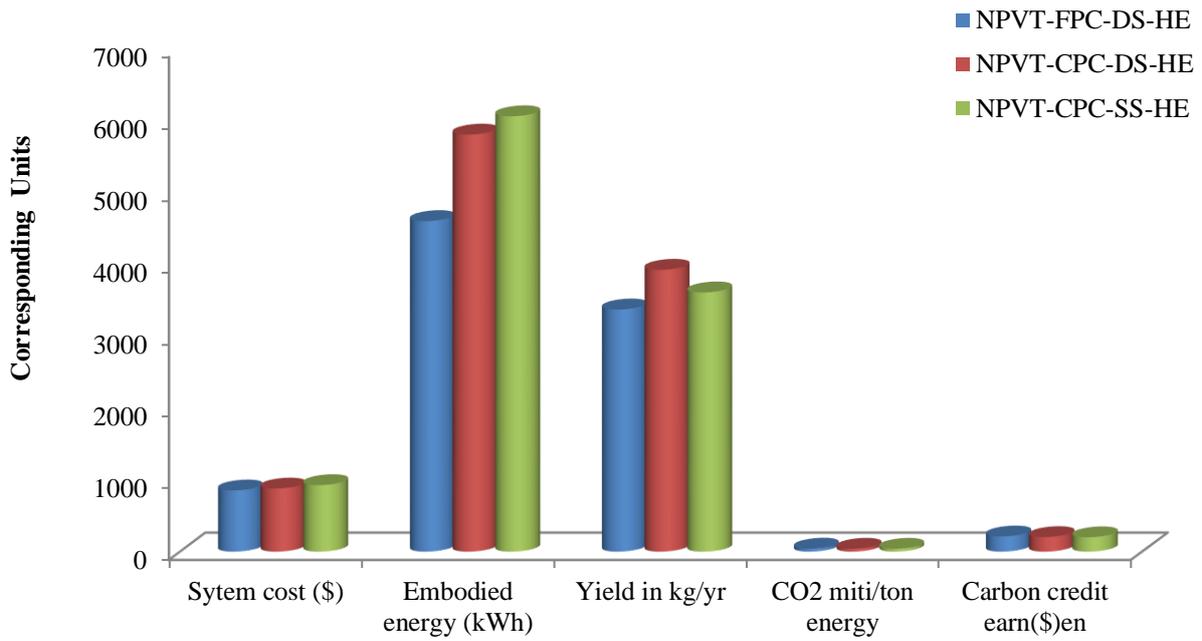


Fig. 4.30 Environ-economic analysis for 15 years

Fig.4.31 shows environ-economic analysis of system-A (N-PVT-CPC-SS-HE), system-B (N-PVT-CPC-DS-HE), and system-C (N-PVT-FPC-DS-HE) [64] for 20 years.

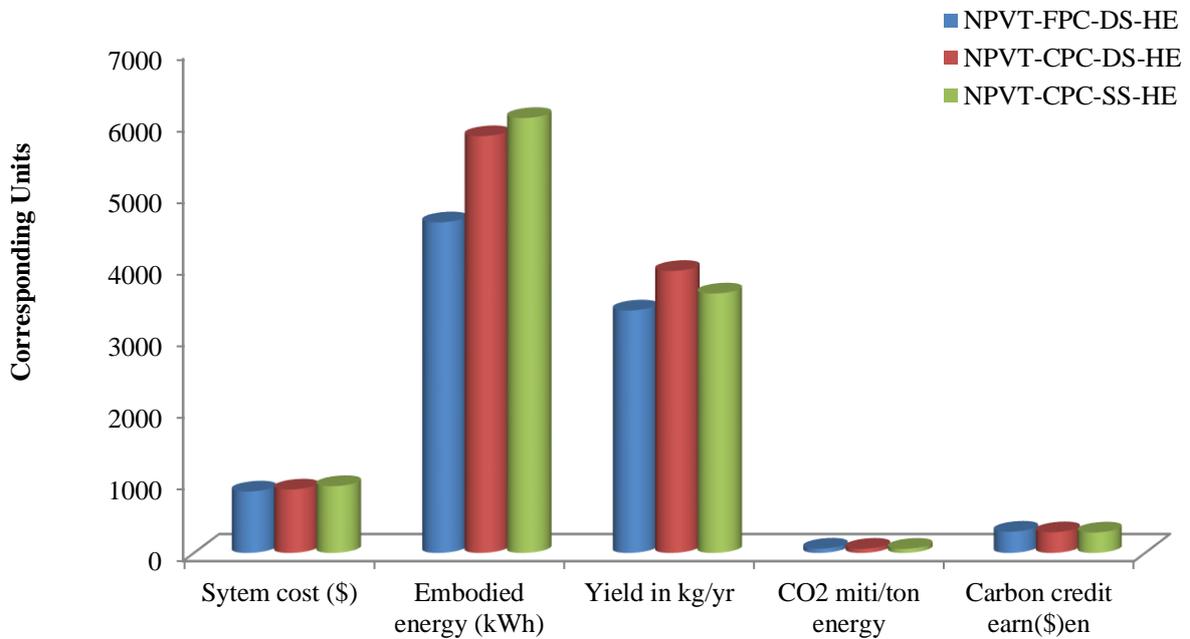


Fig. 4.31 Environ-economic analysis for 20 years

Fig. 4.32 shows environ-economic analysis of system-A (N-PVT-CPC-SS-HE), system-B (N-PVT-CPC-DS-HE), and system-C (N-PVT-FPC-DS-HE) [64] for 30 years.

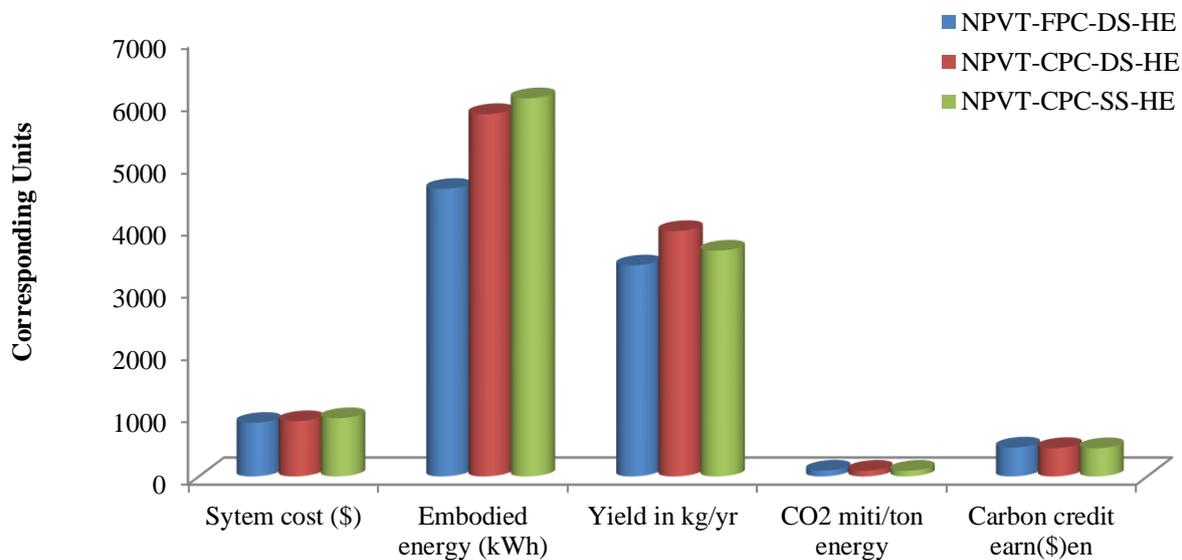


Fig. 4.32 Environ-economic analysis for 30 years

Fig. 4.33 shows environ-economic analysis of system-A (N-PVT-CPC-SS-HE), system-B (N-PVT-CPC-DS-HE), and system-C (N-PVT-FPC-DS-HE) [64] for 50 years.

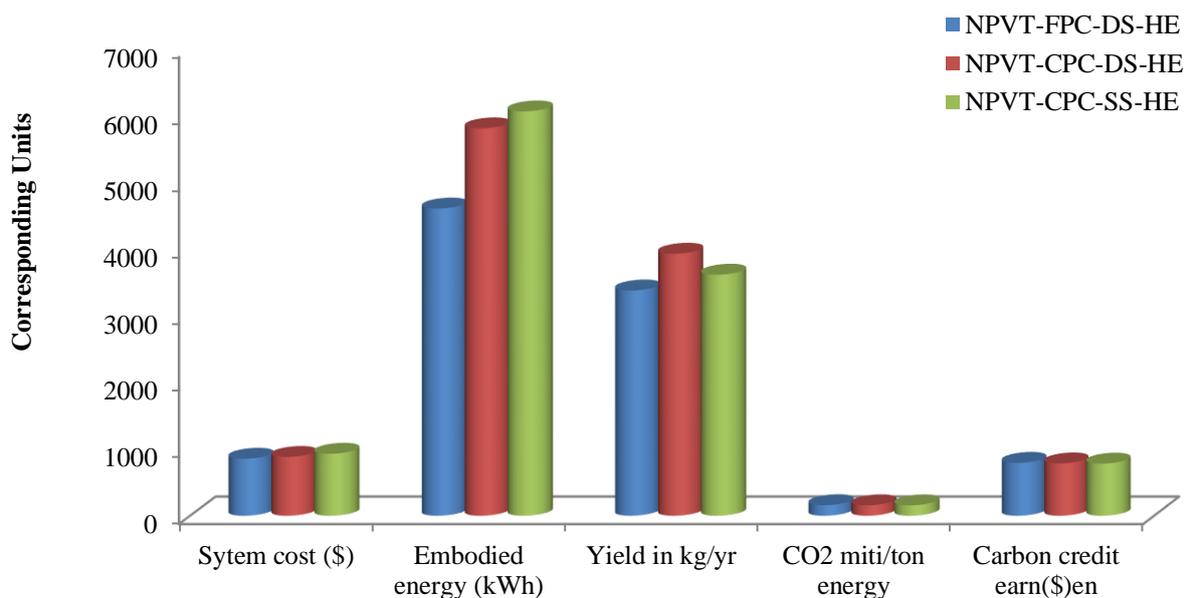


Fig. 4.33 Environ-economic analysis for 50 years

CO₂ mitigation per ton for system-A for 15, 20, 30, 50years are as 40.24, 56.85, 90.06, and 156.49, respectively; system-B are 40.85, 57.46, 90.67, and 157.10, respectively, and; system-C is 42.54, 59.15, 92.36, and 158.79 respectively. Therefore system-A is environ-economic than system-B and system-C and also system-B is better than system-C.

Carbon credit earned based on energy for system-A for 15, 20, 30, 50years are 201.22, 284.25, 450.31, and 782.45, respectively; system-B are 204.26, 287.30, 453.36, and 785.49, respectively, and system-C are 212.71, 295.75, 461.81, and 793.94 respectively show that the system-C is more environ-economic than system-A and system-B, and system-B is more environ-economic than system-A respectively. Because the cost of system-A is high, the embodied energy of system-A is higher. Therefore, the carbon credit earned is less and system-B and system-C simultaneously, as represented in Fig. 4.30, 4.31, 4.32, and 4.33, respectively.

4.3c Exergoeconomic analyses of 25% partly incorporating (N-PVT-CPC-HE) active solar distiller (single and double slope) -

Exergoeconomic analyses of N-PVT-FPC/CPC collector active solar distiller a heat exchanger of helically coiled using CuO nanoparticles of single and double slope at rate of interest 10% for 15 years are shown in Fig 4.34. Exergoeconomic analyses of N-PVT-FPC/CPC active solar distiller with helically coiled heat exchanger using CuO nanoparticles for single and double slope are illustrated in Fig 4.35 at rate of interest 10% for 20 years. Exergoeconomic analyses of N-PVT-FPC/CPC active solar distiller with helically coiled heat exchanger using CuO nanoparticles for single and double slope at rate of interest 10% for 30 years are shown in Fig 4.36.

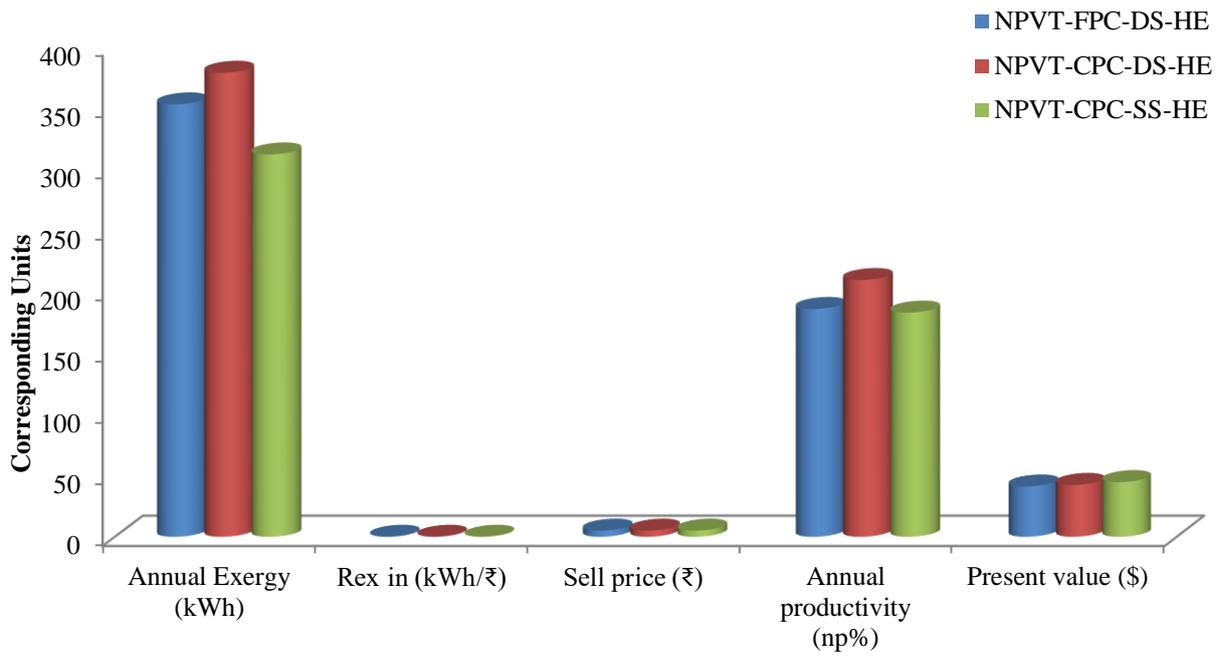


Fig 4.34 Exergoeconomic analyses for 15 years

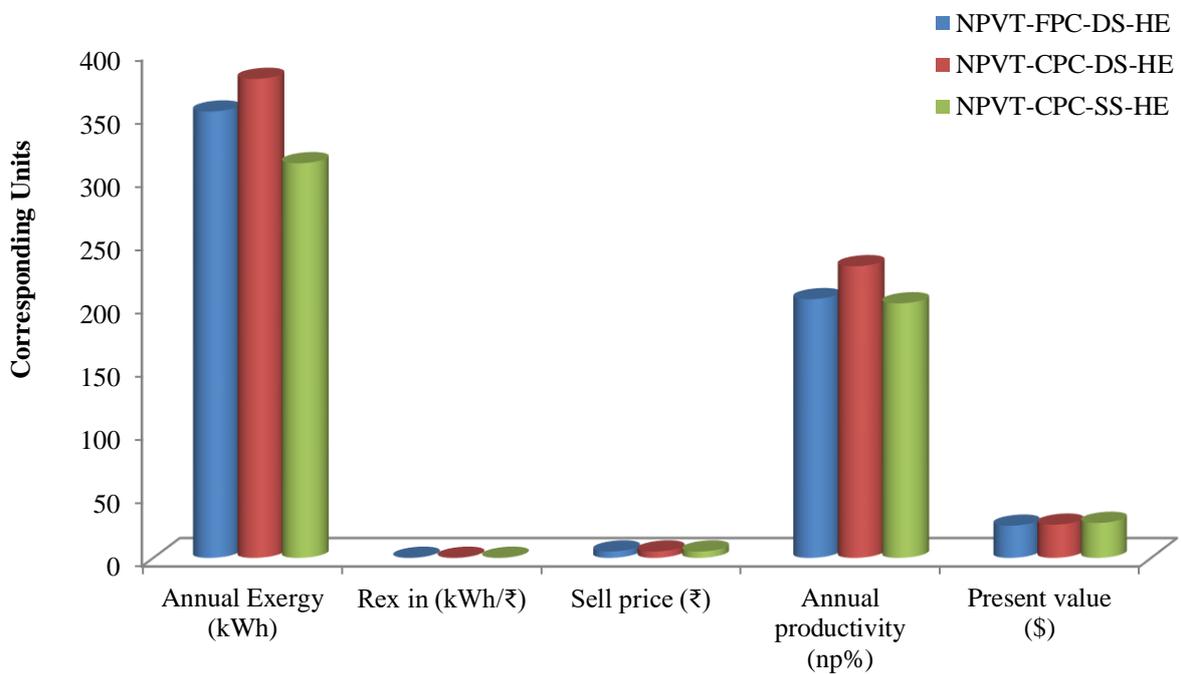


Fig 4.35 Exergoeconomic analyses for 20 years

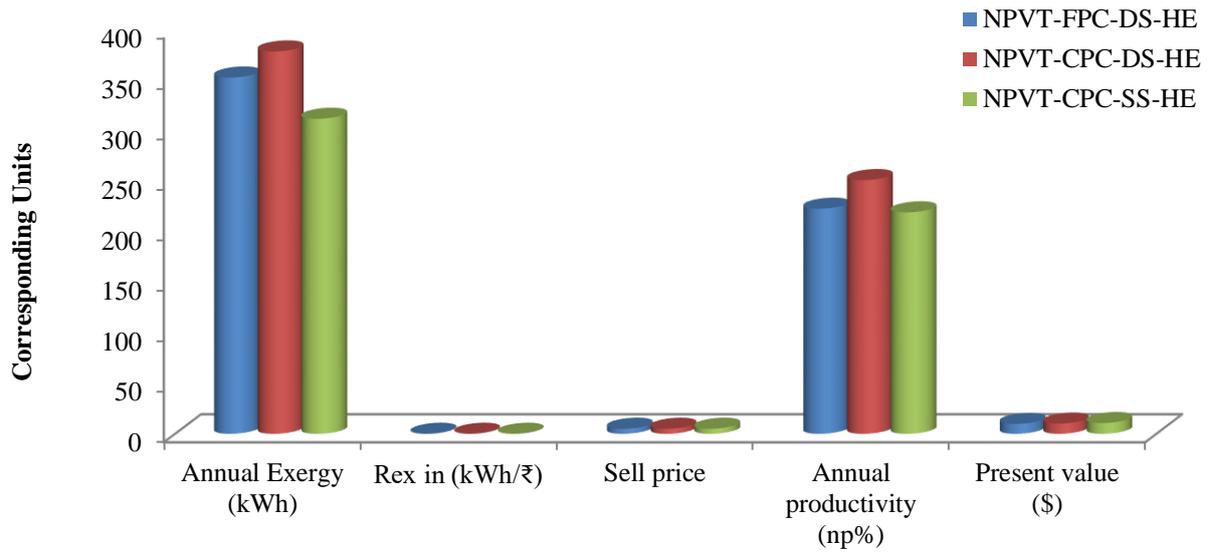


Fig 4.36 Exergoeconomic analyses for 30 years

Exergoeconomic analyses of N-PVT-FPC/CPC active single and double slope solar distillation with heat exchanger (helically coiled) using CuO nanoparticles at rate of interest 10% for 50 years are shown in Fig 4.37.

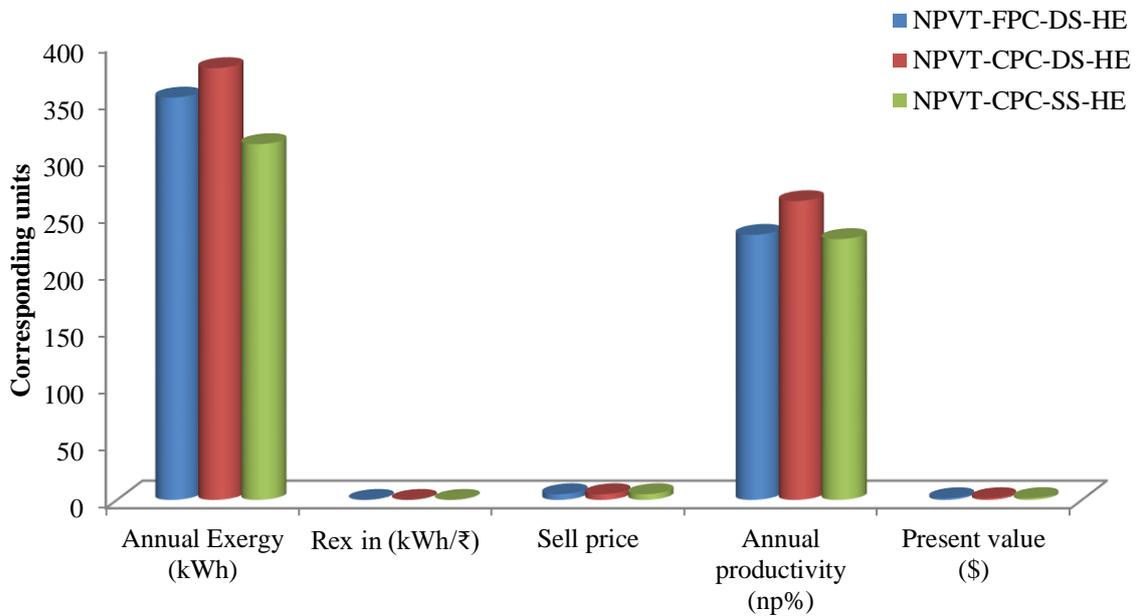


Fig 4.37 Exergoeconomic analyses for 50 years

Exergoeconomic analysis based on exergoeconomic parameter (Rex) kWh/₹ of the system-A for 15, 20, 30, 50years are 0.0312, 0.0344, 0.03746, and 0.03906, respectively; system-B are 0.0399, 0.0440, 0.04791, and 0.04996 respectively; and system-C are 0.0384, 0.0423, 0.04607, and 0.04804 respectively show that the system-A is more economic than system-B and system-C, than system-B respectively. Therefore system-A is better than system-B, system-C.

According to annual productivity(%) of the system-A for 15, 20, 30, 50years are 182.81, 201.31, 219.33, and 228.72, respectively; system-B are 209.44, 230.63, 251.28, and 262.04, respectively; and system-C are 185.80, 204.60, 222.92, and 232.46 respectively show that the system-B is more productive than system-A and system-C, and system-C is more than system-A respectively. Because the exergy of system-B is high, the productivity of system-A is higher and system-A, and system-C is simultaneously low.

According to present value (\$) the system-A for 15, 20, 30, 50years are 44.56, 27.67, 10.66, and 1.58 respectively, system-B are 42.28, 26.25, 10.12, and 1.50 respectively, and system-C are 40.97, 25.44, 9.81, and 1.46 respectively. Based on present value with an interest rate of 10%, system-A is better than system-B and system-C. The system-B is better than system-C, respectively.

The exergoeconomic parameters, annual productivity, and present value based on selling price (₹) 5 are represented in Fig. 4.34, 4.35, 4.36, and 4.37, respectively.

CONCLUSION AND FUTURE SCOPE**5.1 Conclusions**

The proposed systems have been studied based on the temperature of the basin, collector outlet temperature, thermal energy, exergy, electrical exergy, and yield to be higher using CuO nanoparticles in the order followed as $\text{CuO} > \text{Al}_2\text{O}_3 > \text{TiO}_2 > \text{water}$. Moreover, the proposed system is better than the previous system. The temperature differences are also better than in the previous study.

The following concluding remarks are observed by annual analysis of the proposed systems energy, exergy, and yield with CuO nanoparticles.

1. Proposed system-B gives better annual performance than system-A and system-C based on thermal exergy, thermal energy, for system-A 16.75%, 23.16% and for system-B 13.68%, 8.22%, respectively.
2. Production of potable water (yield) CuO nanoparticles. 11.19% in case of system-A, 16.31% in case of system-B, respectively.
3. System-B performs better than system-A and system-C based on thermal energy, thermal exergy, energy, and exergy-based EPT8.38% and 17.48%, EPF is 7.73% and 14.88%, and LCCE is 15.55% and 0.679% greater, respectively.
4. System-B performance is better than system-A and system-C, and as per cost of distillate system-C is better than system-A. The distillate cost on an annual basis and life span basis for system-A is 1.59₹/kg, system-B is 1.98 ₹/kg, and system-C is 2.44 ₹/kg.
5. System-A is environ-economic than system-B and system-C, and system-B is better than system-C. CO₂ mitigation per ton for 15 years system-A 40.24, system-B 40.85, and system-C 42.54.

6. According to carbon credit earned (\$) based on energy, system-C is more environ-economic than system-A and system-B, and system-B is more environ-economic than system-A, respectively. For 15 years, system-A 201.22, system-B 204.26, and system-C 212.71.
7. Exergoeconomic analysis based on exergoeconomic parameter (R_{ex}) kWh/₹, system-A is more economic than system-B and system-C. than system-B. Therefore system-A is better than system-B and system-C.
8. System-B productivity is greater than system-A and system-C. For 15 years, system-A 182.81%, system-B 209.44%, and system-C 185.80%.
9. According to present value (\$), system-A is better than system-B and system-C based on present value with interest rate of 10%. System-B is better than system-C.
10. System performance on 0.02 kg/s flow rate, which is less than prior system 0.03 kg/s flow rate shows that reducing the pump work correspondingly reduces motor power to drive the pump hence reducing the requirement for electricity.
11. Power required to operate the pump is supplied from an integrated solar photovoltaic module with solar stills. Proposed solar distillation system is self-sustainable. Therefore specific electrical energy consumption is based on solar photovoltaic generated power. Pump of 24W rating is used. Specific energy consumption for system-A is 0.02423 kW/kg, system-B is 0.022kW/kg, and system-C is 0.044 kW/kg

The overall best design is active N-PVT-CPC double slope solar distiller incorporating a helically coiled heat exchanger using CuO nanoparticles because of its annual performance based on yield, thermal energy and thermal exergy, energy matrices, exergoeconomic.

5.2 Future scope

The present work can be further expanded by intensive research into CPC-PVT-PCM utilizations up to their optimum level.

1. Energy, exergy, energy matrices, enviroeconomic and exergoeconomic assisted with different nanoparticles and nanofluids can be studied.
2. The effect of mass flow rate, size, and shape of nanoparticles can be investigated.
3. PCM materials can also be used to store energy in the daytime when the sun is shining, which can be further utilized when the sun is absent.
4. The partly covered FPC can be increased beyond 25% to run the system at night with additional supportive electrical subsystems.
5. The profile of CPC may further increase the water temperature during day time and can be further utilized by the PCM at night. It can be another cause for system performance enhancement, and further research is needed to quantify that.

REFERENCES

- [1] <https://www.unicef.org/press-releases> (2021) access as on 15/12/2021.
- [2] WHO, Water, Sanitation and Hygiene Links to Health, Facts and Figures, WHO, updated, 45 (2004)361.
- [3] Burek et al., Water Futures and Solution - Fast Track Initiative (Final Report), (2016).
- [4] Mouchot, A. La Chaleur Solavie et ses Applications. Gauthier- Villars, Paris, (1969).
- [5] Della Porta, G.B. Magiaenaturalis libri XX, Napoli (1589).
- [6] C. F. Colebrook, Turbulent flow in pipes, for particular reference of the transition area between smooth and rough pipe flows, Journal Institute Civil Engineering, 11 (1939) 133-56.
- [7] H. S. Soliman, Solar still coupled with a solar water heater, Mosul, Mosul University, Iraq(1976).
- [8] S. N. Rai, G. N Tiwari, Single basin solar still coupled with flat plate collector, Energy Conversion Management, 23 (1982)145.
- [9] Zaki G.M., Dali T. El and Shafie H. El, Improved performance of solar still, Proc. First Arab International, Solar Energy Conference, Kuwait, (1983) 331-335.
- [10] S. A Lawrence, G. N. Tiwari, Theoretical evaluation of solar distillation under natural circulation with heat exchanger, Energy Conversion Management, 30 (1990) 205-13.
- [11] C. J Popiel, Wojtkowiak, Simple formulas for thermo-physical properties of liquid water for heat transfer calculations (from 0 °C to 150 °C), Heat Transfer Engineering, 19 (1998) 87-101.
- [12] B.C. Pak, Y.I. Cho, Hydrodynamic and heat transfer study of dispersed fluids with sub-

- micronmetallic oxide particles, *Exp Heat Transfer A. Journal, Thermal Energy Generation Transport Storage Conversion*, 11 (1998) 151–70.
- [13] S. Kumar, G. N. Tiwari, Optimization of daily yield for an active double effect distillation with water flow, *Energy Conversion Management*, 40 (1999) 703–15.
- [14] G. N. Tiwari, *Solar energy: fundamentals, design, modeling and applications*, New Delhi/New York, CRC Publication/Narosa Publishing House, (2002).
- [15] E. Delyannis, historical background of desalination and renewable energies, *Solar Energy*, 75 (2003) 357.
- [16] G. N. Tiwari, H.N. Singh, R. Tripathi, Present status of solar distillation, *Solar Energy*, 75 (2003) 367.
- [17] M. Boukar, A. Harmim, Performance evaluation of a one-sided vertical solar still tested in the desert of Algeria, *Desalination*, 183 (2005) 113–126.
- [18] G. N. Tiwari, A. Tiwari, *Solar distillation practice for water desalination systems*, New Delhi, Anamaya Publications, (2007).
- [19] O. O. Barden, Experimental study of the enhancement parameters on a single slope solar still productivity, *Desalination*, 209 (2007) 136-43.
- [20] K. S. Hwang, J. H Lee, S. P. Jang, Buoyancy-driven heat transfer of water-based Al_2O_3 nanofluids in a rectangular cavity, *International Journal of Heat Mass Transfer*, 50 (2007) 4003-4010
- [21] C. J. Ho, M. W. Chen, Z. W. Li, Numerical simulation of natural convection of nanofluid in a square enclosure: effects due to uncertainties of viscosity and thermal conductivity, *International Journal of Heat Mass Transfer*, 51 (2008) 4506-4516.

- [22] S. Dubey, G. N. Tiwari, Analysis of PVT flat plate water collectors connected in series, *Sol Energy*, 83 (2009) 1485-1498.
- [23] R. Dev, G. N. Tiwari, characteristic equation of passive solar still desalination, 245 (2009) 246-265.
- [24] T. P. Otanicar, J. Golden, Comparative environmental and economic analysis of conventional and nanofluid solar hot water technologies, *Environment Science, Technology*, 43 (2009) 6082-6087.
- [25] P. K. Singh, K. B. Anoop, T. Sundararajan, K. D. Sarit, entropy generation due to flow and heat transfer in nanofluids, *International Journal of Heat Mass Transfer*, 53 (2010) 4757-4767.
- [26] R. Dev, G. N. Tiwari, Characteristic equation of a hybrid (PVT) active solar still, *Desalination*, 254 (2010) 126–137.
- [27] M. K Gaur, G.N. Tiwari, Optimization of number of collectors for integrated PV/T hybrid active solar still, *Applied Energy*, 87 (2010) 1763–1772.
- [28] H. K. Patel, T. Sundararajan, S. K. Das, An experimental investigation into the thermal conductivity enhancement in oxide and metallic nanofluids, *Journal of Nanoparticle Research*, 12 (2010)1015-1031.
- [29] K. Sharma, P. Sharma P, W. Azmi, R. Mamat, K. Kadirgama, Correlations to predict friction and forced convection heat transfer coefficients of water based nanofluids for (2010) turbulent flow in a tube, *Int. J Micro-sci. Nanoscale Therm. Fluid Transport Phenomenon*, 3283-3308.
- [30] R. Dev, H. N. Singh, G.N.Tiwari, Characteristic equation of double slope passive solar still, *Desalination*, 267 (2011) 261–266.

- [31] R. Dev, G. N. Tiwari, characteristic equation of the inverted absorber solar still, *Desalination*, 269 (2011) 67–77.
- [32] R. Dev, S.A. Abdul-Wahab, G. N. Tiwari, Performance study of the inverted absorber solar still with water depth and total dissolved solid, *Applied Energy*, 88 (2011) 252–264.
- [33] K. Khanafer, K. Vafai, A critical synthesis of thermo-physical characteristics of nanofluids, *International Journal of Heat Mass Transfer*, 54 (2011) 4410-4428.
- [34] M. G. J. D. Elzen, A. D Hof, A. M. Beltran, G. Grassi, M. Roelfsema, B. V. Ruijven, The Copenhagen accord: abatement costs and carbon prices resulting from the submissions, *Environment Science Policy*, 14 (2011) 28-39.
- [35] V. Khullar, H. Tyagi, A study on environmental impact of nanofluid based concentrating solar water heating system, *International Journal Environment Studies*, 69 (2012) 220-232.
- [36] R. Balan, J. Chandrasekaran, S. Shanmugan, B. Janarthanan, S. Kumar. Review on passive solar distillation, *Desalination and Water Treatment*, (2012).
- [37] T. Yiamsawasd, A. S. Dalkilic, S. Wongwises, Measurement of specific heat of nanofluids, *Current Nanoscience*, 8 (2012) 939-944.
- [38] M. Faizal, R. Saidur, S. Mekhilef, M. A. Alim, Energy, economic and environmental analysis of metal oxides nanofluid for flat-plate solar collector, *Energy conversion and management*, 76 (2013) 162-168.
- [39] X. Liu, W. Chen, M. Gu, S. Shen, G. Cao, Thermal and economic analyses of solar desalination system with evacuated tubular collectors, *Solar Energy*, 93 (2013) 144-150.
- [40] M. A. Khairul, R. Saidur, M. M. Rahman, M. A. Alim, A. Hossain, Z. Abdin, Heat trans-

- ferand thermodynamic analyses of a helically coiled heat exchanger using different types of nanofluids, *International Journal of Heat Mass Transfer*, 67 (2013) 398–403.
- [41] O. Mahian, A. Kianifar, A. Z. Sahin, S. Wongwises, Performance analysis of a mini channel-based solar collector using different nanofluids. *Energy conversion and management*, 88 (2014) 129-138.
- [42] O. Mahian, A. Kianifar, A. Z. Sahin, S. Wongwises, Entropy generation during Al_2O_3 water nanofluid flow in a solar collector: effects of tube roughness, nanoparticle size, and different thermo-physical models, *International Journal of Heat Mass Transfer*, 78 (2014) 64-75.
- [43] Kabeel AE, Omara ZM, Essa FA. Enhancement of modified solar still integrated with External condenser using nanofluids: An experimental approach, *Energy conversion and management*, 78 (2014) 493-508.
- [44] O. Mahian, A. Kianifar, A. Sahin, W. Somchai, Heat transfer, pressure drop, and entropy generation in a solar collector using SiO_2 /water nanofluids: effects of nanoparticles size and pH, *Journal Heat Transfer*, 135 (2015) 61011.
- [45] Shyam, G. N. Tiwari, I. MAI-Helal, Analytical expression of temperature dependent electrical efficiency of N-PVT water collectors connected in series, *Sol Energy*, 114 (2015) 61–76.
- [46] D. Atheaya, A. Tiwari, G. N. Tiwari, I.M. Al-Helal, Analytical characteristic equation for partially covered photovoltaic thermal compound parabolic concentrator (PVT-CPC) collector, *Solar energy*, 111 (2015) 176-185.
- [47] Y. R. Sekhar, K. Sharma, Study of viscosity and specific heat capacity characteristics of water-based Al_2O_3 nanofluids at low particle concentrations, *Journal Experiment naosci-*

Ence. 10 (2015) 86-102.

- [48] T. Elango, A. Kannan, K. K. Murugavel, Performance study on single basin single slope solar still with different water nanofluids. *Desalination* 360 (2015) 45-51.
- [49] Z. M. Omara, A. E. Kabeel, F. A. Essa, Effect of using nanofluids and providing vacuum on the yield of corrugated wick solar still. *Energy conversion and management*, 103 (2015) 965-972.
- [50] G. N. Tiwari, J. K. Yadav, D. B. Singh, I. M. Al-Helal, A. M. Abdel-Ghaney, Exergoeconomic and enviroeconomic analyses of partially covered photovoltaic flat plate collector active solar distillation system, *Desalination*, 367(2015) 186-196.
- [51] H. Sharon, K. S. Reddy, Performance investigation and enviro-economic analysis of active vertical solar distillation units, *Energy*, 84 (2015) 794-807.
- [52] L. Sahota, G. N. Tiwari, Effect of Al_2O_3 NPs on the performance of passive double slope solar still, *Solar Energy*, 130 (2016) 260-72.
- [53] D. B. Singh, G. N. Tiwari, I. M. Al-Helal, V. K. Dwivedi, J. K. Yadav, Effect of energy matrices on life cycle cost analysis of passive solar stills, *Solar Energy*, 134 (2016) 9-22.
- [54] L. Sahota, G. N. Tiwari, Effect of nanofluids on the performance of passive double slope solar still: A comparative study using characteristic curve. *Desalination*, 388 (2016) 9-21.
- [55] D. B. Singh and G. N. Tiwari, Effect of energy matrices on life cycle cost analysis of partially covered photovoltaic compound parabolic concentrator collector active solar distillation system, *Desalination*, 397 (2016) 75-91.
- [56] Shyam, G.N. Tiwari, O. Fischer, R. K. Mishra, I. M. Al-Helal, Performance evaluation of N-photovoltaic thermal (PVT) water collectors partially covered by photovoltaic module

connected in series: an experimental study *Sol. Energy*, 130 (2016) 302–13.

- [57] A. Mwesigye, Z. Huan, J. P. Meyer, Thermal performance and entropy generation analysis of a high concentration ratio parabolic trough solar collector with Cu-Therminol VP-1 nanofluid, *Energy conversion and management* 120 (2016) 449–465.
- [58] R. Tripathi, G. N. Tiwari, Energetic and exergetic analysis of N partially covered thermal compound parabolic concentrator (PVT-CPC) collector connected in series, *Solar energy*, 137 (2016) 441-451.
- [59] MathWorks Inc., MATLAB-R2016a (9.0.0.341360), (2016).
- [60] A. Menbari, A. A. Alemrajabi, A. Rezaei, Heat transfer analysis and the effect of CuO - water nanofluid on direct absorption concentrating solar collector, *Applied Thermal Engineering*, 104 (2016) 176–83.
- [61] G. N. Tiwari, L. Sahota, Review on the energy and economic efficiencies of passive and active solar distillation systems, *Desalination*, 401 (2017) 151–179.
- [62] L. Sahota, G. N. Tiwari, Analytical characteristic equation of nanofluid loaded active double slope solar still coupled with helically coiled heat exchanger, *Energy conversion and management*, 135 (2017) 308-326.
- [63] L. Sahota, Shyam, G. N. Tiwari, Energy matrices, enviroeconomic and exergoeconomic analysis of passive double slope solar still with water based nanofluids, *Desalination*, 409 (2017) 66-79.
- [64] L. Sahota, G.N. Tiwari, Exergoeconomic and enviroeconomic analyses of hybrid double slope solar still loaded with nanofluids, *Energy Conversion and Management*, 148 (2017) 413-430.

- [65] W. Chen, C. Zou, X. Li, L. Li, Experimental investigation of S_iC nanofluids for solar distillation system: Stability, optical properties and thermal conductivity with saline water based fluid, *International Journal of Heat Mass Transfer*, 107 (2017) 264-270.
- [66] O. Mahian, A. Kianifar, S. Z. Heris, D. Wen, A. Z. Sahin, S. Wongwises, Nanofluids effects on the evaporation rate in a solar still equipped with a heat Exchanger. 36 (2017) 134-155.
- [67] D. B. Singh, G. N. Tiwari, Enhancement in energy metrics of double slope solar still by incorporating N identical PVT collectors, *Solar Energy*, 143 (2017) 142-161.
- [68] S.M. Saleha, A.M. Soliman, M.A. Sharaf, V. Kaled, B. Gadgile, Influence of solvent in the synthesis of nano-structured ZnO by hydrothermal method and their application in solar-still, *J. Environ. Chem. Eng.* 5 (1) (2017) 1219–1226.
- [69] S. W. Sharshir, G. Peng, L.Wu, N. Yang, F. A. Essa, A. H. Elsheikh, S. I. T. Mohamed, A.E. Kabeel, Enhancing the solar still performance using nanofluids and glass cover cooling: experimental study. *Appl. Therm. Eng.* 113(2017) 684–693
- [70] G. N. Tiwari, L. Sahota, *Advanced Solar Distillation Systems: Basic Principles, Thermal Modeling and Its Applications*, Springer (Nature), (2017).
- [71] P. Joshi and G. N. Tiwari, Effect of cooling condensing cover on the performance of N identical photovoltaic thermal compound parabolic concentrator active solar still: a comparative study, *International Journal of Energy and Environmental Engineering*, 9 (2018) 473-498.
- [72] A. K. Singh, D. B. Singh, V. K. Dwivedi, N. Kumar, J. K. Yadav, A review of performance enhancement in solar desalination systems with the application of nanofluids, *international Conference on Advances in Computing, Communication Control and Net-w*

-orking (ICACCCN) 2018.

- [73] D. B. Singh, N. Kumar, Harender, S. kumar, S. K. Sharma, A. mallick, Effect of depth ofwater on various efficiencies and productivity of N identical partially covered PVT collectors incorporated single slope solar distiller unit, *Desalination and Water Treatment*, 138 (2019) 99-112.
- [74] D. B. Singh, A. K. Singh, N. Kumar, V. K. Dwivedi, J. K. Yadav, G. Singh, Performanceanalysis of Special Design Single Basin Passive Solar Distillation Systems: A Comprehensive Review, *Lecture Notes in Mechanical Engineering, Advances in Engineering Design*, Springer, Singapore, (2019) 301-310.
- [75] Dharamveer, Samsher, D. B. Singh, A. K. Singh, N. Kumar, Solar Distiller Unit Loaded with Nanofluid-A Short Review. *Lecture Notes in Mechanical Engineering, Advances in Interdisciplinary Engineering Springer*, Singapore, (2019) 241-247.
- [76] H. Prasad, P. Kumar, R. K. Yadav, A. Mallick, N. Kumar, D.B Singh, sensitivity analysis of N identical partially covered (50%) PVT compound parabolic concentrator collectors integrated double slope solar distiller unit, *Desalination and Water Treatment*, 153 (2019) 54-64.
- [77] M.E. Ahmed, A. Abdel-Rehim, Energy and exergy analysis of a thermosiphon and forced-circulation flat-plate solar collector using MWCNT/water nanofluid, *Case studies in thermal engineering* 14 (2019) 1004-1016.
- [78] D. B. Singh, G. Singh, N. Kumar, P. K. Singh, A. Nirala, R. Kumar, Effect of mass flowrate on energy payback time of single slope solar desalination unit coupled with N -identical CPC collectors. <https://doi.org/10.1016/j.matpr.2020.05.137>, (2020).
- [79] G. K. Singh, N. Kumar, D. B. Singh, A. Mallick, exergoeconomic analysis of single slope

solar desalination unit coupled with PVT-CPCs by incorporating the effect of dissimilarity of the rate of flowing fluid mass, 28 (2020) 2364-2368.

- [80] Dharamveer, Samsher, Comparative analysis of energy matrices and enviro-economics for active and passive solar still, *Materials Today: Proceedings*, 45(2020) 6046-6052.
- [81] S. K. Sharma, A. Mallick, S. K. Gupta, D. B. Singh, N. Kumar, G. N. Tiwari, Characteristic equation development for double slope solar distiller unit augmented with *N*-identical parabolic concentrator integrated evacuated tubular collectors, *Desalination and Water Treatment*, 187 (2020) 178-194
- [82] S. K. Sharma, D. B. Singh, A. Mallick, S. K. Gupta, Energy metrics and efficiency analyses of double slope solar distiller unit augmented with *N*-identical parabolic concentrator integrated evacuated tubular collectors: a comparative study, *Desalination and Water Treatment*, 195 (2020) 40-56.
- [83] R. Dhivagar, M. Mohanraj, K. Hindouri, Ye. Belyayev, Energy, exergy, economic and enviroeconomic (4E) analysis of gravel coarse aggregate sensible heat storage assisted single slope solar still, *Journal of Thermal Analysis and Calorimetry*, 145 (2020) 475-494.
- [84] V. S. Gupta, D. B. Singh, S. K. Sharma, N. Kumar, T. Bhatti and G. N. Tiwari, Modeling self-sustainable fully-covered photovoltaic thermal-compound parabolic concentrators connected to double slope solar distiller, *Desalination and Water Treatment* 190 (2020) 12-27.
- [85] G. Zhang, N. D. Kaushika, S. C. Kaushik, R. K. Tomar, *Advances in Energy and Built environment*, Springer Science and Business Media LLC, 2020.
- [86] S. Arora, H. P. Singh, L. Sahota, M. K. Arora, R. Arya, S. Singh, A. Jain, A. Singh, Performance and cost analysis of photovoltaic thermal (PVT)-compound parabolic

concentrator (CPC) collector integrated solar still using CNT-water based nanofluids, *Desalination*, 495 (2020) 114595.

- [87] K. Bharti, S. Manwal, C. Kishore, R. K. Yadav, P. Tiwari, D. B. Singh, Sensitivity analysis of N alike partly covered PVT flat plate collectors integrated double slope solar distiller unit. *Desalination and Water Treatment*, 211 (2021) 45-59.
- [88] Dharamveer, Samsher, Anil Kumar“Analytical study of photovoltaic thermal (PVT) compound parabolic concentrator (CPC) active double slope solar distiller with helical coiled heat exchanger using CuONanoparticles”*Desalination and water treatment*, 233 (2021) 30–51.
- [89] Dharamveer, Samsher, Anil Kumar“Performance analysis of N -identical PVT-CPC collectors an active single slope solar distiller with a helically coiled heat exchanger using CuO nanoparticles”, *Water supply*, (2021) 0-11.

APPENDIX

Appendix A

$$A_1 = C_1 U_1 + C_2$$

$$C_1 = \alpha_g I_{SE} A_{gE} + U_{cgaE} A_{gE} T_a$$

$$C_2 = \alpha_g I_{SW} A_{gE} A_{gW} h_{EW} + U_{cgaW} A_{gE} T_a A_{gW} h_{EW}$$

$$U_1 = h_{1wE} \frac{A_b}{2} + h_{EW} A_{gE} + U_{cgaE} A_{gE}$$

$$A_2 = (h_{1wE} U_2 + h_{1wW} h_{EW} A_{gE}) \frac{A_b}{2}$$

$$U_2 = U_{cgaW} A_{gW} + h_{1wW} \frac{A_b}{2} + h_{EW} A_{gW}$$

$$B_1 = C'_1 U_1 + C'_2$$

$$B_2 = (h_{1wW} U_1 + h_{1wE} h_{EW} A_{gE}) \frac{A_b}{2}$$

$$C'_1 = \alpha_g I_{SW} A_{gE} + U_{cgaW} A_{gE} T_a A_{gW}$$

$$C'_2 = \alpha_g I_{SE} A_{gE} A_{gW} h_{EW} + U_{cgaE} A_{gE} T_a A_{gW}$$

$$D_3 = m_f C_f [T_{HE} - T_{wi}]$$

$$D_1 = \left[\frac{(AF_R(\alpha\tau))1(1 - K_p^N)}{(1 - K_p)} \left(1 - \frac{1}{(1 - e^z K_m^N)} \right) \right]$$

$$D_2 = \left[\frac{(AF_R(UL)1)(1 - K_p^N)}{(1 - K_p)} \left(1 - \frac{1}{(1 - e^z K_m^N)} \right) \right]$$

$$E_1 = U_{gaE} [h_{EW} + h_{1bwW} \left(\frac{A_b}{2A_{gW}} \right)]$$

$$E'_1 = U_{gaW} [h_{EW} + h_{1bwE} \left(\frac{A_b}{2A_{gE}} \right)]$$

$$E_2 = U_{gaW} (h_{EW} + U_{gaE}) A_{gE} A_{gW}$$

$$E'_2 = U_{gaE} (h_{EW} + U_{gaW}) A_{gE} A_{gW}$$

$$H_1 = (U_{gaE} + U_{gaW}) h_{1bwW} h_{1bwE} \left(\frac{A_b}{2} \right)$$

$$H_2 = A_{gE}A_{gW}h_{EW}(U_{gaE}h_{1bwE} + U_{gaW}h_{1bwW})$$

$$H_3 = A_{gE}A_{gW}U_{gaE}U_{gaW}(h_{1bwE} + h_{1bwW})$$

$$H_4 = A_{gE}A_{gW}h_{EW}(U_{gaE}h_{1bwW} + U_{gaW}h_{1bwE})$$

$$H'_{11} = H_1 + H_2 + H_3 + H_4$$

$$H'_{33} = U_bA_b - D_1$$

$$H'_{44} = U_bA_b + D_3$$

$$K_{1E} = [h_{1bwW} \left(\frac{A_b}{2A_{gW}} \right) + h_{EW} \left(1 + \frac{1}{h_{1bwE}} \right) + U_{gaW}]A_{gW}\alpha_gA_{gE}h_{1bwE}$$

$$K_{1W} = [h_{1bwE} \left(\frac{A_b}{2A_{gE}} \right) + h_{EW} \left(1 + \frac{1}{h_{1bwW}} \right) + U_{gaE}]A_{gW}\alpha_gA_{gE}h_{1bwW}$$

$$K'_{1E} = [h_{1bwW} \left(\frac{A_b}{2} \right) + h_{EW} \left(1 + \frac{h_{1wE}}{h_{1wW}} \right) A_{gW} + U_{gaW}A_{gW}] \alpha_g A_{gE} h_{1wE}$$

$$K'_{1W} = [h_{1bwE} \left(\frac{A_b}{2} \right) + h_{EW} \left(1 + \frac{h_{1wE}}{h_{1wW}} \right) A_{gE} + U_{gaE}A_{gE}] \alpha_g A_{gW} h_{1wW}$$

$$P = U_1U_2 - h_{EW}^2A_{gE}A_{gW}$$

Expressions for K_k , $(A F_R(\alpha\tau))_1$ and $(A F_R U_L)_1$ used in Eq. (1) are as follows.

$$K_p = 1 - \frac{(AF_R(UL)1)}{m_f c_f}$$

$$K_m = 1 - \frac{(A_{Rm}F_{Rm}(UL)m)}{m_f c_f}$$

$$U_{tca} = \left[\frac{1}{h_o} + \frac{L_g}{K_g} \right]^{-1} ; U_{tcp} = \left[\frac{1}{h_i} + \frac{L_g}{K_g} \right]^{-1} ;$$

$$h_o = 5.7 + 3.8V, \quad Wm^{-2}K^{-1} ; V = 1 ms^{-1} ; h_i = 5.7, \quad Wm^{-2}K^{-1} ;$$

$$U_{tpa} = \left[\frac{1}{U_{tca}} + \frac{1}{U_{tcp}} \right]^{-1} + \left[\frac{1}{h'_i} + \frac{1}{h_{pf}} + \frac{L_i}{K_i} \right]^{-1} ;$$

$$h'_i = 2.8 + 3V', \quad Wm^{-2}K^{-1} ;$$

$$U_{L1} = \frac{U_{tcp}U_{tca}}{U_{tcp}+U_{tca}} ; U_{L2} = U_{L1} + U_{tpa} ; U_{Lm} = \frac{h_{pf}U_{L2}}{F'h_{pf}+U_{L2}} ; U_{Lc} = \frac{h_{pf}U_{tpa}}{F'h_{pf}+U_{tpa}} ;$$

$$PF_1 = \frac{U_{tcp}}{U_{tcp} + U_{tca}} ; PF_2 = \frac{h_{pf}}{F'h_{pf} + U_{L2}} ; PF_c = \frac{h_{pf}}{F'h_{pf} + U_{tpa}} ;$$

$$(\alpha\tau)_{1eff} = \rho(\alpha_c - \eta_c)\tau_g\beta_c \frac{A_{am}}{A_{rm}} ; (\alpha\tau)_{2eff} = \rho\alpha_p\tau_g^2(1 - \beta_c) \frac{A_{am}}{A_{rm}} ;$$

$$(\alpha\tau)_{meff} = [(\alpha\tau)_{1eff} + PF_1(\alpha\tau)_{2eff}] ; (\alpha\tau)_{ceff} = PF_c \cdot \rho\alpha_p\tau_g \frac{A_{ac}}{A_{rc}} ;$$

$$(AF_R(\alpha\tau))_1 = \left[A_c F_{Rc} (\alpha\tau)_{ceff} + PF_2 (\alpha\tau)_{meff} A_m F_{Rm} \left(1 - \frac{A_c F_{Rc} U_{Lc}}{\dot{m}_f c_f} \right) \right] ;$$

$$(AF_R U_L)_1 = \left[A_c F_{Rc} U_{Lc} + A_m F_{Rm} U_{Lm} + A_m F_{Rm} U_{Lm} \left(1 - \frac{A_c F_{Rc} U_{Lc}}{\dot{m}_f c_f} \right) \right]$$

$$A_{rm} = b_r L_{rm} ; A_{am} = b_o L_{am} ;$$

$$A_c F_{Rc} = \frac{\dot{m}_f c_f}{U_{Lc}} \left[1 - \exp\left(\frac{-F' U_{Lc} A_c}{\dot{m}_f c_f}\right) \right] ; A_m F_{Rm} = \frac{\dot{m}_f c_f}{U_{Lm}} \left[1 - \exp\left(\frac{-F' U_{Lm} A_m}{\dot{m}_f c_f}\right) \right] ;$$

$$z = \frac{2\pi r_{11} U_L}{\dot{m}_f c_f}$$

PUBLICATIONS

International & National Journal/Conference Paper Published (03+ 02 = 05)

International Journal (02+ 01 = 03)

1. **Dharamveer**, Samsher, Anil Kumar “Analytical study of Nth identical photovoltaic thermal compound parabolic concentrator collectors an active single slope solar distiller with a helically coiled heat exchanger using CuO nanoparticles”, Water supply, IWA publication, Oct 2021, **SCI-E**, Impact factor 1.275, <https://doi.org/10.2166/ws.2021.348>
2. **Dharamveer**, Samsher, Anil Kumar “Analytical study of photovoltaic thermal (PVT) compound parabolic concentrator (CPC) active double slope solar distiller with helical coiled heat exchanger using CuO Nanoparticles” Desalination and Water Treatment, Taylor & Francis Publication.233 (2021) 30–51, **SCI-E**, Impact factor 1.254, <http://doi.10.5004/dwt.2021.27526>
3. **Dharamveer**, Samsher, Anil Kumar “Effect of energy matrices on life cycle cost analysis of partly covered N-PVT-CPC active double slope solar distiller with helically coiled heat exchanger using CuO Nanoparticles” Sustainable Energy Technologies and Assessments, Elsevier Publication. Dec 2021, **SCI-E**, Impact factor 5.353, Under Review,

International Conference (02)

1. **Dharamveer**, Samsher “Comparative Analysis of Energy Matrices and Enviroeconomics for Active and Passive Solar Still”. Journal Material’s Today proceedings. <https://doi.org/10.1016/j.matpr.2020.10.001>. **Scopus Index**, Elsevier publication. Presented in International conference on Energy, Material science and Mechanical Engineering 2020 (EMSME2020), October 30- November 01, 2020, at NIT, Delhi.
2. **Dharamveer**, Samsher, Singh D.B., Singh A.K., Kumar N. (2019) Solar Distiller Unit Loaded with Nanofluid-A Short Review. In: Kumar M., Pandey R., Kumar V. (eds) Advances in Interdisciplinary Engineering. Lecture Notes in Mechanical Engineering, Springer, Singapore. https://doi.org/10.1007/978-981-13-6577-5_24. pp 241-247, Paper Published. **Scopus Index**, Springer Publication. Presented in International Conference FLAME- 2018, presented paper at Amity University, Noida, UP.

Brief Bio-Data

Mr. Dharamveer Singh

veerdharam76@gmail.com

Mailing/Permanent Address:

E 223, Choti Market, Govindpuri, Modinagar, Ghaziabad, U. P.-201201, INDIA

Contact No: +91-9760521551, +91-8171763871,

ACADEMIC QUALIFICATION

- **Ph. D. (Thermal Engg.)** Pursuing Jul-2016, **Delhi Technological University**, Delhi 110042, INDIA.
- **M.B.A. (Human Resource Management)**, Aug 2016, **IGNOU**, Delhi, INDIA
- **M.Tech. (Thermal Engg.)**, June 2015, **Rajasthan Technical University**, Kota, Rajasthan, INDIA.
- **B.Tech. (Mech. Engg)**, June 2007, **Delhi College of Engg.** University of Delhi, Delhi -110042, INDIA.
- Diploma: Mechanical Engineering, May 1997, **UPBTE - Lucknow**, INDIA.
- SSC: (10th) June 1992, U.P. Board, INDIA, with Science, Math, English, Technical Drawing and Hindi.

PAPER PUBLISHED

(10+6+4=20)

International Journal

(10)

1. **Dharamveer**, Samsher, Anil Kumar “Performance analysis of N-identical PVT-CPC collectors an active single slope solar distiller with a helically coiled heat exchanger using CuO nanoparticles”, Water supply, Oct 2021, **SCI-E Index**, IWA Publication. **I.F 1.275**, <https://doi.org/10.2166/ws.2021.348/84648>
2. **Dharamveer**, Samsher, Anil Kumar “Analytical study of photovoltaic thermal (PVT) compound parabolic concentrator (CPC) active double slope solar distiller with helical coiled heat exchanger using CuO Nanoparticles” Desalination and water treatment, vol. 233 (2021) 30–51, **SCI-E Index**, Taylor & Francis Publication. **I.F 1.254**, <https://doi.org/10.5004/dwt.2021.27526>
3. **Dharamveer**, Samsher “Comparative Analysis of Energy Matrices and Enviroeconomics for Active and Passive Solar Still”. Journal Materials Today proceedings. **Scopus Index**, Elsevier publication. <https://doi.org/10.1016/j.matpr.2020.10.001>
4. Shiv Kumar, **Dharamveer Singh** “Optimizing Thermal Behavior Of Compact Heat Exchanger” International Journal of Mechanical and Production Engineering Research and Development (IJMPERD) ISSN(P): 2249-6890; ISSN(E): 2249-8001 Vol. 10, Issue 3, Jun 2020, 8113-8130.. **Scopus Index**. <https://doi.org/10.24247/ijmperdjun2020770>
5. Anubhav Kumar Anup, Dharamveer Singh “FEA Analysis of Refrigerator Compartment for Optimizing Thermal Efficiency” International Journal of Mechanical and Production Engineering Research and Development (IJMPERD) ISSN (P): 2249–6890; ISSN (E): 2249–8001 Vol. 10, Issue 3, Jun 2020, 3951-3972. **Scopus Index**. <https://doi.org/10.24247/ijmperdjun2020376>
6. Shiv Kumar, **Dharamveer Singh** “Energy and exergy analysis of active solar still using compound parabolic concentrator” International Research Journal of Engineering and Technology Vols. 6, Issue 12, Dec 2019, ISSN (online) 23950056.
7. Ravi Shanker, **Dharamveer Singh**, DeshBandhu Singh “Performance analysis of C.I. engine using biodiesel fuel by modifying injection timing and injection pressure” International Research Journal of Engineering and Technology Vols. 6, Issue 12, Dec 2019, ISSN (online) 23950056.
8. **Dharamveer**, Samsher, Singh D.B., Singh A.K., Kumar N. (2019) “Solar Distiller Unit Loaded with Nanofluid—A Short Review”. In: Kumar M., Pandey R., Kumar V. (eds) Advances in Interdisciplinary Engineering. Lecture Notes in Mechanical Engineering. Springer, Singapore.

pp 241-247, Paper Published. **Scopus Index**, Springer Publication. https://doi.org/10.1007/978-981-13-6577-5_24

9. Ashwani Rohila, **Dharamveer Singh**, Vikas Chander “Stochastic finite element buckling response of laminated composite plate with random system properties in thermal environment: Micromechanical Model” **International Journal for Research in Technological Studies** Vols. 4, Issue 9, August 2017, ISSN (online): 2348-1439
10. Rajesh Kumar and **Dharamveer Singh**, “Hygrothermal buckling response of laminated composite plates with random material properties Micro-mechanical model,” **International Journal of Applied Mechanics and Materials** Vols. 110-116 (2012) pp 113-119 Trans Tech Publications, Switzerland Published. <https://www.scientific.net/AMM.110-116.113>

International Conference

(6)

1. **Dharamveer**, Samsher “Comparative Analysis of Energy Matrices and Enviro-economics for Active and Passive Solar Still” International conference on Energy, Material science and Mechanical Engineering 2020 (EMSME2020) October 30- November 01, 2020 at NIT, Delhi.
2. **Dharamveer Singh**, D.B Singh, Samsher, Navneet Kumar “solar distiller unit loaded with nanofluid- A short review” - International Conference FLAME 2018 at Amity University, Noida, UP.
3. **Dharamveer Singh**, Rajesh Kumar, “stochastic buckling and postbuckling response of thermally induced laminated composite plate with random system properties using micromechanical model” International Conference STME- 2014 at DTU, Delhi, October 25-26, 2014.
4. **Dharamveer Singh**, Satyaveer Singh, Dr. Achchela, Dr. V.K Singh “Total Quality Management for Technical Institution” International Conference MTIE- 2011 at S.V.N.I.T, Surat, November 17-19, 2011.
5. Rajesh Kumar, **Dharamveer Singh** “Hygrothermal buckling response of composite plate with random material properties: Micro-mechanical” International Conference CMAE- 2011, IEEE, March 19-20, 2011.
6. Rajesh Kumar, **Dharamveer Singh** “Stochastic finite element post buckling analysis of laminated composite plates under non-Uniform Parabolic Temperature Distribution” International Conference VETOMAC-VI at IIT Delhi, December 13-15, 2010.

National Conference

(4)

1. **Dharamveer Singh**, Ashish Nayyar, Dr. NK Bhanthiya, “A Bridge between Petro- and Bio- Fuels” National Conference NCRDMT-12 at S.R.M. University, NCR Campus, March 22-23, 2012.
2. **Dharamveer Singh**, Ashish Nayyar, Dr. B Kumar, “Lean Implementation by Managing Quality Issues” National Conference NCRDMT-12 at S.R.M. University NCR Campus, March 22-23, 2012.
3. **Dharamveer Singh**, Rajesh Kumar, Achchela, D.K. Rao “Generation of energy using load cell (piezoelectric)” National Conference AMPD-2010 at S.V.N.I.T SURAT, November 22-23, 2010.
4. Rajesh Kumar, **Dharamveer Singh**, “Thermo-elastic static bending response of laminated composite plates with random system properties using stochastic finite element method” National Conference NCRDME-2010 at LIET, Alwar (Raj), October 29-30, 2010.

FDP/Seminar/workshop

(6)

1. Participated in one week short term faculty development program (under TEQIP-III) on “**Solar energy- A sustainable future**” organized by department of mechanical engg., Inderprastha Engineering College, Ghaziabad. 15-20 Jul 2019.
2. Participated in one week short term faculty development program (under TEQIP-III) on “**Applied thermodynamics and its application in power plant engineering**” organized by department of mechanical engg., Vidya College of Engineering, Meerut. 22-26 Oct 2018.
3. Participated in Two days international seminar on “**Research and application of renewable energy**” organized by department of mechanical engg., Galgotias college engineering and technology Greater Noida. 11-12 June 2018.

4. Participated in Three days short term training program on “**Solar technology and management**” organized by Centre for advanced management and power studies, National power training institute, Faridabad-121003. 16-18 Jan 2017.
5. Organized in two days faculty development program (workshop) on “**Fusion 360**” organized by department of mechanical engg., R. D. Engineering College Ghaziabad in Association with HR CAD Centre. 06-07 Feb 2016.
6. Participated in AICTE sponsored one week short term training program on “**Advanced applications of finite element method**” organized by department of mechanical engg., SVNIT Surat-395007. 18-22 Jan 2010.

Place: Modinagar, INDIA

Date: 23/02/2022

(Dharamveer Singh)

Publons ID: <https://publons.com/researcher/4458911/dharamveer-singh/>

SCOPUS: <https://www.scopus.com/authid/detail.uri?authorId=57214416811>

Web of Science Researcher ID: [AAO-8047-2021](https://orcid.org/0000-0001-8047-2021)